ISSN: online 2709-2666
print 2663-7006

AZERBAIJAN JOURNAL OF CHEMICAL NEWS

Vol. 4, No.1, 2022

Azerbaijan Journal of Chemical News

ISNN: print 2663-7006; online 2709-2666

Y.N.Qəhrəmanlı	Professor, Azərbaycan Dövlət Neft və Sənaye Universiteti yunisgahramanly@mail.ru
V.L.Bağiyev	Professor, Azərbaycan Dövlət Neft və Sənaye Universiteti vagif.bagiev@yahoo.com
T.M.Naibova	Dosent, Azərbaycan Dövlət Neft və Sənaye Universiteti n.tamilla51@gmail.com
R.V.Qurbanova	Dosent, Azərbaycan Dövlət Neft və Sənaye Universiteti (texniki redaktor) rena06.72@yandex.ru
Əlaqə	
Ünvan: 20 Azadlıq pr., Bakı, AZ1010, Azərbaycan, Tel: +994124986533, E-mail: minira_baku@yahoo.com, mayaabdullayeva@hotmail.com.	

Azerbaijan Journal of Chemical News

ISNN: print 2663-7006; online 2709-2666

CONTENT

ISNN: print 2663-7006; online 2709-2666

AJCN, Vol 4, No 1, 2022, pp. 6-12

https://doi.org/10.32010/AJCN05012022-6

UDC:666.03

THE $SbBiTe_2Se$-$SbBiTe_2S$ PHASE DIAGRAM OF THE Sb-Bi-S-Se-Te SYSTEM

F.R.Aliyev 0000-0003- 1709-0164

Azerbaijan State Oil and Industry University

fariz_ar@hotmail.com

Using powder X-ray diffraction (PXRD) and differential thermal analysis (DTA), the phase equilibria of the SbBiTe2Se – SbBiTe2S section were studied, and its T-x diagram was constructed. The system is non-quasibinary, due to both initial phases melting in the temperature range. The system is stable below the solidus, which is characterized by the formation of continuous solid solutions (α-phase) with a tetradymite-like hexagonal structure. An analysis of the structural features of tetradymite and other tetradymite-like compounds shows that the substitution of atoms by related atoms is possible in all layers of the packet. In this work sulfur atoms in the central layer can be easily replaced by selenium atoms. This tendency allows us to expect the formation of the range of compositions in the Bi-Sb-Te-Se-S system in which substitutions are realized in cationic and anionic positions. Lattice parameters were determined from the results of powder diffraction patterns. It has been established that the crystal lattice parameters of solid solutions change linearly with composition, which complies with the Vegards rule.

Keywords: *$SbBiTe_2Se$ – $SbBiTe_2S$ system, phase diagram, tetradymite-like structure, solid solutions, high entropy alloys.*

INTRODUCTION

The progress of technologies and theories in the field of materials science has led to the need to complicate the composition of structural and functional materials. In recent years, the attention of investigators has been increasingly lured by high-entropy alloys (HEA) [1-5]. HEAs include multicomponent alloys, including at least five basic elements, the content of each of which should not be less than 5 at%. The main requirement for HEAs is the formation of a homogeneous and thermodynamically stable phase. The stabilization of solid phases and the absence of intermetallic phases during crystallization are due to the high mixing entropy of the components. HESs have a wide range of practical applications in nuclear power engineering, aerospace, tool industries, in hydrogen storage, as refractory, magnetically soft, as well as thermoelectric materials etc. [6–10].

Usually, metal alloys are considered as HEAs. However, these requirements are also fulfilled by multicomponent semiconductor phases, in particular, solid solutions of chalcogenides [11–14].

The tetradymite mineral - Bi_2Te_2S has binary and ternary structural analogs, exhibiting interesting thermoelectric and optical properties [15,16]. The discovery of a new quantum state of matter - a topological insulator (TI) [17,18] has snappily increased interest in layered compounds. In the last decades, studies have shown that these phases also exhibit the properties of a topological insulator and have great potential for in various fields including spintronics, medicine, quantum computers, security systems, etc. [19-25].

This paper presents new data on the synthesis and identification of five-component alloys with a tetradymite-like structure in the $SbBiTe_2Se$ – $SbBiTe_2S$ section of the Sb-Bi-S-Se-Te system. Alloys of this section with the content of initial phases from 25 to 75 mol% contain at least 5 at% of elementary components and therefore they can be considered HEA.

EXPERIMENTAL PART

Synthesis of alloys along the $SbBiTe_2Se$ – $SbBiTe_2S$ section, including the initial phases, was carried out by melting corresponding elementary components of high purity (99.999%, Alfa Aesar) in evacuated (~10^{-2} Pa) quartz ampoules. The samples were heated to 800°C, kept at this temperature for 2 h, and quenched by dropping the ampoules into ice water. Then the alloys were annealed at 450°C for 300 h to achieve an equilibrium state.

The synthesized ingots were examined at room temperature by XRD (D2 PHASER diffractometer, Bruker; CuK_α radiation) and DTA. For DTA, a NETZSCH 404 F1 Pegasus system (heating rate 10°C/min-1) was used. Lattice parameters were calculated using the TOPAS V4.0 program.

RESULTS AND DISCUSSION

Annealed alloys of the 20, 40, 50, 60, 80 mol% $SbBiTe_2S$ composition of the $SbBiTe_2Se$-$SbBiTe_2S$ section and its primary phases were studied by the PXRD method. X-ray diffraction patterns of the alloys are shown in fig.1.

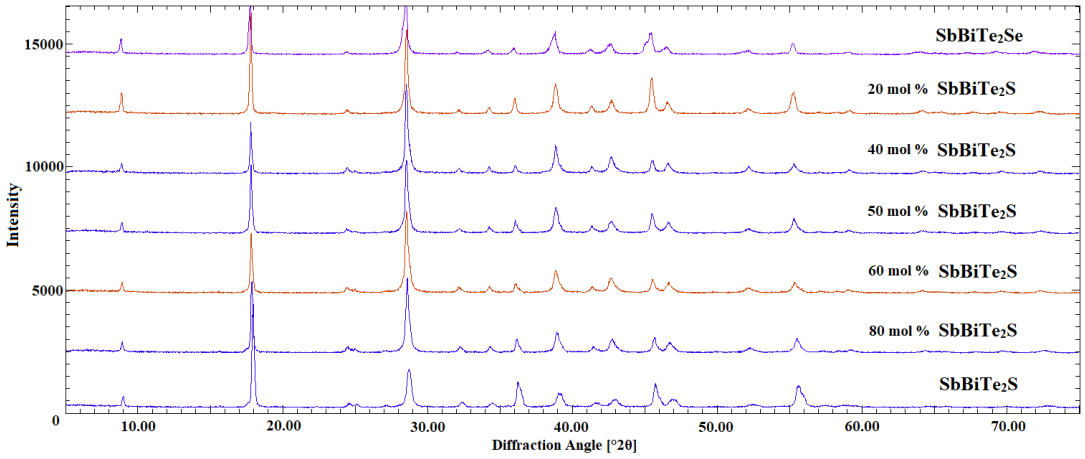

Fig.1. PXRD patterns of the alloys along the $SbBiTe_2Se$ – $SbBiTe_2S$ system.

As can be seen, all samples have qualitatively identical diffraction patterns with some shift of refraction lines, which is typical for systems composed of continuous solid solutions. Analyses of the obtained data using the computer program TOPAS V4.0 showed that all diffraction patterns are completely identified in the tetradymite like hexagonal structure.

ISNN: print 2663-7006; online 2709-2666

Based on the DTA and XRD results, the T-x diagram of the $SbBiTe_2Se$-$SbBiTe_2S$ section was constructed (fig.2.b). As can be seen, even though the system is stable below the solidus and is characterized by the formation of continuous solid solutions (α-phase), it is generally non-quasi-binary, since both initial phases melt in the temperature range. Direction of the tie lines in the L+ α region does not overlap with the T-x plane of this section. Therefore, it is not possible to determine compositions of coexisting phases in this two-phase region from the fig.2b.

From the obtained results, the dependence of lattice parameters on composition was plotted (fig.2a.). As can be seen, the lattice parameters are linearly dependent on the composition which indicates that the Vegard's rule is obeyed.

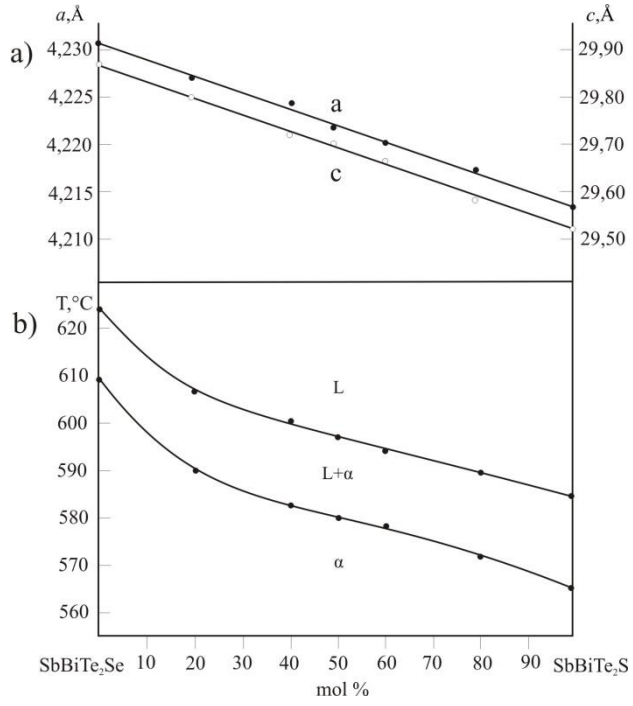

Fig.2. Dependence of lattice parameters on composition (a) and the phase diagram (b) of the system $SbBiTe_2Se$-$SbBiTe_2S$.

By identifying powder diffraction patterns, the parameters of crystal lattices of alloys were determined (table 1).

Table1

DTA results and lattice parameters of $SbBiTe_2Se$-$SbBiTe_2S$ solid solutions

Composition, mol %	Thermal effects, °C	Parameters of the crystal lattice, Å
$SbBiTe_2Se$	625, 610	a=4,2317(3), c=29,871(2)
80	603, 588	a=4,2277(2), c=29,802(1)
60	600, 583	a=4,2241(1), c=29,737(2)
50	595, 580	a=4,2221(2), c=29,709(3)

40	592, 577	*a*=4,2207(2), *c*=29,668(1)
20	589, 574	*a*=4,2177(3), *c*=29,587(2)
$SbBiTe_2S$	585, 563	*a*=4,2131(1), *c*=29,535(3)

CONCLUSION

The manuscript presents new data on phase equilibria in the $SbBiTe_2Se$-$SbBiTe_2S$ system, obtained using the results of differential thermal and XRD analysis. The system is characterized by the formation of continuous solid solutions with a tetradymite-like structure. Lattice parameters of solid solutions have been determined, which are a linear function of the composition. The resulting solid solutions of this system are of potential interest as high-entropy alloys and topological insulators.

REFERENCES

1. Easo P., Robert O., High-entropy alloys. Nature Reviews Materials.2019, Vol. 4, pp. 515–534. https://doi.org/10.1038/s41578-019-0121-4
2. Miracle D., Senkov O. A critical review of high entropy alloys and related concepts. Acta Materialia. 2017, Vol.122, 2017, pp.448-511. https://doi.org/10.1016/j.actamat.2016.08.081
3. Weiran Z., Peter K., Yong Z. Science and technology in high-entropy alloys. Science China Materials. 2018, Vol. 61, pp. 2–22. https://doi.org/10.1007/s40843-017-9195-8
4. Oleg N., Daniel B., Kevin J. Development and exploration of refractory high entropy alloys - A review. Journal of Material Research. 2018, Vol. 33, №19, pp. 3092-3128. https://doi.org/10.1557/jmr.2018.153
5. Jian C., Xueyang Z., Weili W., Bing L., Yukun L., Wei Y., Dapeng X., Yong L. A review on fundamental of high entropy alloys with promising high–temperature properties. Journal of Alloys and Compounds. 2018, Vol.760, 2018, pp. 15-30. https://doi.org/10.1016/j.jallcom.2018.05.067
6. Sathiyamoorthi P., Hyoung S. High-Entropy Alloys: Potential Candidates for High-Temperature Applications – An Overview. Advanced engineering materials.2018, Vol. 20, №1, pp. 1700645. https://doi.org/10.1002/adem.201700645
7. Xuehui Y., Yong Z. Functional properties and promising applications of high entropy alloys. Scripta Materialia. 2020, Vol.187, pp. 188-193. https://doi.org/10.1016/j.scriptamat.2020.06.017
8. Barron P., Carruthers A., Fellowes J., Jones N., Dawson H., Pickering J. Towards V-based high-entropy alloys for nuclear fusion applications. Scripta Materialia. 2020 Vol. 176, pp. 12-16. https://doi.org/10.1016/j.scriptamat.2019.09.028

ISNN: print 2663-7006; online 2709-2666

9. Ka L., Kwang S., Jun S., Jin Y., Hye J., Young S. Dual-phase high-entropy alloys for high-temperature structural applications. Journal of Alloys and Compounds. 2017, Vol. 728, pp. 1235-1238. https://doi.org/10.1016/j.jallcom.2017.09.089
10. Kareer A., Waite J., Li B., Couet A., Armstrong D., Wilkinson A. Short communication: 'Low activation, refractory, high entropy alloys for nuclear applications. Journal of Nuclear Materials. 2019, Vol.526, 2019, pp. 151744 https://doi.org/10.1016/j.jnucmat.2019.151744
11. Min-Jung Y., Yusuf F., Chien-Neng L., Kuei-Hsien C. Synthesis and characterization of Ge-Ag-Sb-S-Se-Te high-entropy thermoelectric alloys. Materials Letters. 2021, Vol.311, pp.131617. https://doi.org/10.1016/j.matlet.2021.131617
12. Riad K., Kazuhisa H., Rajveer J., Masayoshi K., Aichi Y., Yosuke G., Tatsuma D., Yuji A. Superconducting properties of high-entropy-alloy tellurides M-Te (M: Ag, In, Cd, Sn, Sb, Pb, Bi) with a NaCl-type structure. Applied Physics Express.2020, Vol. 13, №3, pp. 33001. https://doi.org/10.35848/1882-0786/ab7482
13. Binbin J., Yong Y., Juan C., Xixi L., Lin X., Jincheng L., Qihao Z., Yi H., Shoucong N., Baohai J., Bin Z. High-entropy-stabilized chalcogenides with high thermoelectric performance. Science. 2021, Vol. 371, pp. 830-834. https://doi.org:/10.1126/science.abe1292
14. Zhao F., Hui W., Yuan W., Xiongjun L., Zhaoping L. Thermoelectric performance of PbSnTeSe high-entropy alloys. Materials Research Letters 2017. Vol.5, №3, pp.187-194. https://doi.org/10.1080/21663831.2016.1244116
15. Liu W., Kevin C., McEnaney K. Studies on the Bi_2Te_3–Bi_2Se_3–Bi_2S_3 system for mid-temperature thermoelectric energy conversion. Energy and Environmental Science.2013, Vol. 6, № 2, pp. 552–560. https://doi.org/10.1039/C2EE23549H
16. Joo S., Ryu B., Son H. Highly anisotropic thermoelectric transport properties responsible for enhanced thermoelectric performance in the hot deformed tetradymite Bi_2Te_2S. Journal of Alloys and Compounds.2019, Vol.783, pp. 448–454. https://doi.org/10.1016/j.jallcom.2018.12.340
17. Joel M. The birth of topological insulators. Nature. 2020, Vol.464, pp. 194–198. https://doi.org/10.1038/nature08916
18. Zahid M., Joel M. Three-dimensional Topological Insulators. Annual Review of Condensed Matter Physics. 2011. Vol.2, 2011, pp. 55–78. https://doi.org/10.1146/annurev-conmatphys-062910-140432
19. Dutta P., Bhoi D., Midya A., Khan N., Mandal P., Ganesan V. Anomalous thermal expansion of Sb_2Te_3 topological insulator. Applied Physics Letters. 2012, Vol. 100, №25, pp. 251912. https://doi.org/10.1063/1.4730390
20. Rabia S., Ganesh G., Patnaik S., Awana V. Crystal growth and characterization of bulk Sb_2Te_3 topological insulator. Materials Research Express. Volume 5, 2018, №4, pp. 46107. https://doi.org/10.1088/2053-1591/aabc33

21. Babanly M., Chulkov E., Aliev Z., Shevel'kov A., Amiraslanov I. Phase diagrams in materials science of topological insulators based on metal chalcogenides. Russian Journal of Inorganic Chemistry. 2017, Vol.62, pp. 1703–1729. https://doi.org/10.1134/S0036023617130034
22. Orujlu E., Aliev Z., Babanly M. The phase diagram of the MnTe–SnTe–Sb_2Te_3 ternary system and synthesis of the iso and aliovalent cation-substituted solid solutions. Calphad. 2022, Vol.76, 2022, pp. 102398. https://doi.org/10.1016/j.calphad.2022.102398
23. Orujlu E., Seidzade A., Mammadov N., Tagiev D., Babanly M. Determination of the Boundaries of Solid Solutions in the MnTe-Sb_2Te_3 and SnTe-Sb_2Te_3 Systems. 11th International Conference on Theory and Application of Soft Computing, Computing with Words and Perceptions and Artificial Intelligence – ICSCCW.2021, Vol.362, pp 513-521. https://doi.org/10.1007/978-3-030-92127-9_69
24. Jörn K., Christian W., Martin L., Melissa S., Elmar N., Gregor M., Thomas S., Detlev G. Selective area growth of Bi_2Te_3 and Sb_2Te_3 topological insulator thin films. Journal Crystal Growth. 2016, Vol.443, 2016, pp. 38-42. https://doi.org/10.1016/j.jcrysgro.2016.03.012
25. Nechaev I., Aguilera I., Renzi V.De., Bona A.Di., Lodi A., Aliev Z., Babanly M., Chulkov E. Quasiparticle spectrum and plasmonic excitations in the topological insulator Sb_2Te_3. Physical Review Journal. 2015, Vol.91, pp.45123. https://doi.org/10.1103/PhysRevB.91.245123

ФАЗОВАЯ ДИАГРАММА $SbBiTe_2Se$-$SbBiTe_2S$ СИСТЕМЫ Sb-Bi-S-Se-Te

Ф.Р. Алиев[0000-0003- 1709-0164]
Азербайджанский Государственный Университет Нефти и Промышленности
fariz_ar@hotmail.com

Методами порошковой рентгенографии (РФА) и дифференциального термического анализа (ДТА) исследовано фазовое равновесие разреза $SbBiTe_2Se$ – $SbBiTe_2S$ и построена его Т-х диаграмма. Система является неквазибинарной так как обе исходные фазы плавятся в интервале температур. Система устойчива ниже солидуса, для которого характерно образование непрерывных твердых растворов (α-фазы) с тетрадимитоподобной гексагональной структурой. Анализ структурных особенностей тетрадимита и других тетрадимитоподобных соединений показывает, что замещение атомов родственными атомами возможно во всех слоях пакета. В этой работе атомы серы в центральном слое можно легко заменить атомами селена. Эта тенденция позволяет ожидать формирования диапазона составов в системе Bi-Sb-Te-Se-S, в которых замещения осуществляются в катионных и анионных позициях. Параметры решетки определяли по результатам порошковых дифрактограмм. Установлено, что параметры кристаллической решетки твердых растворов линейно изменяются с составом, что соответствует правилу Вегарда.
Ключевые слова: *система $SbBiTe_2Se$ – $SbBiTe_2S$, фазовая диаграмма, тетрадимитоподобная структура, твердые растворы, высокоэнтропийные сплавы.*

ISNN: print 2663-7006; online 2709-2666

Sb-Bi-S-Se-Te SISTEMININ $SbBiTe_2Se$-$SbBiTe_2S$ FAZA DIAQRAMI

F.R.Əliyev[0000-0003- 1709-0164]
Azərbaycan Dövlət Neft və Sənaye Universiteti
fariz_ar@hotmail.com

Rentgen-faza analizi (RFA) və diferensial termiki analizindən (DTA) istifadə etməklə $SbBiTe_2Se$ – $SbBiTe_2S$ kəsiyinin faza tarazlığı öyrənilmiş və onun T-x diaqramı qurulmuşdur. Hər iki ilkin fazanın temperatur diapazonunda əriməsi səbəbindən sistem qeyri-kvazibinar hesab olunur. Sistem, solidusdan aşağıda stabil olub tetradimitəbənzər heksoqonal quruluşa malik fasiləsiz bərk məhlulun (α-faza) əmələ gəlməsi ilə xarakterizə olunur. Tetradimit və digər tetradimitəbənzər birləşmələrin struktur xüsusiyyətlərinin təhlili göstərir ki, paketin bütün təbəqələrində atomların oxşar atomlarla əvəzlənməsi mümkündür. Bu işdə mərkəzi təbəqədəki kükürd atomları asanlıqla selen atomları ilə əvəz edilə bilər. Bu tendensiya Bi-Sb-Te-Se-S sistemində kation və anion mövqelərdə əvəzlənmələrin həyata keçirildiyi kompozisiyalar diapazonunun formalaşmasını gözləməyə imkan verir. Qəfəs parametrləri toz nümunələrinin rentgen-faza analizi nəticələri əsasında müəyyən edilmişdir. Müəyyən edilmişdir ki, bərk məhlulun kristal qəfəs parametrləri Veqards qaydasına uyğun olaraq tərkibdən xətti asılıdır.

Açar sözlər: *$SbBiTe_2Se$ – $SbBiTe_2S$ sistemi, faza diaqramı, tetradimitəbənzər qurulus, bərk məhlullar, yüksək entropiyalı ərintilər.*

AJCN, Vol 4, No.1 2022, pp. 13-20

https://doi.org/10.32010/AJCN05012022-13

UDC:*54-76; 543.51; 543.06*

ECOLOGİCAL FEATURES OF THE PHOTOCHEMİCAL PROPERTİES OF $TİO_2$ NANOPARTİCLES

E.M.Gadirova [0000-0002-1302-8227]
Baku State University
elmina2010@mail.ru

TiO_2 nanoparticles have recently been widely used in environmentally important reactions.TiO_2 particles have been studied by XRD, TEM, SEM analysis. It has been determined that the size of nanoparticles is homogeneous and generally varies between 10-30 nm.The results were consistent with the calculations by the Sherrer method. The results of the SEM analysis were the same as the XRD analysis.In the XRD spectra of TiO_2 nanoparticles, the points at all peaks were accurately checked and the TiO_2 nanoparticles matched the rutile phase.According to the Scherrer method, the average size of TiO_2 according to the diffraction point (101) was 10.3, the specific surface area of the crystals was 159.6 m^2/g.The signals for TiO_2 nanoparticles had characteristic peaks at 27.90° (110), 36.01° (101), 41.58°(111), and 54.71°(211).

***Keywords**: XRD, SEM, TEM, nano-TiO_2, photochemical reactions.*

INTRODUCTION

Phenol is a toxic substance in terms of toxicity belongs to class IV according to the degree of danger.It has a negative effect on the nervous system and a strong irritant and inflammatory effect. Inhalation of phenol vapors causes dizziness, headache, shortness of breath muffled sound. In the basins the maximum permeability of phenol is 0.001 mgL^{-1}.Due to the presence of OH-groups in phenol it mixes very well with water to form chlorine derivatives.Chlorinated compounds of phenol are more dangerous than phenol itself.In this regard the formation of such compounds in water poses a serious threat to flora and fauna.In addition to being an environmentally dangerous pollutant phenol also has a carcinogenic effect.Phenol is irritating: leads to tragic consequences for the human body through the food chain.

Complete purification of phenol from water remains a global environmental problem.The reagents used for this must be durable and environmentally friendly. So far various physicochemical and biological methods have been used for cleaning.When using sorbents and chemical reagents these substances remain in the water and they are difficult to clean.Industrial wastewater treatment is especially difficult [1].Therefore modern methods must be developed that use very small amounts of chemical reagents and are environmentally friendly.From this point of view using TiO_2 nanoparticles phenol was purified from wastewater by nanotechnological methods and important results were obtained from the ecological point of view. For this purpose TiO_2 nanoparticles with rutile phase were used.Since TiO_2 nanoparticles are environmentally friendly and a very good photocatalyst their usability is increasing.

One of the destructive methods is the process of photochemical oxidation in which light is always used to carry out the process.The process of using light rays to carry out reactions is both efficient and energy-efficient.Therefore such reactions have recently become very relevant in the fields of chemistry and ecology

[2].Transformations in photochemical processes occur not on the basis of the absorption of light energy by the reactants involved in the reaction, but on the basis of the absorption of energy by the photocatalyst; the photocatalyst is reduced in the process after chemical transformations.Based on this the decomposition of any organic toxic substances occurs in the solution [3].

Rutile modification of TiO_2 is semiconductor; at this time the boundary zone was 3.20 and 3.02 eB. The role of oxygen in the photochemical process is the formation of active oxygen-retaining particles, which in turn lead to the oxidation process.Such particles are in water, for example; interacts with phenol molecules to oxidize it.The effect of metal ions (Ag, Au) on the structure of TiO_2 leads to a reduction of the boundary zone which causes TiO_2 to undergo photochemical reactions in the visible light rather than in the presence of UV radiation.In addition in the TiO_2 photocatalyst the bond energy between Ti-O is greater than the bond energy between Ti-N and therefore the reactions with TiO_2 occur mainly under UV radiation.When Ti-O is replaced by Ti-N the reactions can move from the UV radiation field to another visible field.For this purpose the process in Ti-N systems is considered more expedient.However this poses a challenge as it is very difficult to obtain Ti-N compounds.Recently air nitrogen has been used in the process along with TiO_2 nanoparticles based on UV radiation [4].

It is known from the literature that the process of photochemical decomposition of phenol is carried out in the presence of various substances [5].The reduction of fresh water resources in the world and the increase in the volume of wastewater are increasing the demand for clean water.In this regard effective water treatment methods using nanotechnological methods are becoming more widespread.

EXPERIMENTAL PART

Many properties for nano-TiO_2 have been studied. The physicochemical parameters of TiO_2 were analyzed according to the existing definitions and it was determined that it has a rutile phase.SEM, TEM, XRD analyzes of TiO_2 nanoparticles used in the course of ecologically important reactions as well as in the conduct of photochemical reactions were studied.The size of TiO_2 nanoparticles was homogeneous and ranged from 10 to 30 nm.The results of the TEM analysis were consistent with the XRD results.These analyzes were performed with the support of Baku State University's Nano Research Laboratory.

RESULTS AND DISCUSSION

SEM analysis of TiO_2 nanoparticles in the process was performed on JEOL JSM-7600F (15kV voltage, SEI mode). TEM, XRD analysis of TiO_2 particles are shown in the following figures.

The absorption and irradiance of TiO_2 nanoparticles with rutile phase drawn on a spectrophotometer called Specord-250 are shown below [6]. XRD analysis was performed at room temperature on a Rigaku Mini Flex 600 diffractometer. In all cases Cu K radiation was used in the Cu X-ray tube (operating at 15mA and 30kV).Samples were scanned at 20-70 Bragg angle. Based on the XRD spectra of TiO_2 nanoparticles the points at all peaks were sensitized and the TiO_2 nanoparticles were matched to the rutile phase.According to the Scherrer method the average size of TiO_2 according to the diffraction point (101) was 10.3, the specific surface area of the crystals was 159.6

m^2/g.Signals for TiO_2 nanoparticles it had characteristic peaks at 27.90° (110), 36.01° (101) , 41.58° (111) and 54.71°(211).

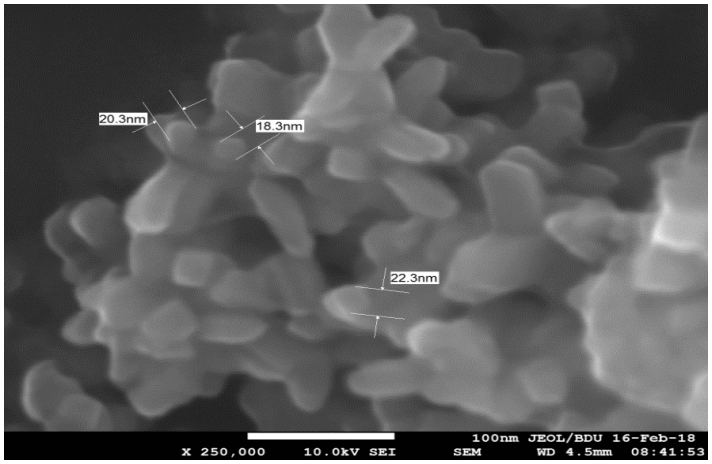

Fig.1. SEM view for TiO2 nanoparticles with rutile phase

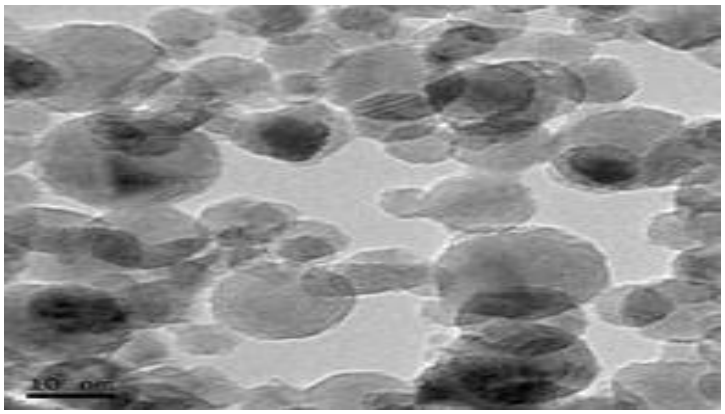

Fig.2.TEM view for TiO_2 nanoparticles

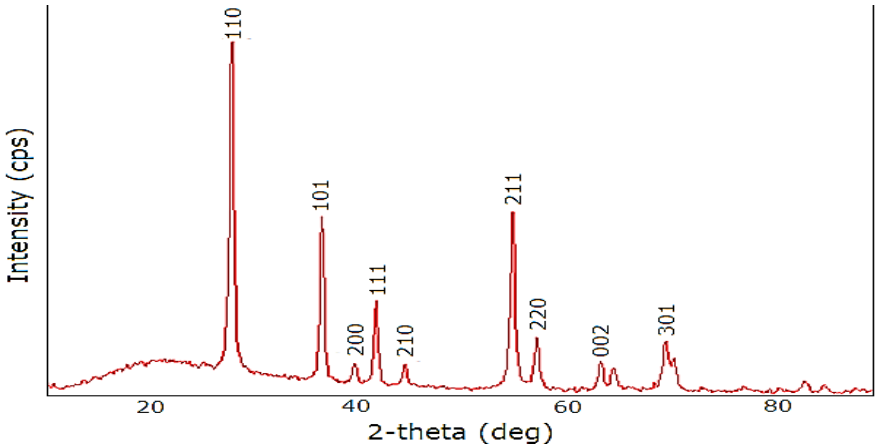

Fig.3. XRD analysis for TiO_2 nanoparticles with rutile phase

ISNN: print 2663-7006; online 2709-2666

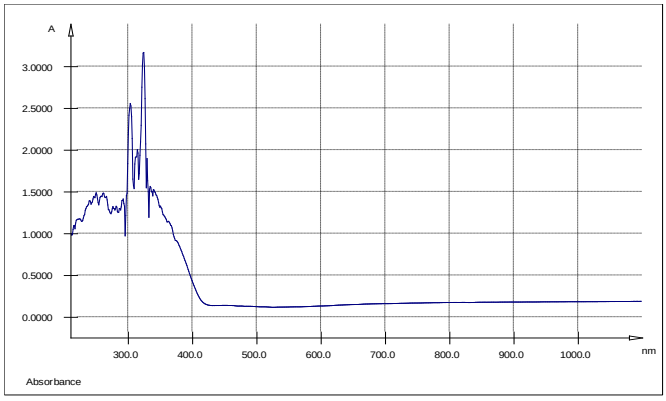

Fig.4. Light absorption of TiO_2 nanoparticles with rutile phase

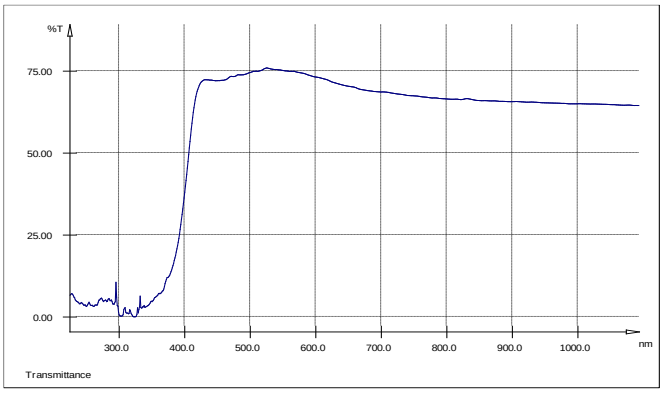

Fig.5. Emission of TiO_2 nanoparticles with rutile phase

As can be seen from Figures 4 and 5 the highest peaks for TiO_2 were obtained at 300-350 nm wavelengths after UV irradiation of TiO_2 nanoparticles.Starting from this wavelength (350 nm) the emission of the UV spectrum increases sharply in the upper figures [7].Figure 6 shows the dependence of the wavelength of light absorption of a solution of TiO_2 nanoparticles on an S-150 monochromator.

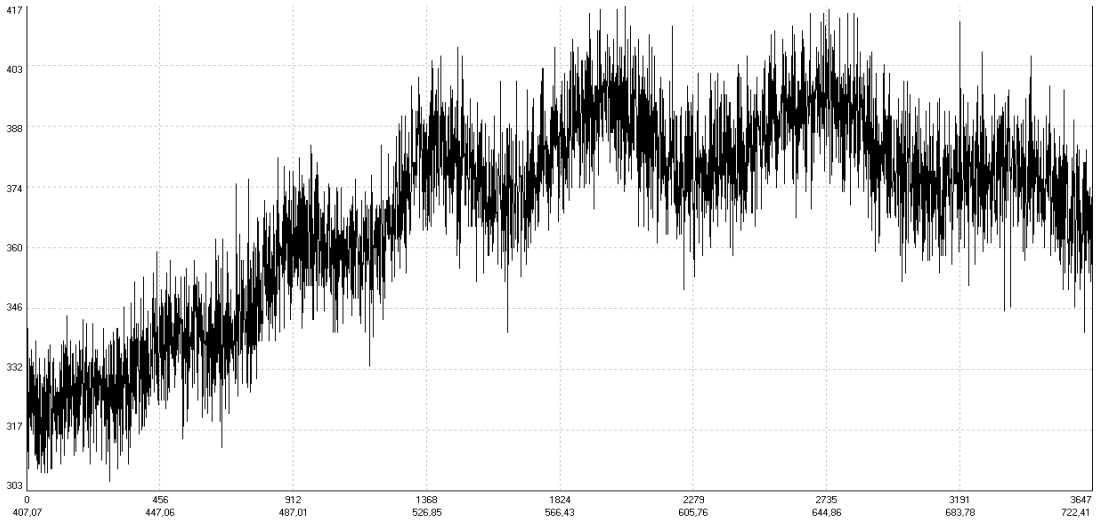

Fig.6. View of the wavelength dependence of light absorption of TiO_2 nanoparticles

The sizes of TiO_2 nanoparticles used in the process ranged from 10 to 30 nm.The wavelength dependence of the light absorption of hollow quartz glass used in the photochemical process and then quartz glass with TiO_2 nanoparticles.In the photochemical process the wavelength dependence of the light absorption of phenol+ TiO_2 and phenol + N/TiO_2 systems with the S-150 device is also shown [8,9].Compared to empty quartz glass with glass containing TiO_2 and chemicals the latter had more light absorption at different intensities than empty glass [10,11].

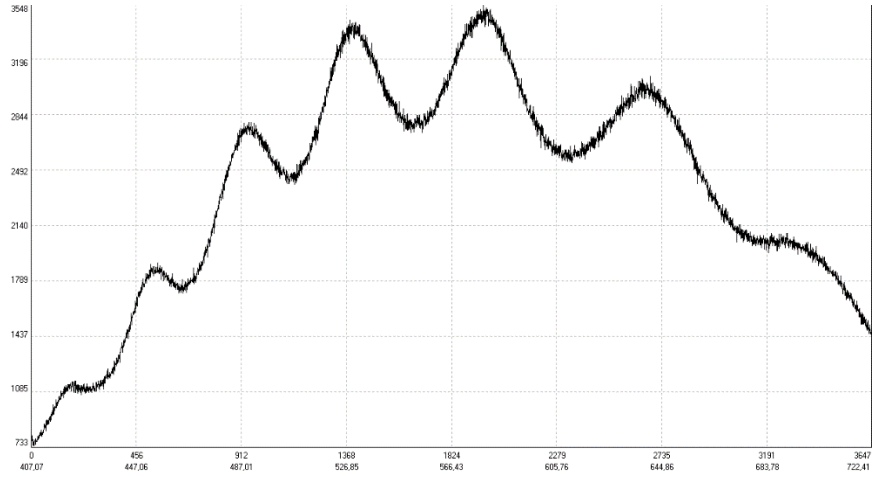

Fig.7. Wavelength dependence of light absorption of empty quartz glass

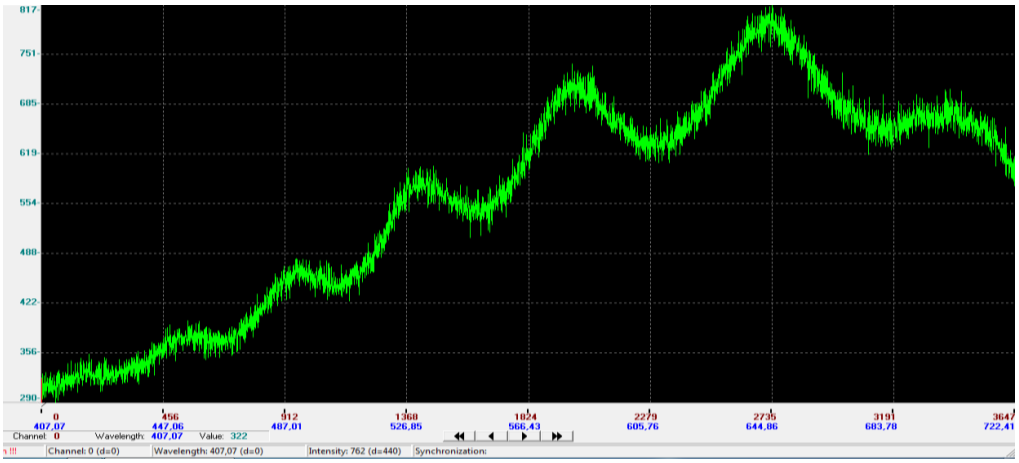

Fig.8. Wavelength dependence of light absorption of phenol + N/TiO_2 system

As can be seen in figures 7-9 the light absorption of the solution was intense in the UV-irradiated area up to 400nm for the phenol+TiO_2 mixture while the light absorption of the phenol+N/TiO_2 mixture covered the area after 400 nm. Photochemical decomposition of phenol in the presence of TiO_2 is already known from the literature [12].

However photochemical processes involving TiO_2 nanoparticles with a complete rutile phase have been studied for the first time [13]. Mathematical models of the processes were also developed. Mathematical modeling was carried out by exponential and logistic methods [14].

ISNN: print 2663-7006; online 2709-2666

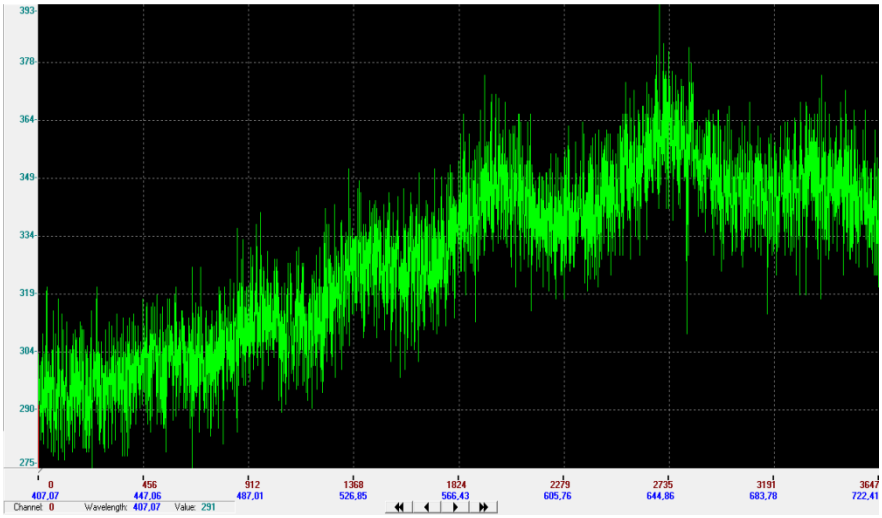

Fig.9. Wavelength dependence of light absorption of phenol + TiO_2 system

CONCLUSION

1. Thus one of the key issues was the development of new methods for the photochemical treatment of wastewater using nanotechnological methods to ensure environmental safety. Rutile phase TiO_2 nanoparticles were used as photochemical catalysts and for this purpose the photochemical properties of nanoparticles were studied.The sizes of TiO_2 nanoparticles used in the process ranged from 10 to 30 nm.

2. TiO_2 nanoparticles have been studied by XRD, SEM, TEM analysis and light absorption and radiation properties have also been studied.The average size of TiO_2 nanoparticles with rutile phase was 10.3nm, the specific surface area of the crystals was 159.6m^2/g.

REFERENCES

1. Hajiyeva S.R.,Gadirova E.M.,Ozdemir N.,Rustamova U.N. Oil Refinery Wastewater and Environmental Assessment//Baku: Processes of Petrochemistry and Oil Refining.2021, Vol.22, №.4, pp.457-467. ISSN:1726-4685
2. Gadirova E.M. Cleaning of phenol from wastewater with TiO_2 nanoparticles // 3rd International UNIDOKAP Black Sea Symposium “Sustainable Agriculture and Environment”, Tokat:21-23 June,2019, pp.10
3. Gadirova E.M. Photochemical degradation of phenol in the presence of titanium dioxide nanoparticles//Actual problems of ecology and soil science in the XXI century, materials of the VIII Republican scientific conference. Baku 2019, BSU, may 3-4, pp.45-46
4. Laoufi A.N., Djilali Tassalit, Fatiha Bentahar.The degradation of phenol in water solution by TiO_2 photocatalysis in a helical reactor//Global Nest Journal,2008,Vol 10,(3),pp.404-418. ISSN: 17907632
5. Lodha S., Vaya, D., Ameta, R.,etc. Photocatalytic degradation of phenol red using complexes of some transition metals and hydrogen peroxide // J. Serb. Chem. Soc.2008,73,pp.631-639

6. Hajiyeva S.R.,Gadirova E.M. Photochemical reactions in the participation of TiO_2 nanoparticles and methyl 3-aminocrotonate// Actual problems of ecology and soil sciences in the XXI century;materials of the VIII Republican scientific conference,-Baku:-2019,BSU,3-4 may,pp.88-89
7. Gadirova E.M. Photochemical degradation of phenol in the presence of titanium dioxide nanoparticles//Actual problems of ecology and soil sciences in the XXI century,materials of theVIII Republican scientific conference.Baku BSU,3-4 may, 2019, pp.45-46
8. Gadirova Elmina,Hajiyeva Sevinj, Sujayev Afsun. Investigation of photocatalytic properties of TiO_2 nanoparticles belonging to rutile phase //Journal of Molecular Structure.Amsterdam, Elsevierç,2021, Vol.1227, doı.org/10.1016.j/molstruc,129534.
9. Gadirova E.M.Photochemical reactions occurring in UV-visible area//Tadqiqot uz, Alchemist.Tashkent:2019, pp.3-8, doı.org/10.1016.j/molstruc,129534.
10. Hagfeldt A.and Gratzel M. Light-induced redox reactions in nanocrystalline systems//Chem. Rev.1995, 95, pp.49-68
11. Yoong L.S. Development of copper-doped TiO_2 photocatalyst for hydrogen production under visible light/Yoong L.S., Chong F.K., Binay K.and Dutta L.S.// Energy,2009, Vol. 34, pp.1652-1661
12. Gadirova E.M.Photochemical degradation of phenol in the presence of titanium dioxide nanoparticles//Applied chemistry and biotechnology,2019,9(2), pp.176-182
13. Laoufi A.N.The degradation of phenol in water solution by TiO_2 photocatalysis in a helical reactor/A.N.Laoufi, Djilali Tassalit, Fatiha Bentahar// Global Nest Journal, 2008, Vol 10, (3), pp.404-418
14. Weir M.D.,Giordano, F.R., Fox, W.P. Mathematical modelling, 2003,pp.14-17

ЭКОЛОГИЧЕСКИЕ ОСОБЕННОСТИ ФОТОХИМИЧЕСКИХ СВОЙСТВ НАНОЧАСТИЦ TİO$_2$

Э.М.Кадырова[0000-0002-1302-8227]
Бакинский Государственный Университет
elmina2010@mail.ru

Наночастицы TiO_2 в последнее время широко используются в экологически важных реакциях. Наночастицы TiO_2 изучались с помощью рентгеноструктурного анализа, ПЭМ и СЭМ. Установлено, что размер наночастиц однороден и обычно колеблется в пределах 10-30 нм.Результаты СЭМ-анализа были такими же, как и рентгенодифракционный анализ.В рентгенодифракционных спектрах наночастиц TiO_2 были точно проверены точки на всех пиках и наночастицы TiO_2 соответствовали фазе рутила.Согласно методу Шеррера,средний размер TiO_2 по точке(101) был 10,3,а удельная поверхность наночастиц составил 159,6 м^2/г. Сигналы наночастиц TiO_2 имели характерные пики при 27,90° (110), 36,01° (101), 41,58° (111) и 54,71° (211).

Ключевые слова: *СЭМ, ПЭМ, нано-TiO_2, рентгеноструктурный анализ, фотохимические реакции.*

ISNN: print 2663-7006; online 2709-2666

TiO_2 NANOHİSSƏCİKLƏRİNİN FOTOKİMYƏVİ XASSƏLƏRİNİN EKOLOJİ XÜSUSİYYƏTLƏRİ

E.M.Qədirova[0000-0002-1302-8227]
Bakı Dövlət Universiteti
elmina2010@mail.ru

Son zamanlar TiO_2 nanohissəcikləri ekoloji cəhətdən əhəmiyyətli reaksiyalarda geniş istifadə edilmişdir. TiO_2 hissəcikləri XRD, TEM, SEM analizləri ilə tədqiq edilmişdir. Müəyyən edilmişdir ki,nanohissəciklərin ölçüləri homogendir və10-30 nm arasında dəyişir.SEM analizinin nəticələri XRD analizinin nəticələri ilə eyni olmuşdur.TiO_2 nanohissəciklərinin XRD spektrlərində bütün zirvələrdəki nöqtələr dəqiqliklə yoxlanılmış və TiO_2 nanohissəcikləri rutil fazaya uyğun gəlmişdir.Şerrer metoduna əsasən (101)difraksiya nöqtəsinə əsasən TiO_2-nin orta ölçüsü 10,3, nanohissəciklərin xüsusi səth sahəsi 159,6 m^2/q təşkil etmişdir.TiO_2nanohissəcikləri üçün xarakterik siqnallar 27,90° (110), 36,01° (101), 41,58° (111) və 54,71° (211) zirvələrdə müəyyən edilmişdir.

Açar sözlər: *SEM, TEM, nano-TiO_2, XRD, fotokimyəvi reaksiyalar.*

AJCN, Vol 4, No. 1, 2022, pp. 21-31

https://doi.org/10.32010/AJCN05012022-21

UDC:666.965.2

RESEARCH OF WATER ABSORPTION OF GEOCONCRETES ON BASIS OF WASTE OF IRON ORE ENRICHMENT AND BOTTOM ASH

Y.N.Gahramanli [0000-0002-1041-7227], M.I.Aliyeva[0000-0001-76269-4457], M.R.Mikailova[0000-0002-0009-8779], G.Sh.Adgozalova[0000-0002-8466-6277]
Azerbaijan State Oil and Industry University
y.gahramanli@asoiu.edu.az

Specimens of geopolymeric concrete on basis of waste of iron ore enrichment of Dashkesan's deposit and bottom ash of combustion of domestic waste were obtained. Herewith ratio of waste mixture to binder made up 80:20. At obtaining of geoconcrete specimens the concentration of bottom ash in waste mixture was variated in limits of 10-50%wt. Normality of water solution of alkali activator was variated from 1N up to 8N. Maximal values of water absorption of geoconcrete specimens containing 10, 20, 30, 40 and 50%wt of bottom ash correspondingly made up 9,9, 12,3, 11,9, 12,8 and 16%.
Keywords: *geopolymeric concrete, enrichment waste, iron ore, bottom ash, water absorption.*

INTRODUCTION

The continuous increasing of the world population and need for more buildings increase demand for building materials. The conventional Portland cement is among them. Portland cement is the most widely used material due to its low cost, wide abundance and binding properties. World production of Portland cement is estimated more than 4 billion metric tons annually and its world consumption can reach 200% till 2050 year [1].

However, manufacturing of Portland cement is related to emission of huge amounts of carbon dioxide during obtaining of clinker [2]. International Energy Agency reported that these emissions of carbon dioxide make up 6-7% from world emissions of this gas [3]. Therefore, with the aim of decreasing of environmental pollution many researchers offered to use new hydraulic binders for substitution of conventional Portland cement. Among these binders the geopolymeric concretes became more attractive due to their characteristics [4]. Geopolymeric concretes or inorganic polymers are synthesized using several types of raw materials. These are mainly metakaolin and bottom ash [5]. Hence, researchers recently began to use other solid anthropogenic waste such as waste of mineral resource industry due to limitedness of resources of metakaolin and bottom ash [6]. Mineral resource industry and processes of ores enrichment generate huge amount of dry waste or by-products which are mainly barren rocks, waste, slugs, ashes and sludges [7]. There are several environmental problems related to utilization of these waste. These are physical instability and leaching of heavy metals which lead to contamination of rivers and lakes [8]. Mineral resource industry is an important part of economic development of any country. However, growing of the mining waste makes one of the greatest issues in the world. This is a problem of utilization of waste of mineral resource industry [9].

Thus, they must be developed more efficient measures on management and reusing of waste of mineral resource industry. Thereupon, the review of literature indicates that different methods of reusing of waste of mineral resource industry can be

used for an obtaining of building materials. It is offered a using of mining waste as aggregates for preparation of concrete [10]. Other researchers offer to synthesize fired bricks from by-products of red clays [11]. Besides that, it is offered a using of coal mine waste for development of ecofriendly bricks [12]. Some researchers offered to use waste of mineral resource industry as a precursor in the synthesis of geopolymeric concretes which are considered as an alternative cementitious material. Such waste can be mixed with other aluminosilicate materials [13, 14]. They can also be used only as a precursor.

Since 50th years of the 20th century a production of iron ore was being conducted in Dashkesan region of Azerbaijan. As a result of which a huge amount of waste of barren rocks and waste of magnetic separation of iron ore were accumulated on the production site. According to preliminary data, the amount of these waste make up several tens millions tons. In the same time great amount of bottom ash and slugs of combustion of domestic waste are accumulated on "Temiz Sheher" plant situated in Baku. Therefore, utilization of abovementioned waste is rather actual problem.

Thereupon, the aim of the given research is a studying of water absorption of geoconcrete specimens obtained on basis of waste of enrichment of Dashkesan's iron ore and bottom ash obtained by combustion of domestic waste.

EXPERIMENTAL PART

Materials on basis of waste of iron ore enrichment and bottom ash obtained by combustion of domestic waste were obtained. Waste of enrichment of iron ore had a following chemical composition (table l).

Table 1

Chemical composition of waste of iron ore enrichment

Na_2O	MgO	Al_2O_3	SiO_2	P_2O_5	SO_3	K_2O	CaO	TiO_2	MnO	Fe_2O_3	Cl^-
0,26	2,81	7,22	25,17	0,2	0,25	0,58	21,6	0,38	0,75	24,45	0,02

Alkali silicate corresponding to GOST 13078-81 was used as a binder. Sodium hydroxide (GOST 4328-77) was used for preparation of water solutions of alkali activator of setting process. Bottom ash corresponded to technical specifications AZ 1700914011-001-2013. Preparation of geoconcrete mixtures was carried out by way of a mixing of initial constituents. Herewith the ratio of waste:binder made up 80:20. Amount of bottom ash in the "waste of enrichment + bottom ash" mixture was variated from 10%wt up to 50%wt. The mixing of initial constituents was conducted at ambient temperature. After obtaining of pasty and homogeneous mixture the geoconcrete was filled into cylindrical form prepared beforehand. A forming process was conducted during a day. Then the hardened specimen of geoconcrete was extracted from the mold and was subjected to thermal processing at 80^0C during 16-20 hours.

Research of water absorption (W_M, %) of geoconcrete specimens was conducted by way of complete submersion of the specimen into water according to the GOST 12730.3-2020. Water absorption was calculated in accordance with formula:

$$W_M = \frac{m_w - m_d}{m_d} \cdot 100\%$$

where m_w – is a weight of wet specimen, g; m_d – is a weight of dry specimen, g.

Weighing of geoconcrete specimens was carried out by the use of "$KERN_{PLC}$" analytical balance with accuracy of 0,001g.

RESULTS AND DISCUSSION

As is known the capability to absorb water is one of properties of materials made from concrete. Knowledge in this field make it possible to define the areas and conditions of a using of concrete. Water absorption of concretes is studied at the expense of full submersion of specimen into water medium or of the partial submersion of specimen into water. The researches with full submersion of specimens of the geopolymeric concrete into water were conducted according to GOST 12730.3-2020. Tests were conducted at ambient temperature and water absorption was defined by gravimetric method. Specimens of geopolymeric concrete were obtained by geopolymerization. Herewith ratio of waste mixture to alkali silicate made up 80:20. Herewith the concentration of bottom ash in the mixture of waste was variated from 10% up to 50%wt. Concentration of alkali activator was changed from 1N up to 8N.

Results of the conducted experiments of geopolymeric concretes obtained from mixes containing 10%wt of bottom ash are represented in fig.1. Herewith the concentration of alkali activator was variated from 1N up to 8N. As follows from the figure, the water absorption of geopolymeric concrete rapidly increases within the first 5 minutes of the exposition in the water medium. At increasing of exposition time of the specimens up to 72 hours some decreasing of water absorption is observed. Then it is stabilized. Thus, in this case the water absorption which takes place within the first minutes of exposition can be considered as a desired water absorption. As follows from fig.1 all kinetic curves have a maximum which is reached within 5-10 minutes of exposition. It should be noted that at increasing of concentration of alkali activator from 1n up to 8n the maximal value of water absorption is decreased from 9,9% up to 7,3%.

Such decreasing of water absorption can be explained in the following way. As is known, a using of bottom ash which is a main binder in this case leads to a parallel behavior of a foaming process and to a forming a pore structure. Presence of aluminum in the initial waste is a reason of a foaming process. At low content of alkali activator and at low concentration of alkali in the solution of activator the setting process occurs slowly. Thus, a foaming process takes place in the less viscous medium. Increasing of concentration of alkali activator accelerates the process of increasing of viscosity of geoconcrete mix. Completeness of the material and its volume weight are increased as a result of viscosity increasing and at slow occurring of a foaming process. This circumstance is a reason of a decreasing of material porosity.

Decreasing of water absorption of the material at increasing of concentration of alkali activator can be explained by that. On the one hand it is clear from the figure that after reaching of maximum some decreasing of water absorption of the material occurs at increasing of exposition time. From our point of view, it occurs so-called seeming decreasing of water absorption. It is explained by that experiments were conducted by gravimetric method, that is, by way of a weighing of specimens' weight before and after exposition. It was established that at geopolymerizing of specimens the non-crystallized amorphous part of geoconcretes is washed away by water and passes into the solution during exposition. In the same time, it promotes loss of weight of specimen.

ISNN: print 2663-7006; online 2709-2666

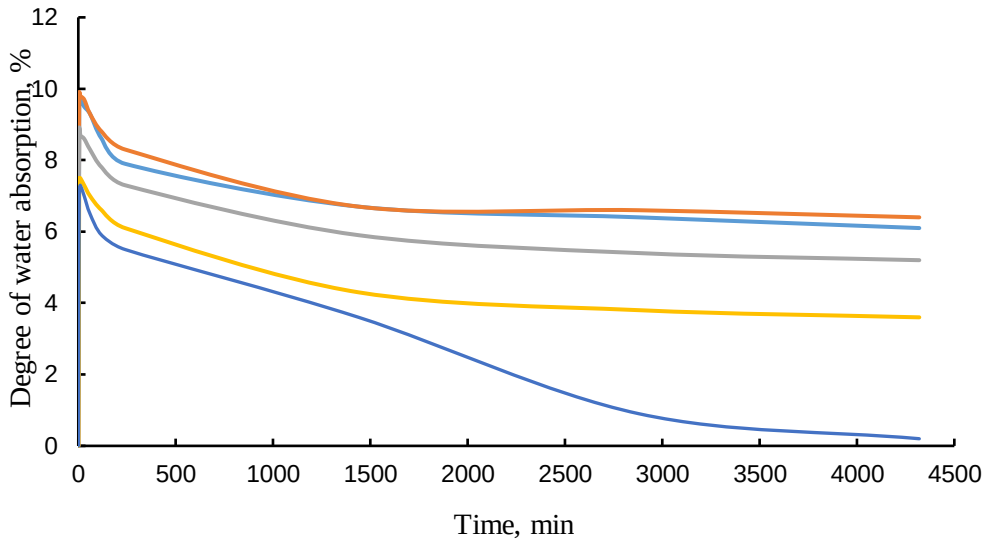

Fig.1. Kinetic curves of water absorption of geoconcrete specimens containing 10%wt. of bottom ash:
alkali concentration 1N; alkali concentration 2N; alkali concentration 3N; alkali concentration 5N; alkali concentration 8N.

It should be noted here, that at increasing of concentration of alkali activator a weight loss of specimen also rises and in accordance with fig.1 it achieves its maximal value at 8n concentration. The fact is that during geopolymerization an alkali activator acts as agent which dissolves and decomposes amorphous part of aluminosilicates contained both in bottom ash and in waste of iron ore enrichment. Low concentration of bottom ash and high content of alkali promote acceleration of setting process and lead to increasing of system's viscosity. Herewith due to rapid growth of viscosity and decreasing of lifetime of geoconcrete mass the crystallization process does not occur completely. This circumstance leads to increasing of amorphous part of geoconcrete and to increasing of washing away of mass by water. Therefore, using of high concentrations of alkali activator at low containing of bottom ash is unreasonable.

Researches of specimens containing of 20%wt of bottom ash were conducted. Research results are represented in fig.2. One can see from the figure that maximal value of water absorption is reached within the first 5-10 minutes of exposition. Then the exposition in water medium leads to some seeming decreasing of water absorption. This circumstance was explained above and is related to loss of weight of geoconcrete specimens. Thus, maximal value of water absorption is reached within the first several minutes of water exposition. Herewith increasing of concentration of alkali activator from 1N up to 3N is conducive to increasing of a water absorption as distinct from the case described in fig.1. Then the further increasing of concentration of alkali up to 8N only leads to decreasing of water absorption. Maximal value of water absorption takes place at normality of alkali solution equal 3. Such changing of water absorption can be explained. So, increasing of concentration of bottom ash up to 20%wt is conducive to increasing aluminum content. This in turn accelerates a foaming process of the material and forming of porous structure. The higher normality of solution of alkali activator, the faster a foaming process and the higher a porosity of the material.

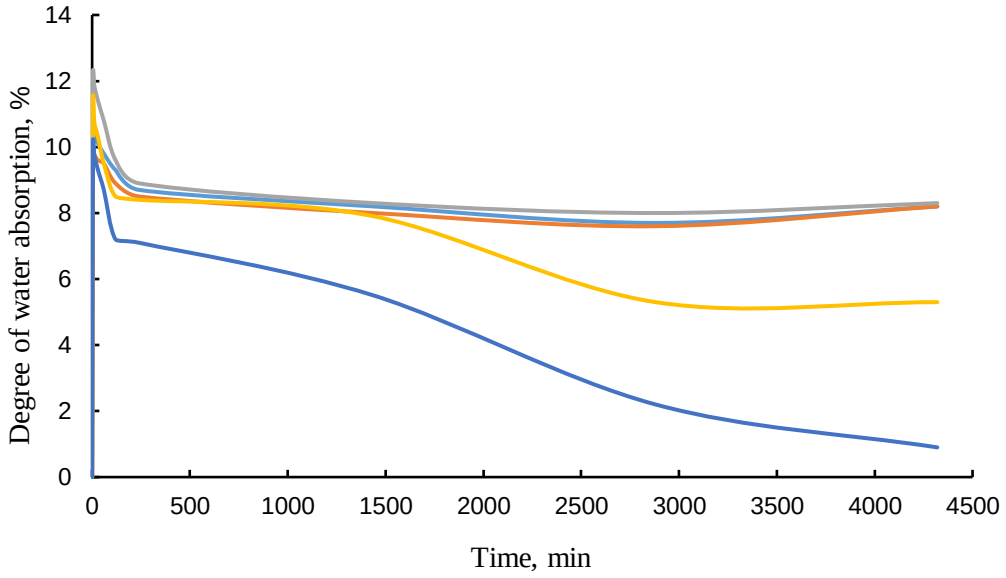

Fig.2. Kinetic curves of water absorption of geoconcrete specimens containing 20%wt. of bottom ash:
alkali concentration 1N; alkali concentration 2N; alkali concentration 3N; alkali concentration 5N; alkali concentration 8N.

A growth of water absorption as a result of increasing of alkali concentration is explained by this. However, a further increasing of alkali normality more than 3N leads to decreasing of water absorption. It is explained by that an increasing of solution normality of alkali activator accelerates a process of setting of the material, reducing a lifetime of geoconcrete mixture. Herewith viscosity of the system is increased with high rate. This circumstance impedes a forming of porous structure and leads to decreasing of water absorption. One can see that 72-hour exposition of specimens obtained at changing of concentration of alkali activator from 1n up to 3N is conducive to lesser mass loss due to reasons described above (see fig.2). An increasing of normality of alkali solution up to 8 leads to a rapid increasing of mass loss or to a seeming decreasing of water absorption. It should be noted here, that an increasing of bottom ash concentration from 10%wt up to 20%wt is conducive to some decreasing of mass loss as a result of wash-out of amorphous part by water. In this case in spite of excess of alkali the increasing of bottom ash concentration is conducive to more involvement of alkali in process of geopolymerization and destructive effect of the remaining excess of alkali, to a lesser extent, influences process of forming of crystal structure. That is, the crystallinity of the specimen is increased but volume of amorphous part is decreased.

Further it was studied water absorption of geoconcrete specimens containing 30%wt of bottom ash at different concentrations of alkali activator. Results of conducted experiments are represented in fig.3. As is shown in fig.3, maximal values of water absorption are reached during the first 5-10 minutes of exposition like in previous cases. Then the further exposition in water leads to some seeming decreasing of water absorption. It should be noted here, that specimens obtained by using of 1n solution of alkali activator were possessed by maximal resistance to effect of water and had the least mass loss.

ISNN: print 2663-7006; online 2709-2666

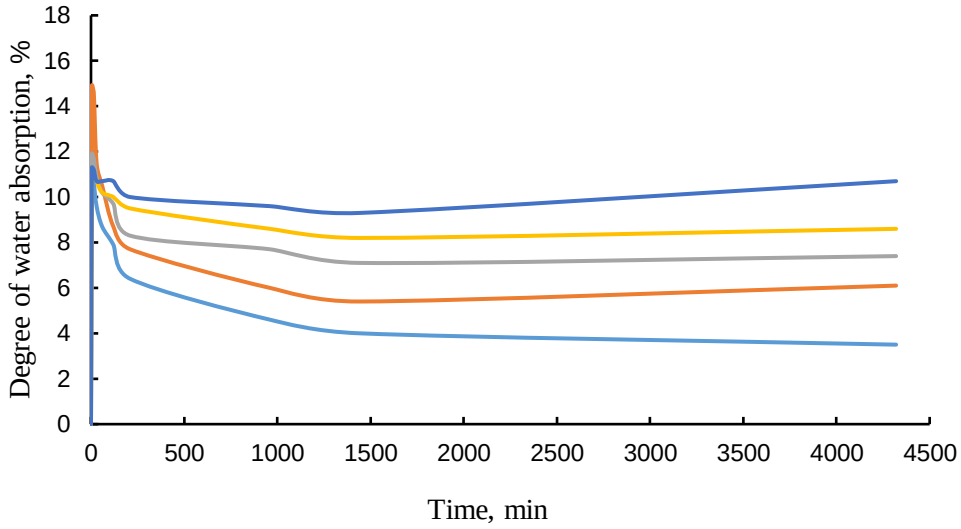

Fig.3. Kinetic curves of water absorption of geoconcrete specimens containing 30%wt. of bottom ash:
alkali concentration 1N alkali concentration 2N; alkali concentration 3N; alkali concentration 5N; alkali concentration 8N.

However, the further increasing of concentration of alkali activator leads to increasing of mass loss (see fig.3). Maximal increasing of mass loss is observed at increasing of normality of alkali solution up to 8N. It should be noted here, that an increasing of content of bottom ash from 10%wt up to 30%wt leads to decreasing of mass loss of specimens, even at normality of alkali solution equal 8. Such phenomenon is explained by that the increasing of concentration of bottom ash is conducive to the more involvement of alkali as an activator of dissolution and decomposition processes of amorphous part of aluminosilicates because bottom ash is their main source in the geoconcrete. In the same time, this circumstance reduces a destructive influence of alkali upon crystallization and gel forming processes. Herewith crystallization process occurs more completely and volume of amorphous phase is decreased. Thus, it occurs the decreasing of wash-out of amorphous phase by water and also the decreasing of mass loss. It should be also noted that the increasing of bottom ash concentration from 10%wt up to 30%wt leads to some intensification of a foaming process of geoconcrete mixture which occurs in parallel. It occurs due to increasing of aluminum concentration in geoconcrete mixture. Intensification of foaming leads to a forming more developed porous structure and correspondingly to the increasing of water absorption in comparison with cases represented in fig.1 and fiq.2. Herewith maximal value of water absorption is observed at normality of alkali solution equal 5. At 10% containing of bottom ash this maximum is observed at concentration 2N but 20% containing of bottom ash the maximum takes place at 3n concentration of alkali activator. Thus, at increasing of content of bottom ash the displacement of the maximal value of water absorption towards the higher concentrations of alkali activator is observed. This fact can be also explained. The point is that at increasing of content of bottom ash the concentration of aluminum added together with the ash is also increased. For the ensuring of maximal water absorption, the more foamed structure is necessary because a foaming process is directly related to quantity of added aluminum. Therefore, greater amount of alkali is necessary for more quantity of aluminum. Thus, greater amount of

bottom ash and correspondingly added aluminum is conducive to maximal foaming at higher concentrations of alkali activator. A more intensive foaming process gives more porous structure which is conducive to increasing of water absorption.

The further research was related to a studying of process of water absorption of geoconcrete specimens containing 40%wt of bottom ash. At conducting of researches a normality of alkali solution was changed from 1 up to 8. Results of conducted experiments are represented in fig.4. In accordance with the results represented in fig.4, maximal values of water absorption are reached during the first 5-10 minutes of exposition of specimens obtained from concrete mixtures containing alkali solution with normality 3, 5 and 8N. The further increasing of exposition leads to some seeming decreasing of water absorption. Herewith in this case a maximal value of water absorption is observed at studying of specimens obtained from mixtures containing alkali solution with normality 8N. It should be also noted here, that specimens obtained in the presence of alkali solution with normality 1 and 2 have a greater resistance to water influence. In comparison with cases described in fig.1, 2 and 3, in this case the mass loss is also observed. However, wash-out of amorphous phase occurs to a lesser extent. The important fact is that at exposing of specimens obtained in the presence of 1n solution of alkali activator the maximal value of water absorption takes place only during 30-minute exposition in water. This fact indicates that the given specimen has a rather dense and microporous structure. It impedes diffusion and flowing of water into deep layers of material, that is, it takes more time for that. Maximal water absorption of specimens obtained from geoconcrete mixtures containing alkali solution with normality 2N takes place at 10-minute exposition in water. This indicates some decreasing of material density and predominance of structure with relatively large pores.

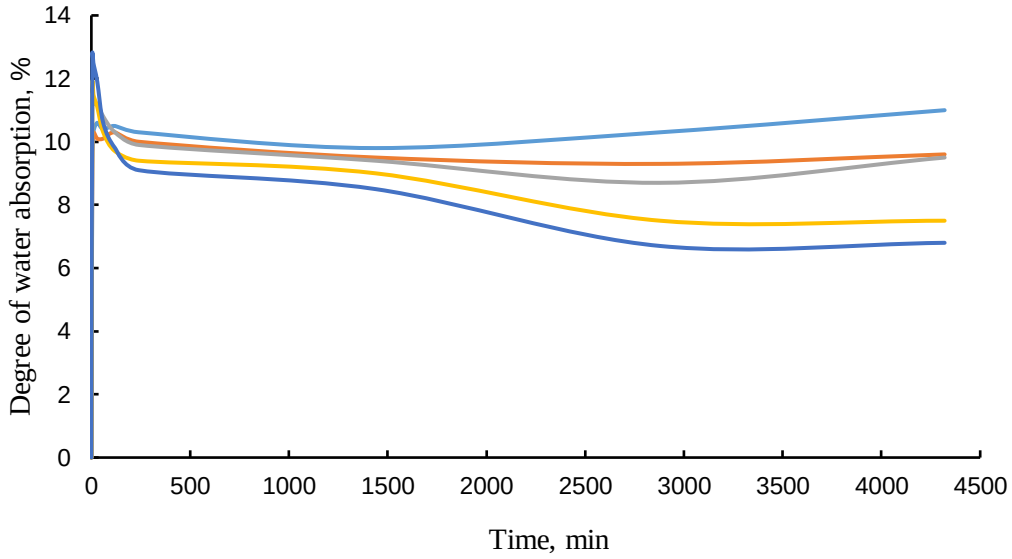

Fig.4. Kinetic curves of water absorption of geoconcrete specimens containing 40%wt. of bottom ash:
alkali concentration 1N; alkali concentration 2N; alkali concentration 3N;
alkali concentration 5N; alkali concentration 8N.

Then the conducted researches were devoted to a studying of water absorption of geoconcrete specimens containing 50%wt of bottom ash. As well as in previous cases the normality of alkali activator was variated within the limits of 1-8N. The results of

ISNN: print 2663-7006; online 2709-2666

conducted experiments are represented in fig.5.

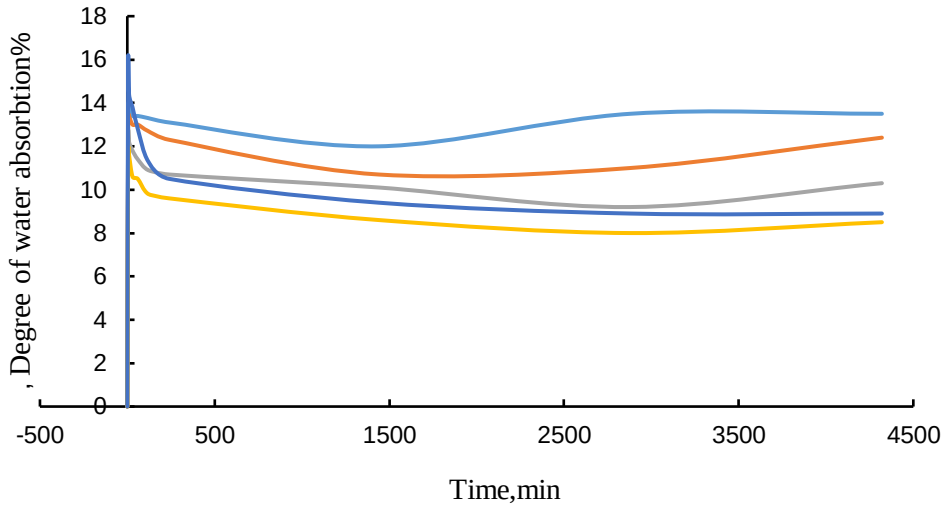

Fig.5. Kinetic curves of water absorption of geoconcrete specimens containing 50%wt. of bottom ash:
alkali concentration 1N; alkali concentration 2N; alkali concentration 3N; alkali concentration 5N; alkali concentration 8N.

Herewith one can see that the maximal values of water absorption are reached during the first 5-10 minutes of exposition. It should be noted that materials containing 50%wt of bottom ash have a relatively greater resistance to water influence than materials which contain 10, 20, 30 and 40%wt of bottom ash. In this case the presence of two maximums of water absorption are observed at 5-minute exposition of specimens obtained from geoconcrete mixtures containing alkali activator solutions with normality 1N and 8N. An appearing of such maximums is explained by the fact that at using of alkali activator with normality 1N a lifetime of geoconcrete mixture is more. Herewith a foaming process taking place in the geoconcrete mixture occurs more completely in spite of its low rate. This makes it possible to obtain a certain porous structure in the specimen. Presence of such porous structure is conducive to the increasing of water absorption. At increasing of normality of alkali activator solution from 2N up to 5N some compacting of the material occurs. This circumstance leads to some decreasing of water absorption. Such compacting of the material is explained by the fact that the increasing of concentration of alkali activator accelerates a process of setting of geoconcrete mixture and reduces its lifetime. Herewith viscosity of the system is rapidly increased and puts certain obstacles to forming a porous structure. This leads to decreasing of water absorption. The further rising of normality of alkali activator solution up to 8N leads to acceleration of a foaming process. In this case a rate of a foaming process is equalized with rate of setting process of geoconcrete mixture which occurs simultaneously. This makes it possible to reach a relatively high porosity of the material within short lifetime of geoconcrete mixture. Presence of the second maximum of water absorption for specimens obtained from geoconcrete mixtures containing alkali activator solution with normality of 8n is explained by that.

CONCLUSION

1.It is established that water absorption of geoconcrete specimens is reached its maximal value during the first 5-10 minutes of exposition.

2. Geoconcrete specimens containing in mixture of waste 10, 20, 30, 40 and 50%wt of bottom ash have maximal values of water absorption which correspondingly make up 9,9, 12,3, 11,9, 12,8 and 16%.

3. Geoconcrete specimens containing in the mixture of waste 10 and 20%wt of bottom ash are least resistant to influence of water.

4. Geoconcrete specimens containing in the mixture of waste 40 and 50%wt of bottom ash are most resistant to influence of water.

5. A using of solutions of alkali activator with normality of 8N is reasonable if containing of bottom ash in the mixture of waste makes up 40 and 50%wt.

REFERENCES

1. Huseien G.F., Mirza J., Ismail M., Ghoshal S.K., Hussein A.A. Geopolymer mortars as sustainable repair material: a comprehensive review. Renewable and Sustainable Energy Reviews. 2017, Vol. 80, pp.54–74. https://doi.org/10.1016/j.rser.2017.05.076
2. Schneider M., Romer M., Tschudin M., Bolio H. Sustainable cement production - present and future. Cement and Concrete Research.2011, Vol. 41 (7), pp. 642–650
3. Palomo A., Fernandez-Jimenez, A., Lopez-Hombrados C., Lleyda J.L. Railway sleepers made of alkali activated fly ash concrete. Revista Ingenieria de Construccion. 2007, Vol.22 (2), pp.75–80. https://doi.org/10.4067/S0718-50732007000200001
4. Duxson P., Provis J.L., Lukey G.C., Mallicoat S.W., Kriven W.M., Van Deventer J.S. Understanding the relationship between geopolymer composition, microstructure and mechanical properties. Colloids and Surface A. Physicochemical and Engineering Aspects. 2005, Vol.269 (1-3), pp.47–58. https://doi.org/10.1016/j.colsurfa.2005.06.060
5. Yip C.K., Provis J.L., Lukey G.C., Van Deventer J.S. Carbonate mineral addition to metakaolin-based geopolymers. Cement and Concrete Composites. 2008, Vol.30(10), pp.979–985. https://doi.org/10.1016/j.cemconcomp.2008.07.004
6. Ahmari S., Zhang L. Production of eco-friendly bricks from copper mine tailings through geopolymerization. Construction and Building Materials.2012, Vol.29, pp.323–331. https://doi.org/10.1016/j.conbuildmat.2011.10.048
7. Palmer M.A., Bernhardt E.S., Schlesinger W.H., Eshleman K.N. Foufoula-Georgiou E., Hendryx M.S., et al. Mountaintop mining consequences. Science. 2010, Vol.27 (5962), pp.148–149. https://doi.org/10.1126/science.1180543
8. Plumlee G.S., Morman S.A. Mine wastes and human health. Elements. 2011, Vol. 7 (6), pp.399–404. https://doi.org/10.2113/gselements.7.6.399
9. Tiruta-Barna L., Benetto E., Perrodin Y. Environmental impact and risk assessment of mineral wastes reuse strategies: review and critical analysis of approaches and applications. Resources, Conservation and Recycling.2007, Vol. 50, Issue 4, pp. 351–379. https://doi.org/10.1016/j.resconrec.2007.01.009
10. El Machi A., Mabroum S., Taha Y., Tagnit-Hamou A., Benzaazoua M., Hakkou R., 2020. Valorization of phosphate mine waste rocks as aggregates for concrete.

ISNN: print 2663-7006; online 2709-2666

Materials Today: Proceedings. 2011, Vol. 37, Part 3, pp.3840-3846 https://doi.org/10.1016/j.matpr.2020.08.404
11. Loutou M., Taha Y., Benzaazoua M., Daafi Y., Hakkou R. Valorization of clay byproduct from moroccan phosphate mines for the production of fired bricks. Journal of Cleaner Production.2019, Vol. 229, pp.169-179. https://doi.org/10.1016/j.jclepro.2019.05.003
12. Taha Y., Benzaazoua M., Hakkou R., Mansori M. Coal mine wastes recycling for coal recovery and eco-friendly bricks production. Minerals Engineering. 2017,Vol. 107, pp.123–138. https://doi.org/10.1016/j.mineng.2016.09.001
13. Kiventera J., Golek L., Yliniemi J., Ferreira V., Deja J., Illikainen M. Utilization of sulphidic tailings from gold mine as a raw material in geopolymerization. International Journal of Mineral Processing.2016, Vol. 149, pp.104–110. https://doi.org/10.1016/j.minpro.2016.02.012
14. Mabroum S., Aboulayt A., Taha Y., Benzaazoua M., Semlal N., Hakkou R., 2020. Elaboration of geopolymers based on clays by-products from phosphate mines for construction applications. Journal of Cleaner Production. 2020, Vol. 261, 121317.https://doi.org/10.1016/j.jclepro.2020.121317

ИССЛЕДОВАНИЕ ВОДОПОГЛОЩЕНИЯ ГЕОБЕТОНОВ НА ОСНОВЕ ОТХОДОВ ОБОГАЩЕНИЯ ЖЕЛЕЗНОЙ РУДЫ И ЗОЛЬНОГО ОСТАТКА

Ю.Н.Кахраманлы [0000-0002-1041-7227], М.И.Алиева[0000-0001-76269-4457],
М.Р.Микаилова[0000-0002-0009-8779], Г.Ш.Адгезалова[0000-0002-8466-6277]
Азербайджанский Государственный Университет Нефти и Промышленности
y.gahramanli@asoiu.edu.az

Были получены образцы геобетона на основе отходов обогащения железной руды Дашкесанского месторождения и зольных остатков сжигания бытовых отходов. При этом соотношение смеси отходов к связующему компоненту составляло 80:20. При получении образцов геобетонов содержание щелочного активатора твердения варьировалось в пределах 10-50%масс. Нормальность водного раствора щелочного активатора варьировалась в пределах 1-8N. Максимальные значения водопоглощения образцов геобетона содержащих 10, 20, 30, 40 и 50%масс. зольного остатка соответственно составили 9,7; 11,5; 14,9; 12,5 и 14,4%.
Ключевые слова: *геополимерный бетон, отходы обогащения, железная руда, зольный остаток, водопоглощение.*

DƏMİR FİLİZİNİN ZƏNGİNLƏŞMƏSİ TULLANTILARI VƏ KÜL QALIQLARI ƏSASINDA OLAN GEOBETONLARIN SU UDMA DƏRƏCƏSİNİN TƏDQİQİ

Y.N.Qəhrəmanlı[0000-0002-1041-722],M.İ.Əliyeva[0000-0001-76269-4457],
M.R.Mikayılova[0000-0002-0009-8779], G.Ş.Adgözəlova[0000-0002-8466-6277]
Azərbaycan Dövlət Neft və Sənaye Universiteti
y.gahramanli@asoiu.edu.az

Daşkəsən yatağının dəmir filizinin zənginləşməsi tullantıları və məişət tullantıların yandırılmasının kül qalıqları əsasında geobeton nümunələri alınmışdır. Tullantılar qarışığının əlaqələndirici komponentə olan nisbəti 80:20 təşkil etmişdir. Geobeton nümunələrinin alınması

zamanı bərkimənin qələvi aktivatorunun miqdarı 10-50%küt hədlərində dəyişirdi. Qələvi aktivatorunun sulu məhlulunun normallığı 1-8N hədlərində saxlanılırdı. Tərkibində 10, 20, 30, 40 və 50%küt kül qalığı olan geobeton nümunələrinin su udma dərəcəsinin maksimal qiymətləri uyğun olaraq 9,7; 11,5; 14,9; 12,5 və 14,4% təşkil etmişdir.
Açar sözlər: *geopolimerli beton, zənginləşdirmə tullantıları, dəmir filizi, kül qalığı, su udma dərəcəsi.*

ISNN: print 2663-7006; online 2709-2666

AJCN, Vol 4, No 1, 2022, pp. 32-41

https://doi.org/10.32010/AJCN05012022-32

UDC:541.183

THE STUDY OF HEAVY METAL ION SORPTION KINETICS

E.S.Karimova [0000-0001-7577-2900]
Baku State Universitet
elladakarimova1903@gmail.com

Phosphorus-containing polymeric sorbent based on butadiene-styrene rubber was used to remove zinc, iron and chromium ions from water. The research was carried out to study the sorption characteristics by determining the effects of various parameters, such as the pH of the solution, the initial concentration of metal ions, the sorbent mass, the phase contact time, and temperature. The regularities of the kinetics of the sorption of zinc, iron and chromium ions on the phosphorus-containing sorbent synthesized on the basis of butadiene-styrene rubber were studied. On the basis of the results it was defined that the process of sorption of zinc, iron and chromium ions on the cation exchanger proceeds by an ion-exchange mechanism. The kinetics of this process is a combination of external and internal diffusion kinetics (with some predominance of external diffusion kinetics) and is better described by the pseudo-second order reaction model. In addition, a certain contribution to the overall speed of the process is made by the interaction of the sorbed ions with the functional groups of the cation exchanger.
***Keywords**: phosphorus-containing cation exchanger, zinc, iron, chromium, sorption, kinetics.*

INTRODUCTION

It is necessary to use complex-forming ion exchangers, which possess high affinity for polyvalent and heavy metals in order to solve technological problems associated with obtaining high-purity substances in the processes of separation, recovery, concentration of rare and non-ferrous metals. Such compounds include phosphorus-containing cation exchangers with phosphoric acid groups [1, 2].

The aim of this work was to study the effectiveness of phosphorus-containing sorbent based on butadiene-styrene rubber of the DSKK grade, used to remove Zn(II), Fe(III) and Cr(III) ions from aqueous solutions. The method of synthesis of phosphorus-containing sorbent by chemical modification (oxidative chlorophosphorylation reaction) of industrial polymer - butadiene-styrene rubber was developed by our scientists and described earlier [3-5]. It was found that this reaction proceeds using readily available commercial reagents under mild conditions and using simple equipment. This paper presents the influence of various parameters, such as the concentration of the initial Zn(II), Fe(III) and Cr(III) solution, the pH of the solution, the sorbent mass, contact time and temperature.

The study of sorption kinetics makes it possible to determine the rate of attainment of equilibrium, the maximum working capacity of an ion exchanger for a certain solution composition, and the mechanism of interaction of metal ions with ion exchanger during sorption.

EXPERIMENTAL PART

The modified butadiene-styrene rubber was used as the sorbent for studying the sorption behavior of Zn(II), Fe(III) and Cr(III) ions in aqueous solution. Phosphorus-

containing sorbent was synthesized on the basis of butadiene-styrene rubber using PCl_3, CCl_4, H_2SO_4 and O_2. Butadiene-styrene rubber was purchased from the Voronezh Synthetic Rubber Manufactory (Russia). PCl_3, CCl_4, H_2SO_4 were purchased from Vecton (Russia) and used without further purification. The working solutions of zinc sulfate were prepared by dissolving a sample of $ZnSO_4 \times 7H_2O$ in an appropriate amount of distilled water. The ferric chloride working solution was prepared by dissolving the $FeCl_3 \times 6H_2O$ sample in an appropriate amount of distilled water. The working solutions of chromium nitrate were prepared by dissolving a sample of $Cr(NO_3)_3$ in an appropriate amount of distilled water. The pH value in the solution was established using an acetate-ammonia buffer solution.

The concentrations of $ZnSO_4 \times 7H_2O$, $FeCl_3 \times 6H_2O$ before and after sorption were determined using a photometric colorimeter with an optical density determination at a wavelength of 490 nm. The concentrations of $Cr(NO_3)_3$ before and after sorption were established using an ISP MS 7700e mass spectrometer.

Preliminary experiments began with the aim of studying the effect of the pH of the solution, sorbent mass, contact time, temperature and the initial concentration of metal ions on the sorption of Zn(II), Fe(III) and Cr(III) ions by a phosphorus-containing sorbent. Precisely weighed amounts of sorbent (0.05 g) were placed in flasks and filled with $ZnSO_4 \times 7H_2O$, $FeCl_3 \times 6H_2O$ and $Cr(NO_3)_3$ solutions of different initial concentrations. In this case, the initial concentrations of the samples were changed in the range from 10^{-4} to 5×10^{-2} M. When studying the effect of the sorbent mass on sorption, the mass of the sorbent was varied in the range from 0.01 to 0.1 g. The solutions of Zn(II), Fe(III) and Cr(III) with a pH of 1 to 11 were used in order to determine the effect of the pH of the solution. A study of the dependence of the sorption on contact time was carried out using 0.3 g of sorbent and 90 ml of $ZnSO_4 \times 7H_2O$, $FeCl_3 \times 6H_2O$ and $Cr(NO_3)_3$ solutions with 10^{-3}M concentration and changing the contact time in a range from 3 to 65 minutes, and temperatures of 25, 35 and 50°C. In recent experiments, the sample was taken every 3-5 minutes and analyzed on a spectrophotometer. The sorption capacity ($mg \cdot g^{-1}$) and the degree of adsorption (%) were calculated using equations (1) and (2):

$$SC = (c_0 - c_e)\frac{V}{m} \qquad (1)$$

$$R = \frac{100(C_0 - C_e)}{C_0} \qquad (2)$$

where C_0 and C_e are the initial and equilibrium concentrations of Zn(II), Fe(III) and Cr(III) ions in the solution, respectively ($mg \cdot ml^{-1}$), V is the volume of the solution (ml), and m is the sorbent mass (g).

The results showed that 10^{-3} M solutions, 0.05g adsorbent, was used as the optimal concentration for studying the effect of pH on the sorption of ions. Based on the results obtained, adsorption isotherms are determined.

The results were statistically processed using standard methods [6]. The average error of the experiment was estimated to be less than 4%.

The kinetics of the sorption of ions from aqueous solutions with phosphorus-containing cation exchanger synthesized on the basis of butadiene-styrene rubber was comparatively studied in this paper under static conditions. The phosphorus-containing cation exchanger was synthesized on the basis of industrial polymer – butadiene-styrene rubber of the DSSK brand by the reaction of oxidative chlorophosphorylation using

ISNN: print 2663-7006; online 2709-2666

PCl_3 in the presence of oxygen, followed by hydrolysis of the resulting modificant. The method of obtaining the sorbent was described in the early works [3]. The pH value in the solution was established using an acetate-ammonia buffer solution.

A 200 ml flask equipped with a magnetic stirrer was used in order to study the sorption kinetics by limited volume method [6]. 90 ml of a previously prepared solution with a component concentration of 10^{-3} mol·L^{-1} was placed in a flask. The experiments were carried out at a constant temperature of 23 ± 2°C and pH 6 (the indicated acidity of the medium is optimal). 0.3 g (in terms of absolutely dry) cation exchanger was placed in the solution. Analysis of the content of elements in all solutions was performed by spectrophotometric method. The volume of taken samples did not exceed 2% of the total volume.

RESULTS AND DISCUSSION

Fig.1 shows the dependence of the sorption of ions on time using the synthesized phosphorus-containing sorbent. It is seen that for the phosphorus-containing sorbent achieving equilibrium cationite-salt solution occurs after 65 minutes.

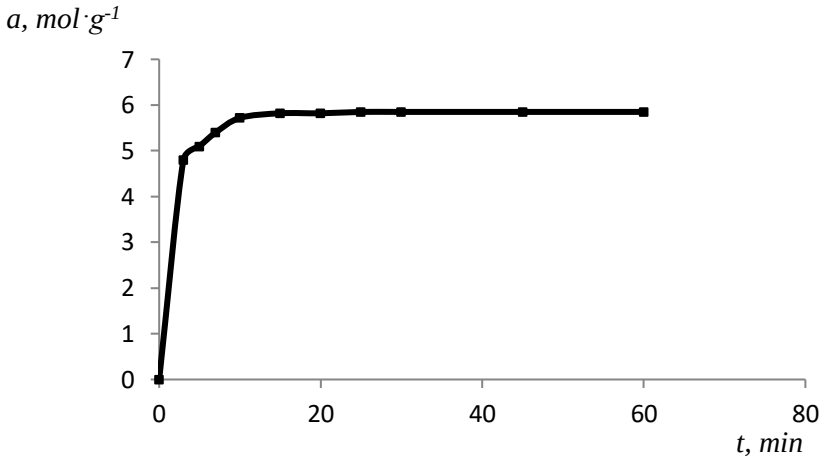

a

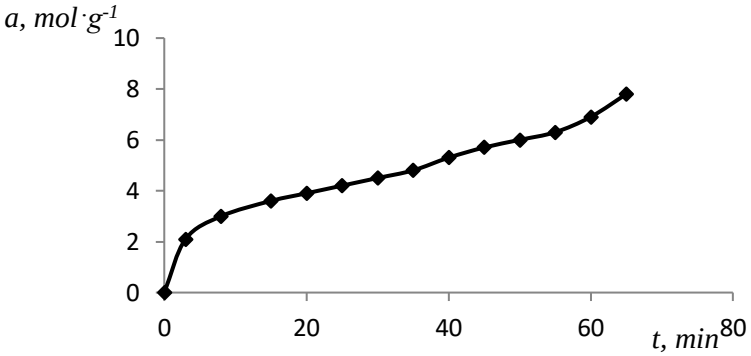

b

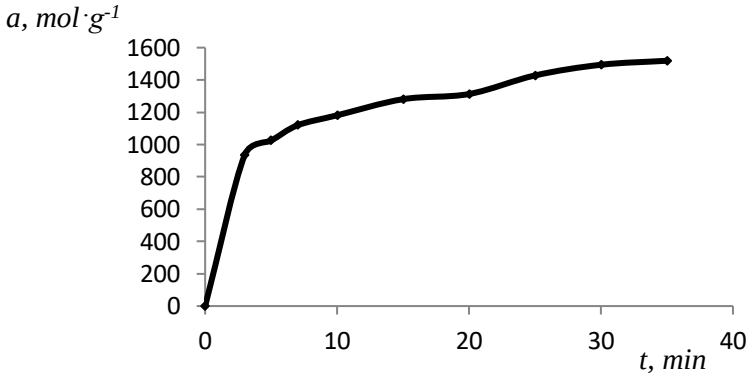

c

Fig.1. Kinetic curves of sorption: a - of zinc ions, b - of iron ions, c - of chromium ions

It is known that the sorption process is complex and multi-stage, and the cumulative consideration of all stages of this process is difficult to implement, therefore, it is usually resorted to simplifications using the principle of the limiting stage [4].

The contribution of external diffusion to the sorption of ions on the phosphorus-containing rubber sorbent can be described by the equation (3):

$$ln(1 - F) = -\gamma \cdot t, \qquad (3)$$

where F is the rate at which equilibrium is reached, calculated by formula $F = {a_t}/{a_e}$ (a_t – the amount of sorption (mmol/g) at time t, a_e is the amount of sorption in the equilibrium state (mmol/g)); γ is some constant value for these conditions; t - sorption time (min).

The dependence $-ln(1-F) = f(t)$ is shown in Fig.2.

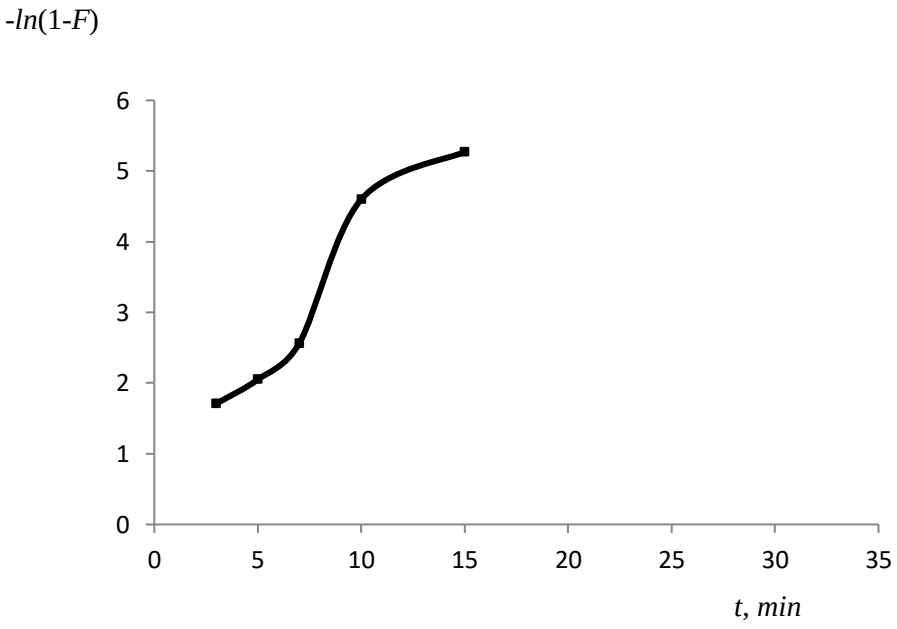

a

ISNN: print 2663-7006; online 2709-2666

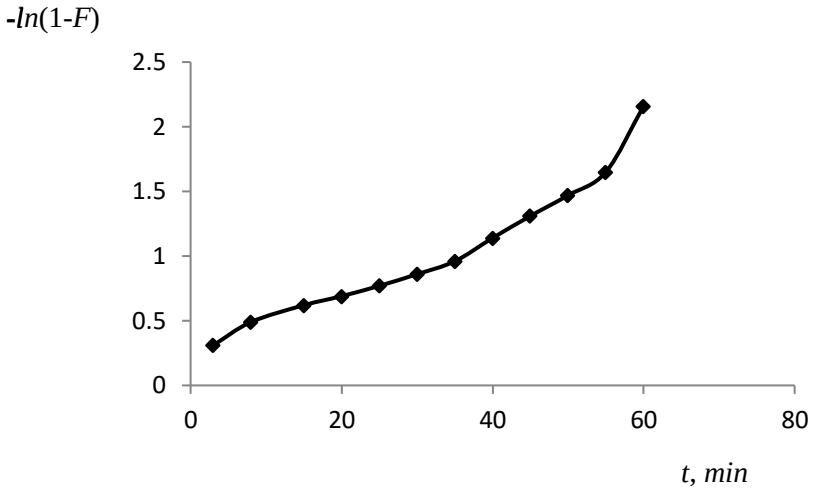

b

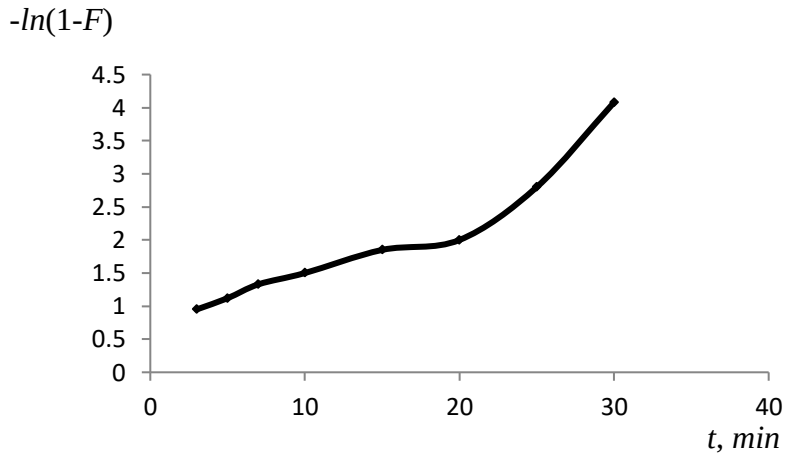

c

Fig.2. Dependence of -*ln*(1− *F*) on time *t* for sorption of: a - of zinc ions, b - of iron ions, c - of chromium ions

As can be seen from fig.2, only in the initial sections there is a rectilinear dependence of the function -*ln*(1− *F*) = *f*(*t*), and the kinetic curves do not describe only the external diffusion mechanism throughout the entire process. In the course of the process, the influence of the external diffusion factor decreases, while the intradiffusion factor increases, and for the phosphorus-containing cation exchanger synthesized by us this effect occurs much earlier than for the industrial cation exchanger. This means that the process proceeds in a mixed diffusion mode, i.e. It is controlled by diffusion in the solution film and diffusion in the cationite grain [5]. In order to evaluate the contribution of internal diffusion to the sorption process, the empirical equation (4) is used:

$$a_t = k_d \cdot t^{1/2}, \qquad (4)$$

where a_t is the amount of sorbed ion per unit cation exchange mass at time t, mol/g; k_d is the rate constant of internal diffusion, mmol·g $^{-1}$·min$^{-0.5}$; t-sorption time, min.

Evidence that the stage limiting the sorption process is internal diffusion is the observance of a rectilinear relationship in the coordinates a_t - $t^{1/2}$ (fig.3).

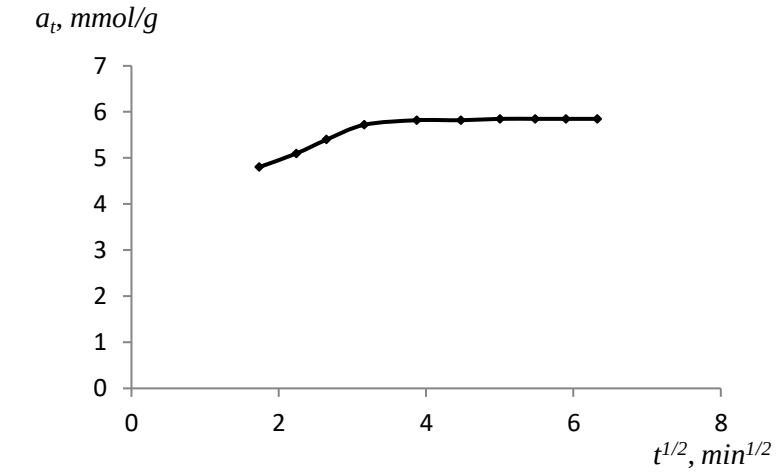

a

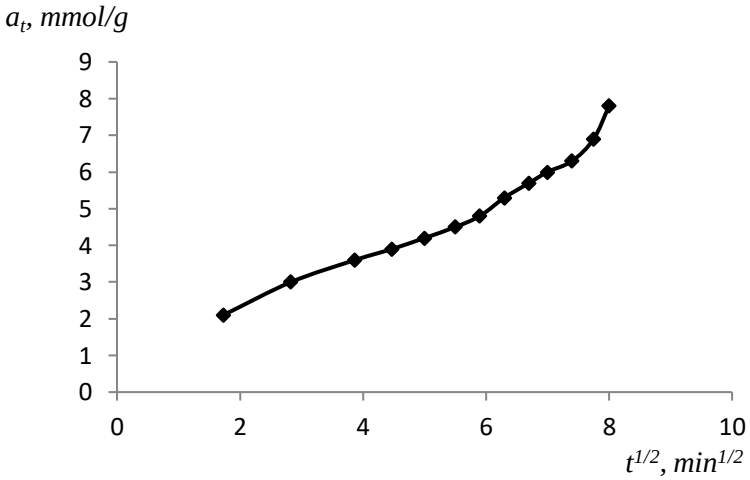

b

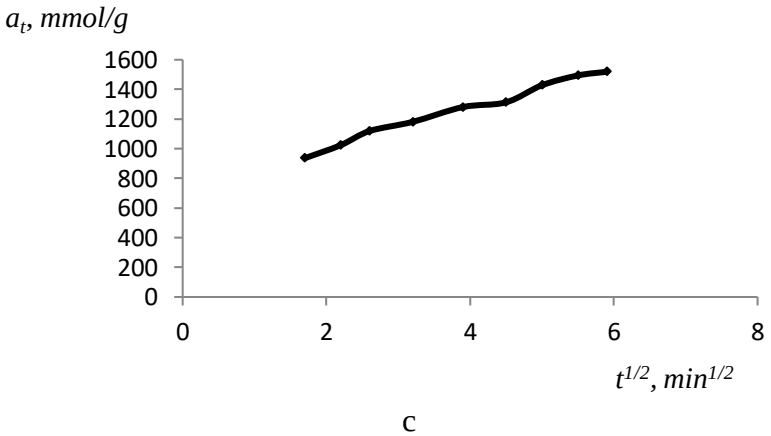

c

Fig.3. Dependence a_t - $t^{1/2}$ for sorption of: a - of zinc ions, b - of iron ions, c - of chromium ions

ISNN: print 2663-7006; online 2709-2666

In most cases this dependence is multilinear and is characterized by 2-3 sections, and is described by the equation (3):

$$a_t = k_d \cdot t^{1/2} + A, \qquad (5)$$

where A is the segment cut off on the ordinate axis of the $a_t = f(t^{1/2})$ dependence.

The quantity A in equation (3) characterizes the thickness of the boundary layer. The initial section describes the diffusion of sorbate through the solution layer to the surface of the sorbent (external diffusion kinetics). The second section, from whose slope the rate of internal diffusion is determined, describes the intrinsic diffusion process itself . It should be noted that in all cases, the process of diffusion of iron ions on the phosphorus-containing sorbent synthesized on the basis of butadiene-styrene rubber is described by equation (3), i.e. there is a mixed kinetics. In this case, the kinetic parameters corresponding to internal diffusion characterize the slope angle of the second section; The segment cut off by the continuation of this straight line on the ordinate axis is proportional to the thickness of the film surrounding the ion exchanger grain [7,8]. The rate constants of the external and internal diffusions are presented in table 1.

Table 1

The rate constants of the external and internal diffusions

Ion	The rate constants of the external diffusion		The rate constants of the internal diffusion		
	γ	R^2	k_d, mmol·g^{-1} min$^{-0,5}$	A	R^2
Zn(II)	0,3881	0,8866	0,1993	4,7925	0,7118
Fe(III)	0,0312	0,9136	0,8152	0,3879	0,952
Cr(III)	0,1256	0,8265	136,59	731,41	0,988

R - is the correlation coefficient

It is assumed that a substantial contribution to the kinetics of the entire process can be made by the sorption proper phase. Therefore, to describe the pattern of this kinetic stage, the pseudo-first and pseudo-second order patterns of the reaction were used, which in linear form are expressed by equations (6**)** and (7):

$$ln(a_e - a_t) = lna_e - k_1 \cdot t, \qquad (6)$$

$$t/a_t = 1/(k_2 \cdot a_e^2) + (1/a_e) \cdot t, \qquad (7)$$

where a_e and a_t - the value of equilibrium sorption and the value of sorption at time t, respectively, mmol/g; k_1, k_2 are the rate constants of the sorption of the pseudo-first (min^{-1}) and pseudo-second orders (g/mmol·min), respectively. According to the equation (6) the $ln(a_e-a_t)$-t dependence must represent a straight line from which the values of k_1 and a_e can be determined. The values of k_1 and a_e calculated from these dependencies are given in table 2.

Table 2

The rate constants of the external and internal diffusions

Ion	The pseudo-first-order model			The pseudo-second-order model		
	a_e	k_1	R^2	a_e	k_2	R^2
Zn(II)	13,7816	0,3259	0,9308	6,0168	0,2562	0,9991
Fe(III)	6,7727	0,0278	0,9302	8,8809	0,0052	0,8918
Cr(III)	907,96	0,0999	0,9177	1666,7	0,0002	0,9933

It should be noted that, in spite of sufficiently high correlation coefficients, the values of a_e, obtained from the line $\ln(a_e-a_t)$ - t, in most cases do not coincide with the experimental values of a_e. From the dependences t/a_t - t, according to equation (7), k_2 and a_e were calculated.

CONCLUSION

1. In this study, the sorption capacity of the phosopher-containing sorbent synthesized by oxidative chlorophosphorylation of butadiene-styrene rubber followed by hydrolysis with respect to Zn(II), Fe(III) and Cr(III) ions was studied, determining the influence of various parameters such as the pH of the solution, the initial concentration of the salt, the sorbent mass, phase contact time and temperature. Experimental results have shown that a phosphorus-containing sorbent based on butadiene-styrene rubber can be successfully used to extract ions from aqueous solutions.

2. Processing the kinetic curves of ions sorption on the phosphorus-containing sorbent synthesized on the basis of butadiene-styrene rubber, it is defined that the mechanism of the process is rather complicated. The low concentration of the iron salt solution leads to the fact that diffusion of the solution film contributes to the overall process speed. The mixed diffusion mechanism indicates the effect of diffusion on the cationite grain. The application of the equations of chemical kinetics has shown that a certain contribution to the overall process speed is made by the interaction stage of the sorbed ions with the functional groups of the cation exchanger. The results obtained can be useful in developing the sorption technology for purification of natural and waste water from iron ions using phosphorus-containing sorbent based on butadiene-styrene rubber.

REFERENCES

1. Saladze K.M., Kopilova-Valova V.D. Complexing ion exchangers. Moscow: Chemistry. 1980, 336 p
2. Kopilova V.D., Mekvabishvili T.V., Gefter Y.L. Phosphorus-containing ion exchangers. Voronej: Voronej University, 1992, 192 p
3. Karimova E.S., Azizov A.A., Alosmanov R.M., Buniyatzadeh I.A. Polymer modification for using as a sorbent. Young scientist.2017, Vol.16, pp.117-119
4. Maharramov A.M., Alosmanov R.M., Melikova A.Y. Phosphochlorination of polybutadiene with phosphorus (III)chloride in the presence of oxygen. Chemistry and chemical technology. 2003, Vol.46, pp.25-27

ISNN: print 2663-7006; online 2709-2666

5. Azizov A.A., Rahimov R., Alosmanov R.M. Patent of the Azerbaijan Republic №:0108, 2003
6. Alosmanov R.M. Kinetics investigation of the lead and zinc sorption by the phosphorus containing cationite. Bulletin of Moscow University.2011 Vol.52, 145 p
7. Polyanskiy N.G., Gorbunov G.V., Polyanskaya N.L. Ionite research methods. Moscow: Chemistry. 1976,208 p
8. Cestari A.R., Vieira E.F.S., Pinto A.A. Adsorption of anionic dyes on chitosan beads. 1. The influence of the chemical structures of dyes and temperature on the adsorption kinetics. J. Colloid Interface Science. 2005 Vol. 292, pp. 363-386. doi.org/10.1016/j.jcis.2004.08.007

ИССЛЕДОВАНИЕ КИНЕТИКИ СОРБЦИИ ИОНОВ ТЯЖЕЛЫХ МЕТАЛЛОВ

Э.С.Керимова[0000-0001-7577-2900]
Бакинский Государственный Университет
elladakarimova1903@gmail.com

Фосфорсодержащий полимерный сорбент на основе бутадиен-стирольного каучука был использован для удаления ионов цинка, железа и хрома из воды. Исследование проводилось с целью изучения сорбционных характеристик путем определения влияния различных параметров, таких как pH раствора, начальная концентрация ионов металлов, масса сорбента, время контакта фаз и температура. Изучены закономерности кинетики сорбции ионов цинка, железа и хрома на фосфорсодержащем сорбенте, синтезированном на основе бутадиен-стирольного каучука. На основании полученных результатов определено, что процесс сорбции ионов цинка, железа и хрома на катионообменнике протекает по ионообменному механизму. Кинетика этого процесса представляет собой комбинацию кинетики внешней и внутренней диффузии (с некоторым преобладанием кинетики внешней диффузии) и лучше описывается моделью реакции псевдовторого порядка. Кроме того, определенный вклад в общую скорость процесса вносит взаимодействие сорбированных ионов с функциональными группами катионообменника.
Ключевые слова: *фосфорсодержащий катионообменник, цинк, железо, хром, сорбция, кинетика.*

AĞIR METAL İONLARININ SORPSİYASI KİNETİKASININ ÖYRƏNİLMƏSİ

E.S.Kərimova[0000-0001-7577-2900]
Bakı Dövlət Universiteti
elladakarimova1903@gmail.com

Sudan sink, dəmir və xrom ionlarını çıxarmaq üçün stirol-butadien kauçuk əsasında fosfor tərkibli polimer sorbentdən istifadə edilmişdir. Tədqiqat məhlulun pH, metal ionlarının ilkin konsentrasiyası, sorbentin kütləsi, fazaların təmas müddəti və temperatur kimi müxtəlif parametrlərin təsirini təyin etməklə sorbsiya xüsusiyyətlərini öyrənmək məqsədilə aparılmışdır. Stirol-butadien kauçuku əsasında sintez edilmiş fosfor tərkibli sorbentdə sink, dəmir və xrom ionlarının sorbsiya kinetikasının qanunauyğunluqları tədqiq edilmişdir. Alınmış nəticələr əsasında müəyyən edilmişdir ki, sink, dəmir və xrom ionlarının kation dəyişdiricidə sorbsiya prosesi ion mübadiləsi mexanizmi üzrə gedir. Bu prosesin kinetikası xarici və daxili diffuziya kinetikasının birləşməsidir (xarici diffuziya kinetikasının bir qədər üstünlüyü ilə) və

psevdoikinci dərəcəli reaksiya modeli ilə daha yaxşı təsvir edilmişdir. Bundan əlavə, prosesin ümumi sürətinə müəyyən töhfə sorbsiya ionların kation dəyişdiricisinin funksional qrupları ilə qarşılıqlı təsiri ilə edilir.
***Açar sözlər**: fosfor tərkibli kation dəyişdirici, sink, dəmir, xrom, sorbsiya, kinetika.*

ISNN: print 2663-7006; online 2709-2666

AJCN, Vol4, No.1, 2022, pp. 42-47

https://doi.org/10.32010/AJCN05012022-42

UDC: 542.97

DEHYDROALKYLATION OF BENZENE WITH PROPANE ON MECHANICAL MIXTURES OF CATALYSTS

F.A. Babayeva 0000-0003-4815-1070

Institute of Petrochemical Processes of Azerbaijan National Academy of Sciences

feridan@rambler.ru

The conversion of C_6H_6 : C_3H_8 mixtures on mixed catalysts (MMC) composed of the metal oxide catalysts M,ReO_x/Al_2O_3 (Pt or Ni -0.5 wt.%, Re-1.0 wt.%) and zeolites Y, MOR, and ZSM-5 in the H form was studied. The products of benzene dehydroalkylation by propane and propane dehydrogenation products are formed at 200–400°C. It has been shown that C_3H_8 is activated on the metal oxide catalysts and C_6H_6 interacts with the zeolites yielding the C_6H_{7+} intermediate, which acts as an agent of proton transfer from a zeolite to a metal catalyst, and another intermediate C_9H_{13+} . Cumene, alkylbenzenes, and propene are formed as a result of the conversion . Acomparison of the results of the conversion of these mixtures on the composite catalysts with different zeolites shows that the formation of cumene and propene is thermally controlled and the formation of the other products is kinetically controlled. It has been concluded that the coupling of the redox properties of the metal oxide catalysts with the acid–base properties of the zeolite catalysts facilitates the low–temperature transformations of the C_6H_6 : C_3H_8 mixtures.

Keywords: *dehydroalkylation, dehydrogenation, benzene, propane, mechanical mixture of catalysts, zeolite isopropylbenzene, propylene*

INTRODUCTION

The involvement of propane in the processes of the synthesis of valuable products, such as cumene and propylene, is of great theoretical and practical importance. The solution of this problem is related to the feasibility of the catalytic activation of the conversion of this alkane into an intermediate capable of alkylating aromatic compounds or the conversion into propene [1-5].

Formation of products conversion of benzene-propane mixtures MMC is accompanied by the occurrence of three reactions: a) the alkylation of benzene; b) the propane dehydrogenation; c) the formation of alkylaromatic hydrocarbons (ArH). The course of these reactions depends on the contact conditions of the studied mixtures with MMC [6,7].

Our studies on the M,Re/Al_2O_3+ H-zeolite catalytic system showed the feasibility of benzene dehydroalkylation by propane even at 200°C and cumene production under temperature conditionsclose to the conditions of benzene alkylation with propene [7].

Catalysts such conversions of methane and other gaseous alkanes may be metal oxide and zeolite system. Therefore, the research aimed at the development of processes involving methane and other gaseous alkanes in the processes of the formation of intermolecular C-C bonds with new catalytic systems containing highly dispersed metal particles on oxide and a zeolite carrier and their composites, relevant and promising [8,9].

ISNN: print 2663-7006; online 2709-2666

The present work is devoted to the results of researches in this direction with the purpose of finding-out of influence of the conditions of experiment and the nature of zeolite component of catalytic system M, Re/Al_2O_3+H-zeolite (where zeolite Y, MOR, ZSM-5) on conversion of C_6H_6: C_3H_8 mixes.

EXPERIMENTAL PART

Research has been carried out on the mechanical mixture of aluminaplatinumrhenium catalyst (APRC) prepared by the known technique [6] and H-forms of zeolites (Y, MOR, ZSM-5).

H-forms of zeolites have been prepared proceeding from the Na-form of industrial zeolite. Completely replaced H-form of Y-zeolite was obtained by ionic exchange of initial zeolite with water solution of ammonium chloride at 80ºC (6 h). Obtained zeolites have been formed with binding alumogel (20 mas. % Al_2O_3).

Dealuminized form of mordenite has been prepared by triple processing of initial Na-form of 2,5 N by HCl solution, cleaning of Cl^- ions and subsequent decationization (3 multiple NH_4Cl exchange), drying at 120ºC and glowing at 450ºC (on 4 h). Further, the samples mixed with hydrocarbon gel aluminium oxide, formed, dried at 120ºC and calcinated at 350ºC – 450ºC (8 h). ZSM-5 has been translated into the H-form by 3 multiple processing of 2 N by NH_4Cl solution with subsequent cleaning from ions Cl^- and glowing at 400ºC (4 h). Initial reagents propane and benzene had cleanliness = 99 % (Gas-liquid chromotografic analysis).

Conversion of propane-benzene mixes has been studied in the flowing reaction Kr at 200–450°C, atmospheric pressure and reaction mix supplying weight hour space velocity 125-1000 h^{-1}.

When carrying out the experiments with C_6H_6: C_3H_8 =1 : 9 mix barbotage supply of reactants in reactor has been used. In the experiments with other mole ratio of components benzene in the calculated quantities has been supplied by the dosing pump to the evaporator - mixer, further the mix entered the reactor. Variation of weight hour space velocity (WHSV) has been carried out by respective change of the used catalyst volume. WHSV 500 h^{-1} corresponded to the loading of the catalyst of 5 sm^3. Before experiments the catalyst has been processed by air at 400ºC (4 h).

The products were analyzed using chromatography (AutoSystem XL, Perkin_Elmer) and the amount of the components was expressed in % C, i.e., the overall amount of carbon atoms participating in the reaction.

RESULTS AND DISCUSSION

Results of studying the conversion of C_6H_6 : C_3H_8 mixtures MMC showed that only in the presence of benzene MMC has activity in a low temperature (≥ 180 °C) conversion of propane. The introduction of small amounts of benzene into propane (for example, 10 mol %) leads to its transformations and the formation of hydrogen, the molar value of which corresponds to the total molar conversion of propane. Eduction of hydrogen in the conversion of benzene-propane mixtures is a total reflection of the noted reactions.

ISNN: print 2663-7006; online 2709-2666

Table 1

The effect of the ratio of benzene conversion of propane and a mixture of C_6H_6: C_3H_8. T = 250 °C, V = 500 h^{-1}

Content, mol. %		Conversion, %		The product yield, % C		
C_6H_6	C_3H_8	C_6H_6	C_3H_6	IPB	C_3H_6	ArH
125	100	-	0	-	-	-
250	90	12	1.9	3.6	0.5	-
500	75	14	7.2	6.2	0.7	2.2
750	50	23	7.7	6.4	0.4	2.6
1000	0	0	-	-	-	-

Conversion C_6H_6 : C_3H_8 mixtures depends on the pretreatment of the catalyst. Eduction hydrogen subjected to standard processing air MMC characterized by a period of activation. This activation period MMC is associated exclusively with the interaction of propane with AMR catalyst and, by analogy with methane, may be a consequence of the partial reduction of the metal component of MMC (table 1).

It is seen from table 1, that the yield of conversion products C_6H_6 : C_3H_8 mixtures depends on their ratio. Changing the molar ratio of C_6H_6: C_3H_8 from 1 : 9 to 1 : 1 leads to an increase in conversion of benzene and C_9 growth ArH composition.

Table 2

Effect of temperature on the conversion of a mixture of C_6H_6 : C_3H_8 (1 : 9 mol). On MMC- AMRC + HY; V = 500 h^{-1}

T, °C	Conversion, %		Product yield, %				
	C_6H_6	C_3H_8	IPB	C_3H_6	NPB	ArH	C_1-C_2
200	4.8	0.6	1.4	0	0	0	0
250	11.4	2.0	3.1	0.6	traces	0	0
300	31.7	7.6	8.7	2.9	0.8	0	0
320	59.6	4.8	13.9	7.1	3.2	0.8	0
350	37.0	22.8	6.5	15.3	3.4	1.2	0
375	18.7	23.8	1.7	21.4	1.7	2.2	0
400	8.1	5.4	Traces	3.5	0.4	1.5	traces
450	11.3	3.3	0	1.5	traces	1.5	2.2

The results show that regardless of the nature of the zeolite component of the MMC, carrier Bronsted acid centers, propylene begins to form at a temperature of 250 °C and its yield increases with temperature reaching a maximum value at 375 °C, i.e. the maximum values of benzene conversion, and yield IPB (320 °C), and propylene are different (table 2).

Varying the volume speed of from 125 to 1000 h^{-1} changes as the conversion of components of C_6H_6:C_3H_8 mixture and distribution of the reaction products (table 3) – below than 500 h^{-1} is increased yield IPB and formations NPB and ArH with slight amounts of propylene. Increasing the volume speed leads to a monotonic decrease of benzene conversion, while the conversion of propane in the range of V = 125-500 h^{-1} is reduced, and then increases again with growth the volume speed of from 500 to 1000 h^{-1}.

Table 3

The effect of volume speed rate of reactants on the conversion of benzene-propane mixture at MMC:AMPK + HZSM-5;T = 250 ° C

V, h^{-1}	Conversion, %			Product Yield, %		
	C_6H_6	C_3H_8	IPB	C_3H_6	NPB	ArH
125	18.2	2.7	4.3	0.1	0.3	0.4
250	15.8	2.2	4.0	0.4	0.2	0.1
500	11.4	2.0	3.1	0.6	traces	0
750	10.2	2.9	2.8	1.4	0	0
1000	8.5	5.7	2.3	3.9	0	0

Varying the ratio of metal and acid MMC components leads to a change in the transformation products C_6H_6 : C_3H_8 mixtures. The data show that the type of zeolite influences the conversion of individual components of the reaction mixture and the yield (selectivity) of the reaction products.

The results obtained show that at sufficiently low temperatures contacting benzol-propane mixture on the mechanical mixture of catalysts leads to the formation of products of two thermodynamically difficult reactions: dehydrogenation of propane and dehydroalkylization of benzol propane presence of a catalyst activation period associated with partial recovery of the MMC metal component may suggest the following scheme of MMC activation

$$M, ReOx/\ Al_2O_3 \xrightarrow[-CO_2,\ -H_2O]{C_3H_8} M \cdot\cdot O \cdot\cdot ReOx^1$$

contributing to the formation of some active bridge form of bound oxygen involved in the activation of C_3H_8

$$M \cdot\cdot O \cdot\cdot ReOx_1 + C_3H_8 \rightleftharpoons M \begin{array}{l} \diagup\ C_3H_7 \cdots H \\ \diagdown\ O \diagdown ReOx \end{array}$$

The interaction of benzene with the H-zeolite component of MMC promotes the formation of a stable benzolonium ion.

$$H\text{ - zeolite} + C_6H_6 \rightleftharpoons [zeolite]^{\ominus} + C_6H_7^{\oplus}$$

able to migrate to the metal-containing component of MMC and interact with activated propane.

$$M \begin{array}{l} \diagup C_3H_7 \cdots H \\ \diagdown O^{\delta-} \end{array} ReO_{x'} + C_6H_7^{+} \rightleftharpoons \left[M \begin{array}{l} \diagup C_3H_7 \\ \diagdown C_6H_6 - H \end{array} O^{+}H \diagdown ReO_{x'} \right] \xrightarrow{-H_2O} \left[C_6H_6^{\oplus} \cdot C_3H_7 \right] + M, ReO_{x'}$$

The formed carbocatione $[C_6H_6^{\oplus} \cdot C_3H_7]$ undergoes stabilization (with isomerization, depending on reaction conditions) on the zeolite component of MMC

$$[zeolite]^{\ominus} + C_6H_6^{\oplus} \cdot C_6H_7 \rightleftharpoons H\text{- zeolite} + \text{products}$$

CONCLUSION

1. It was found for the first time that on mechanical mixtures of catalysts consisting of bimetal-aluminum oxide catalysts M, Re/Al_2O_3, where (M=Pt, Ni) and H-zeolite (Y, HM or ZSM-5), low-temperature (≥ 180 ºC) alkylation of benzene with

ISNN: print 2663-7006; online 2709-2666

propane to form isopropylbenzene and the product of its dealkylation and isomerization.

2. It was shown that the alkylation of benzene of propane on spatially separated centers of mechanical mixtures (bimetal alumina and H-zeolite) catalysts proceeds by cyclic transport of protons from acid centers on the metal reduction-oxidation and and back ions C_6H_{7+} and C_6H_6 C_3H_{7+}.

REFERENCES

1. Abasov S.I., Babayeva F.A., Tagiyev D.B., Rustamov M.I. Low-temperature catalytic alkylation of benzene by propane. Applied Catalysis A: General. 2003, № 251, pp.267-274 (doi.orq/10.1016/50926-860x(03)00342-9)
2. Abasov S.I., Babayeva F.A., Tagiyev D.B., Rustamov M.I. Inıtıatıon of unfavorable reactıons by proton cyclıc transfer over zeolıte-containing catalysts. Proceedings of the 14th International Zeolite Conf., Cape Town, South Africa. 25-30th April 2004, pp.2339-2346
3. Li Y., Xue B., He X. Catalytic synthesis of ethylbenzene by alkylation of benzene with diethyl carbonate over HZSM-5. Catal. Commun. 2009, Vol.10, № 5, pp.702-707
4. Huang X., Sun X., Zhu S., Liu Z. Benzene Alkylation with Propane over Mo Modified HZSM-5. Catalysis Letters. 2007, Vol.119, №3-4, pp.332-338
5. Abasov S.I., Babaeva F.A., Rustamov M.I. On the catalytic activation of low molecular weight C1-C3 alkanes. Catalysis in industry, 2009, №.6, pp.23-27
6. Abasov S.I., Babaeva F.A., Nasibova A.R., Rashidova A.A., Tagiev D.B. Influence of the zeolite nature on low-temperature conversions of C_6H_6 : C_3H_8 mixes on catalytic systems Pt, Re/Al_2O_3-H-zeolite. Processes of petrochemistry and oil refining.2004, №3(18), pp 87-93
7. Babayeva F.A., Abasov S.I., Rustamov M.I. Conversions of Mixtures of Propane and Benzene on Pt, Re/Al_2O_3 + H-Zeolite Systems. Petroleum Chemistry. 2010, Vol.50, №1, pp.42-46
8. Zhasibaeva, A.M., Masenova A.T., Zhasibaev M.Zh. Modified zeolite catalysts for the alkylation of benzene with propane. Kaznu Bulletin. Chemical series, 2013, № 2, pp.70-73
9. S.I. Abasov, E.S. Isaeva, F.A. Babaeva [et al.] Catalytic reactions involving sterically separated active cites// Journal of Applied Chemistry. 2015, Vol.88, № 5, pp.787-795

ДЕГИДРОАЛКИЛИРОВАНИЕ БЕНЗОЛА ПРОПАНОМ НА МЕХАНИЧЕСКИХ СМЕСЯХ КАТАЛИЗАТОРОВ

Ф.А.Бабаева 0000-0003-4815-1070

Институт Нефтехимических Процессов НАН Азербайджана

feridan@rambler.ru

Изучено превращение смесей C_6H_6 : C_3H_8 на механически смешанных катализаторах (МСК), состоящих из металлооксидных катализаторов M,ReOx/Al_2O_3 (Pt или Ni -0,5 мас.%, Re-1,0 мас.%) и цеолитов Y, MOR и ZSM- 5 в Н-форме. Продукты дегидроалкилирования бензола пропаном и продукты дегидрирования пропана образуются при 200–400°C. Показано, что C_3H_8 активируется на металлооксидных

*катализаторах, а C_6H_6 взаимодействует с цеолитами с образованием интермедиата C_6H_{7+}, который действует как агент переноса протона от цеолита к металлическому катализатору, и другого интермедиата C_9H_{13+}. В результате превращения образуются кумол, алкилбензолы и пропилен. Сравнение результатов превращения этих смесей на композиционных катализаторах с различными цеолитами показывает, что образование кумола и пропилена контролируется термически, а образование остальных продуктов - кинетически. Сделан вывод, что сочетание окислительно-восстановительных свойств металлооксидных катализаторов с кислотно-основными свойствами цеолитных катализаторов облегчает низкотемпературные превращения смесей C_6H_6 **:** C_3H_8.*
***Ключевые слова**: дегидроалкилирование, дегидрирование, бензол, пропан, механическая смесь катализаторов, цеолит изопропилбензол, пропилен.*

BENZOLUN PROPAN İLƏ DEHIDROALKILLƏŞMƏSI KATALİZATÖRLƏRİN MEXANİK QARŞIQLARI ÜZRƏ

F.Ə.Babayeva[0000-0003-4815-1070]
Azərbaycan Milli Elmlər Akademiyasının Neft-Kimya Prosesləri İnstitutu
feridan@rambler.ru

*C_6H_6 **:** C_3H_8 qarışıqlarının metal oksid katalizatorları M, ReO_x/Al_2O_3 (Pt və ya Ni -0,5 ağırlıq %, Re -1,0 çəki%) və Y, MOR və ZSM-5 seolitlərindən ibarət mexaniki qarışıq katalizatorlarda (MQK) C_3H_8 qarışıqlarının çevrilməsi H şəklində. Benzolun propan ilə dehidroalkilləşmə məhsulları və propan dehidrogenləşmə məhsulları 200–400°C-də əmələ gəlir. Göstərilmişdir ki, C_3H_8 metal oksid katalizatorlarında aktivləşir, C_6H_6 isə seolitlərlə reaksiyaya girərək seolitdən metal katalizatora proton ötürücü agent kimi çıxış edən C_6H_{7+} ara məhsulunu və digər C_9H_{13+} ara məhsulunu əmələ gətirir. Transformasiya nəticəsində kumen, alkilbenzollar və propilen əmələ gəlir. Bu qarışıqların müxtəlif seolitlərlə kompozit katalizatorlarda çevrilməsinin nəticələrinin müqayisəsi göstərir ki, kumen və propilen əmələ gəlməsinə termik, digər məhsulların əmələ gəlməsinə isə kinetik nəzarət edilir. Belə nəticəyə gəlmək olar ki, metal oksid katalizatorlarının redoks xassələrinin seolit katalizatorlarının turşu-əsas xassələri ilə birləşməsi C_6H_6**:**C_3H_8 qarışıqlarının aşağı temperaturda transformasiyasını asanlaşdırır.*
***Açar sözlər**: dehidroalkilləşmə, benzol, propan, katalizatorların mexaniki qarışığı, seolit izopropilbenzol, propilen.*

ISNN: print 2663-7006; online 2709-2666

AJCN, Vol 4, No. 1, 2022, pp. 48-53

https://doi.org/10.32010/AJCN05012022-48

UDC 628.5 (07)

MODIFIED CONCRETES BASED ON NON-CLINKER BINDERS

E.F.Aslanov[0000-0002-1894-1242], *N.A. Jafarova* [0000-0001-5669-6631],
T.K. Sherifova [0000-0001-6689-3102]
Azerbaijan State Oil and Industrial University
hteyfa@gmail.com

The study of the properties of high-strength concrete on the basis of new binders made from technogen waste is discussed. Theoretical provisions for the hardening of a clinker-free binder, consisting of co-crushed dump steel-smelting slag, cullet, a modifying aluminum-containing additive, and an alkaline component hardening under conditions of heat and moisture treatment, have been developed. The optimal compositions of clinker-free binder and fine-grained concrete based on it have been determined. At 25.0 MPa of the activity of the clinker-free binder, the composition contains (metallurgical waste) slag -52%; cullet - 37%; modifying aluminum-containing additive -11%; alkalis (activator) - 7.4% (by weight of the binder). It has been established that to obtain fine-grained concrete grade M 150, it is necessary: 25% clinker-free binder and 75% mixed aggregate, consisting of 35% steel-smelting waste slag and 65% sand. With a water / binder ratio of 0.33.

Keywords: *clinker-free cement, waste, modified concrete, metallurgical slag, glass-alkali binder, slag cement.*

INTRODUCTION

Concrete is a composite material consisting of various components, such as artificial stone, obtained by mixing and hardening a mixture of adhesives and aggregates with water, which can achieve the various properties required over a wide range of components due to changes in proportions. Concrete structures are widely used because they are technologically easy to obtain. Thus, the annual production of concrete mixes in the world is more than a billion tons, and in Azerbaijan - more than 1,555000 tons [1].

The production of large volumes of materials in the construction materials industry has a significant impact on the environment. To improve the environmental situation, technologies that can use industrial wastes or their products as raw materials, which are economically viable and resource-saving in industrial production, are being widely used. For example, the production of Portland cement accounts for 5% of energy production. The Norm cement plant alone produces 2 million tons of cement a year.

Due to the large volume of concrete produced, it is very important to use resource-saving technologies for recycling waste. The use of metallurgical slag as small and large aggregates in the production of heavy concrete has been well studied and incorporated into industrial production in many countries [2].

The most promising way to reduce energy consumption in the building materials industry is to replace Portland cement with clinker-free cement, ie with alkaline adhesives in addition to activators, which has an environmentally friendly effect. Thus, the economic efficiency of their production is high, as there is no need for capital

ISNN: print 2663-7006; online 2709-2666

investment in production equipment, field development, energy-intensive technological operations.

Slag-alkaline cement is a high-strength hydraulic binders consisting of finely ground slag (up to 95% of the total content) and an alkaline hardening activator (soda, liquid glass, etc.), dominated by CaO, SiO_2, Al_2O_3 [3,4]. In the production of slag cement, granular blast furnace, electrothermophosphorus and non-ferrous metallurgical slags are used. Slag is similar to volcanic rocks and has a unique high-temperature mineral composition that can vary even within the same plant due to the different composition of the ore and flux used. The main property of slag is the presence of a glass phase that interacts with alkalis during hardening on a special surface of 300m^2/kg. As the number of small particles in the slag increases, the number of structural defects with high surface energy increases, which increases the hardening rate and strength of concrete. As an activating alkaline component, caustic and anhydrous soda, potash, soluble glass-sodium silicate, as well as various man-made alkaline wastes are more commonly used, which allows to obtain a significant amount of slag binders.

The optimal composition of alkaline compounds in the binders is 2-5% by weight of slag. The high activity of alkali metal compounds compared to calcium compounds allows to obtain a fast-setting and high-strength concrete. The presence of alkalis intensifies the disintegration and dissolution of the slag glass in the solution, creating an environment conducive to the formation and high stability of alkaline hydroaluminosilicates and low-base calcium hydrosilicates. The low solubility of the newly formed particles determines the stability of the structure over time, the durability of the slag-alkali stone.

When slag cement is used in the production of concrete, there are fewer voids and pores in the structure of the resulting cement stone, unlike ordinary Portland cement. The difference between this binders and Portland cement is its high resistance to water and frost and its low adhesion and fraction properties.

Azerbaijan State Oil and Industry University has prepared fine-grained concrete consisting of 5-10% man-made waste (burnt foundry sand) [5]. As a continuation of this work, we set a goal to prepare slag-alkali concrete.

The mineral component used is ground and granulated blast furnace slag from the metallurgical waste of “Elektrotechonline”, Sumgayit. Granulated kiln slag is a man-made waste formed during the smelting of iron ore and is formed as a result of rapid cooling of the slag melt with water. This was made possible by the simultaneous installation of laboratory grinding equipment - a centrifugal mill and a magnetic separator - for fine grinding of metallurgical slages. In this case, the free iron particles inside the slag are completely removed.

EXPERIMENTAL PART

In a centrifugal mill, the crushed slag has isometric particles with an amorphous surface, which increases the activity of the slag. The bulk of granulated kiln slag is the glass phase, which varies between 66.6 and 95% [6]. Minerals in slags - bicalcium silicate, basaltic melilite, gelenite, melvinite crystallize (table 1).

The basic modulus is a characteristic of the activity of metallurgical slags and their resistance to decomposition, and is determined by the ratio of basic oxides in slag to acid oxides according to the following formula:

ISNN: print 2663-7006; online 2709-2666

Table 1

Chemical composition of granulated high-temperature kiln slag and glass waste (%)

mass, %	Ingredients, %							
	SiO_2	CaO	MgO	Al_2O_3	Fe_2O_3+FeO	MnO	SO_3	Na_2O+K_2O
Blast furnace slag	21	38	10	4,8	18	5	0,46	0,34
Glass waste	73,8	7-9	3-4	1,2-3,3	0,2-0,5	-	0,5	14

$$M_0 = \frac{CaO + MgO}{SiO_2 + Al_2O_3}$$

Here CaO, MgO - the composition of the main oxide in the slag;

SiO_2, Al_2O_3 - the composition of acid oxide in the slag.

For slags with more than one base modulus, all alkaline compounds or mixtures there of may be used. The basic modulus of the granulated kiln slag under study is 1.9.

Preliminary grinding of blast-furnace slags was carried out in a centrifugal impact mill with a built-in separator. The principle of operation of the mill is based on the mechanical acceleration of particles and their impact on an obstacle. The grain composition of the slag crushed in is shown in table 2. The physical properties of granulated kiln slag are given in table 2.

Table 2.

Physical properties of granulated kiln slag

Feature	Parametr
Fractional composition < 80 mkm	96,0
Fractional composition < 20 mkm,	60,0
Special surface area, m2/kg	450
basic module	1,9
actual density, kg/m3	2850
bulk density, kg/m3	1140

Grinding of the material takes place under high pressure and, by means of a centrifugal separator, allows to obtain a product with a high specific surface area of 450 m^2/kg.

Technical NaOH alkali was used as an alkaline activator (GOST R 55064-2012).

An aluminum-containing additive was used as a modifier. The composition of waste from Ganja Aluminum Plant according to macro components is as follows composition, (% of mass): $A1_2O_3$ -45-47; MgO-0,73; SO_2 -7.9; TiO_2 - 4.4; Fe_2O_3 -13-18; CaO - 3; K_2O- 0,16.

The qualitative composition of the sand, the modulus of size of the grains were determined in accordance with the methodology [7] by laboratory scales and sieves. Absheron sand with medium size modulus (M = 1,1) was used for concrete preparation. This sand meets the standard requirements developed for construction works.

Obtaining liquid glass with the help of alkaline and modifying aluminum additives was carried out in accordance with the developed technology:

- Obtaining a powdered waste mixture with 30% NaOH solution;
- processing at low temperature (90-95°C) with continuous stirring for 4-6 hours;

- cooling of the purchased mineral glass.

A YAW-300D laboratory machine were used to perform the strength and compression tests.

RESULTS AND DISCUSSION

The properties of slag cement are regulated by changing the composition of the components and depend on the type of slag, the mineral composition and specific surface, the type and concentration of the solution of the alkaline component. The optimal composition for maximum activity without autoclave hardening was determined: steel slag -52%; crushed glass - 37%; modifying aluminum-containing additive - 11%; alkaline activator - 7.4% (depending on the weight of the binder). All components are ground together to a specific surface area of 4500 sm^2/g.The ratio of water/binder and the type of activator affect the strength of the slag cement.

In the process of research, the optimal mode of heat and moisture treatment was determined, which allows to obtain an binders with an activity higher than 25,0 MPa.

The influence of the properties and proportions of the components on the rheological, structural and strength properties of slag-alkaline cement was studied during laboratory researches. Also, research was conducted on the main technological parameters of the production of fine-grained clinker-free concrete obtained on the basis of modified slag glass binder.

The study of the effect of binder : filler ratio 1: 1, 1: 2, 1: 3 and 1: 4 on the properties of concrete made with slag-glass binder shows that fine-grained concrete without clinker (fig.1) has higher strength with mixed aggregate. With the formation of gel-like compounds in the contact zone, the binder chemically interacts with alkaline and moisturizing products, due to the self-compression effect leads to an increase in the density of cement stone not only in the contact zone but also in concrete as a whole. Increasing the density of concrete helps to improve its physical and mechanical properties and structural properties.

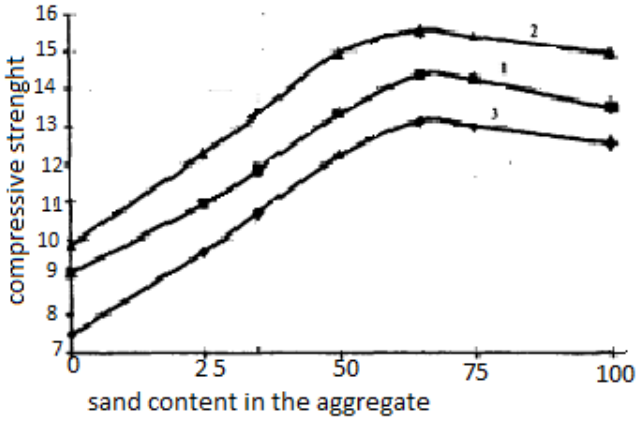

Fig.1. Percentage of sand in the aggregate

Figure 1. and the effect of 1: 2, 1: 3 and 1: 4 ratio of glass-slag binder and filler on the strength of concrete.

As a results of the work clinker-free concrete was prepared on the basis of slag-alkaline cemento using waste.

At the same time, the effect of the properties of the components and the ratio of

ISNN: print 2663-7006; online 2709-2666

components on the quality characteristics of the concrete obtained during the study was studied and its composition was optimized. The conditions of hardening of concrete depending on the effect and duration of wet-heat treatment were studied.

Studies have shown that fine-grained clinker-free concrete without autoclave hardening has high performance: in terms of mechanical strength - 15-20 MPa, frost resistance - more than 200 cycles; water absorption - not more than 6%, has increased operational stability and corrosion resistance in aggressive environments.

CONCLUSION

1. Developed theoretical positions of solidification of non-clinker binder, consisting of waste fined slag, crushed glass, modifying alumina-containing compound and alkali activator.

2. The possibility of using a clinker-free binder to obtain fine-grained concrete and products based on them has been theoretically substantiated and practically confirmed, which opens up a new effective way for the disposal of waste from steelmaking, broken glass and aluminum-containing waste from the industry.

3. Optimal composition of non-clinker binding activity of 25.0 MPa: dump steel slag -52%; crushed glass - 37%; modifying aluminum-containing additives -11%; alkaline aktivatior - 7.4% (from the mass of binding).

4. It is established that for the production of fine-grained concrete grades M 150 is not required: 25% of clinker binder and 75% of mixed aggregate, consisting of 30% of dumped slag and 65% of sand. With a water-binding ratio of 0.33.

As a result of the research, a high-strength hydraulic binders (modified concrete) without clinker was obtained on the basis of steel slag, which makes up a large percentage of man-made waste in the metallurgical industry of Azerbaijan. Economic calculation of costs and laboratory experiments show the practical feasibility and economic feasibility of industrial production of slag cement binders.

REFERENCES

1. Dvorkin L.I., Dvorkin O.L. Construction materials from industrial wastes: textbook-reference manual. Rostov nD: Phoenix, 2007, 368 p
2. Adilkhodjaev A.I., Mahamataliev I.M., Tsoi V. M., Shaumarov S.S. Scientific-based method of selection of additives when designing the composition of complex-modified concrete. Scientific and technical bulletin of Bryansk State University. 2019, №2, pp.269-279.doı. org/10.22281/413-9920-2019-05-02-269-279
3. Nahaev M., Salamanova M., Ismailova Z.Regularıtıes of the processes of formatıon of the structure and strength of a clınker-free bınder of alkalıne actıvatıon. 2020, Construction Materials and Products 3(1) pp. 21-29. doı.org/10.34031/2618-7183-2020-3-1-21-29
4.. Rudnov V.S., Belyakov V.A. New knitting materials from man-made waste / Congress TECHNOGEN-2017. "Basic Research and Applied Development processes of processing and utilization of technogenic formations",. Ekaterinburg. 2011, pp.82-84
5. Babayev I., Jafarova N. Use of burned mold soil. “Annali d’Italia” 2021, №17, Vol.1, pp.25

6.. Xobatova Э.B.,. Kalmykova Yu. C.Oxide composition of slag-binding slags on the basis of decomposed blast-furnace slag.NTP and production efficiency. Kharkov, 2014, №3, (121), pp.47-52
7. AZS 474 - 2011. (GOST 8735-88) State standard of the Republic of Azerbaijan. GUM for construction work. Specifications.

МОДИФИЦИРОВАННЫЕ БЕТОНЫ НА ОСНОВЕ БЕСКЛИНКЕРНЫХ ВЯЖУЩИХ

Э.Ф.Асланов[0000-0002-1894-1242], Н.А. Джафарова[0000-0001-5669-6631], Т.К. Шерифова[0000-0001-6689-3102]
Азербайджанский Государственный Университет Нефти и Промышленности
hteyfa@gmail.com

Обсуждается исследование свойств высокопрочных бетонов на основе новых вяжущих веществ, изготовленных из техногенных отходов. Разработаны теоретические положения твердения бесклинкерного вяжущего, состоящего из совместноизмельченного отвального сталеплавильного шлака, стеклобоя, модифицирующей алюмосодержащей добавки и щелочного компонента, твердеющего в условиях тепловлажностной обработки. Определены оптимальные составы бесклинкерного вяжущего и мелкозернистого бетона на его основе. При 25,0 МРа активности бесклинкерного вяжущего в составе бетона имеется (металлургического отхода) шлак - 52 %; стеклобоя - 37%; модифицирующей алюмосодержащей добавки -11%; щелочи (активатор) - 7,4 % (от массы вяжущего). Установлено, что для получения мелкозернистого бетона марки М 150 необходимо: 25 % бесклинкерного вяжущего и 75 % смешанного заполнителя, состоящего из 35 % отвального сталеплавильного шлака и 65 % песка. При водо/вяжущем отношении 0,33.
Ключевые слова: *бесклинкерный цемент, отходы, модифицированный бетон, металлургические шлаки, стеклощелочное вя жущее вещество, шлакцемент.*

KLİNKERSİZ YAPIŞDIRICILAR ƏSASINDA MODİFİKASİYALI BETONLAR

E.F.Aslanov[0000-0002-1894-1242], N.Ə. Cəfərova[0000-0001-5669-6631], T.K.Şərifova[0000-0001-6689-3102]
Azərbaycan Dövlət Neft və Sənaye Universiteti
hteyfa@gmail.com

Məqalə texnogen tullantılardan hazırlanan yeni yapışdırıcılar əsasında yüksək möhkəmlikli betonun xassələrinin öyrənilməsindən bəhs edilir. Klinkersiz bağlayıcının bərkiməsinə dair nəzəri müddəalar işlənib hazırlanmışdır ki, bunlar birgə əzilmiş poladəritmə posaları və şüşə tullantılarından, modifikasiyaedici alüminium tərkibli əlavədən və istilik - nəm emal şəraitində bərkiməni aktivləşdirən qələvi komponentdən ibarətdir. Klinkersiz yapışdırıcı və onun əsasında incə dənəli betonun optimal tərkibləri müəyyən edilmişdir. Klinkersiz bağlayıcının aktivliyinin 25,0 MPa həddində tərkib (metallurgiya tullantıları) şlak -52%; şüşə qırıntıları - 37%; modifikasiya edici alüminium əlavəsi -11%; qələvi (aktivator) - 7,4% (yapışdırıcının çəkisinə görə) ibarət olmalıdır. Müəyyən edilmişdir ki, M 150 markalı incə dənəli beton almaq üçün 25% klinkersiz bağlayıcı və 75% doldurucudan, doldurucu kütləsi isə 35% poladəritmə şlakından və 65% qumdan ibarət olan qarışıq hazırlamaq lazımdır. Bu halda, su/bağlayıcı nisbəti 0,33 təşkil edir.
Açar sözlər*: klinkersiz sement, tullantılar, modifikasiyalı beton, metallurgiya posaları,şüşə-qələvi bağlayıcı, posalı sement.*

ISNN: print 2663-7006; online 2709-2666

AJCN, Vol 4, No. 1, 2022, pp. 54-59

https://doi.org/10.32010/AJCN05012022-54

UDC:547.56.563.364

AMINOMETHOXY DERIVATIVES OF CYCLOHEXANOL AS BIOCORROSION INHIBITORS

S.V. Ismayilova [0000-0001-7399-5510]

I*nstitute of Petrochemical Processes of Azerbaijan National Academy of Sciences,*

ismayilova_s_ch@mail.ru

Based on cyclohexanol, aliphatic amines (diethylamine, dipropylamine, dibutylamine, dihexylamine), and formaldehyde, new Mannich bases have been synthesized. The reaction was carried out at a temperature of 78–80°C for 4–5 h in a benzene solution at an equimolar ratio of the starting components. The yield of compounds was 63–80%. The physicochemical data of the synthesized compounds were determined. The composition and structure of the target products were confirmed by elemental analysis, IR, ^{1}H and ^{13}C NMR spectroscopy. Their influence on the vital activity of sulfate-reducing bacteria (SRB) of the "Desulfovibrio desulfuricans" type at three concentrations (25; 50; 100 mg/l) was studied. The resulting compounds showed high bactericidal properties. 1% solutions of these compounds in isopropyl alcohol at a concentration of 100 mg/l showed a 100% bactericidal effect. Given that these aminomethoxy derivatives of cyclohexanol affect bacteria at very low concentrations, they can be proposed as effective inhibitors against sulfate reducing bacteria.

***Keywords**: cyclohexanol, aliphatic amines, Mannich bases, sulfatereducing bacteria, inhibitor-bactericides, biocorrosion.*

INTRODUCTION

One of the economic and environmental problems of oil companies is the difficulties that arise due to corrosion during oil production and transportation of oil. Corrosion leads to the destruction of production units, tubing and drilling equipment. A significant part of the corrosion damage of oilfield equipment is due to the vital activity of a number of microorganisms that enter oil reservoirs with river, lake, sea and waste water pumped into it, previously untreated from bacteria [1]. In this case, the wells become infected with SRB and other microorganisms. This complicates the operation of the field and thereby accelerates the corrosion of oil industry equipment, and also significantly reduces the quality of oil, thereby complicating oil refining. Oil companies are showing increased interest in inhibitors, which, along with slowing down hydrogen sulfide and carbon dioxide corrosion of metal equipment, have a bactericidal effect on SRBs [2–4].

Organic compounds containing various functional groups and heteroatoms, such as sulfur and nitrogen, along with biological activity, are characterized by antimicrobial activity. Among the biologically active compounds of the cyclohexane series, their amine-containing derivatives stand out, the value of which is associated with the presence of two pharmacophore fragments in their molecules - a nitrogen-containing group and a cyclohexane ring [5,6].

One of the easy and widely used methods for obtaining nitrogen-containing compounds is the aminomethylation reaction. Mannich bases, having pronounced antimicrobial and antifungal properties, have found their application as bactericide inhibitors [7,8]. Mannich bases with a cyclohexane fragment, which have a wide range

ISNN: print 2663-7006; online 2709-2666

of properties, also exhibit bactericidal properties, but their effect against the growth of SRBs has been little studied [9,10].

EXPERIMENTAL PART

This paper presents the results of the synthesis and study of the properties of aminomethoxy derivatives of cyclohexanol. For this purpose, the Mannich condensation reaction of cyclohexanol (I), formaldehyde (II) and secondary aliphatic amines [diethylamine (III), dipropylamine (IV), dibutylamine (V), dihexylamine (VI)] was carried out. The reaction proceeds according to the following scheme:

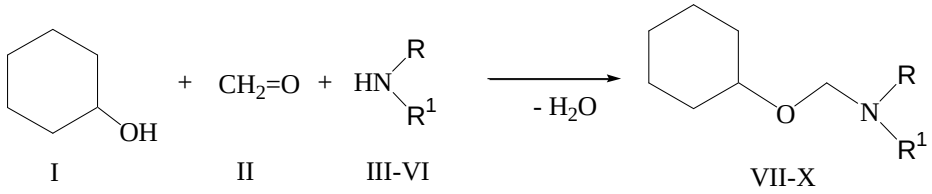

I II III-VI VII-X

R=R_1= C_2H_5 (III, VII), C_3H_7 (IV, VIII), C_4H_9 (V, IX), C_6H_{13} (VI, X)

The reaction was carried out at a temperature of 78–80°C for 4–5 h in a benzene solution at an equimolar ratio of the starting components. The yield of the compounds was 63–80%, with the maximum yield obtained using diethylamine.

To a mixture of 0.1 mol of formaldehyde (II) and 0.1 mol of cyclohexanol (I) in benzene, add 0.1 mol of secondary amine (III–VI) dropwise at 20–22°C with stirring. After cooling, the mixture was washed with 10% ammonia solution, then with distilled water until neutral and dried over anhydrous $MgSO_4$. After distilling off benzene, the residue was distilled in vacuo. Target compounds are liquids with a characteristic odor, insoluble in water, and readily soluble in organic solvents. The composition and structure of compounds (VII–X) were established on the basis of elemental analysis, IR, ^1H, and ^{13}C NMR spectroscopy. The physicochemical properties of the obtained compounds (VII–X) are presented in table 1.

Table 1

Physico-chemical properties of compounds (VII–X)

Compounds	T_{boil}, °C (p, mm.Hg)	n_D^{20}	d_4^{20}	Yield, %	Brutto-formul
N,N-Diethylaminomethoxy-cyclohexane (VII)	111 (3)	1.4531	0.8861	80	$C_{11}H_{23}NO$
N,N- Dipropylaminomethoxy-cyclohexane (VIII)	119 (3)	1.4551	0.8717	71	$C_{13}H_{27}NO$
N,N- Dibutylaminomethoxy-cyclohexane (IX)	121–122 (4)	1.454	0.8606	63	$C_{15}H_{31}NO$
N,N- Dihexylaminomethoxy-cyclohexane (X)	138–141 (8)	1.457	0.8771	65	$C_{19}H_{39}NO$

In the IR spectra of all synthesized cyclohexanol derivatives (VII–X), there is no absorption band in the region of 3334 cm^{-1}, which is characteristic of the hydroxyl group, and absorption bands are observed in the regions of 1232 and 1024 cm^{-1}, related to the stretching vibrations of the R_3N group, absorption bands in the regions 1150,

ISNN: print 2663-7006; online 2709-2666

1134, and 1070 cm^{-1} refer to the stretching vibrations of the ether bond (C–O–C). The IR spectra of compounds (VII-X) also confirm the structure of the synthesized compounds (fig. 1).

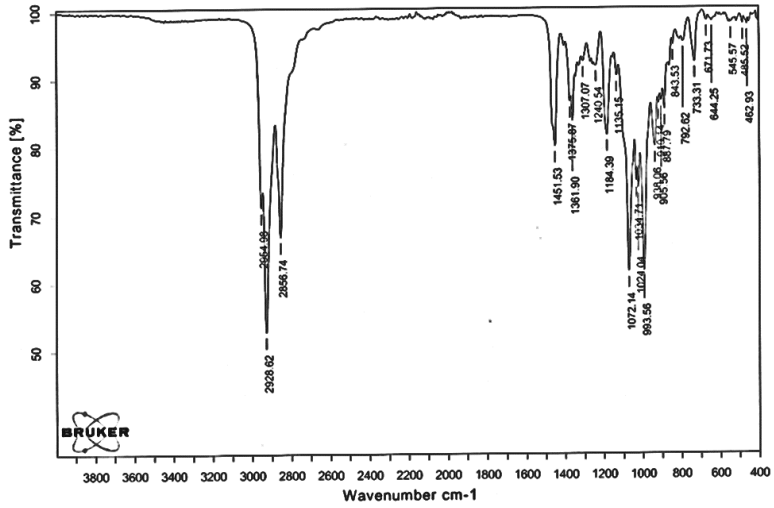

Fig. 1. IR spectrum of N,N-dihexylaminomethoxycyclohexane (X)

The ^{1}H and ^{13}C NMR spectra of compounds (VII–X) also confirm the structure of the synthesized compounds. The protons of the methyl group in the position of the amine fragment give a signal at approximately δ = 0.86 ppm. in the form of a triplet (fig. 2). The protons of the methylene groups give signals in the ranges δ = 1.2–1.86 ppm. in the form of a multiplet, and the protons of the CH_2–N–CH_2 group, in the regions δ = 2.4–2.78 ppm. The CHO proton of the cyclohexane ring gives signals approximately in the region of δ = 4.07 ppm. in the form of a doublet of doublets. The protons of the OCH_2N group give signals approximately in the regions δ = 4.4 ppm. in the form of a doublet of doublets (J = 2.5 Hz, J = 6.5 Hz).

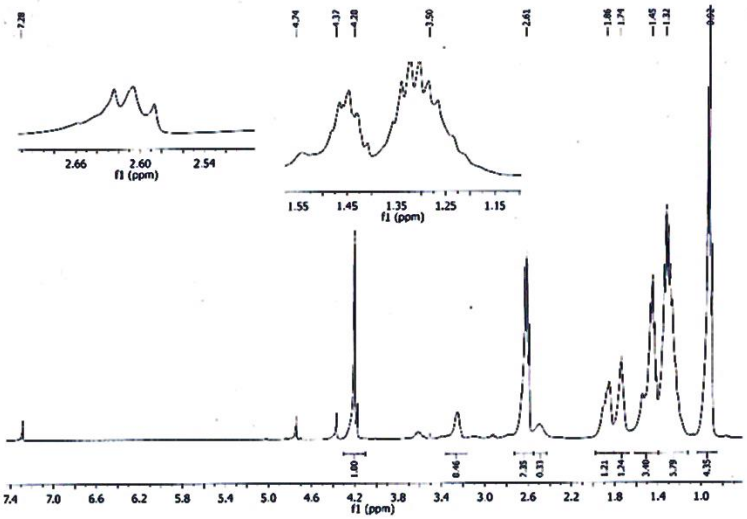

Fig. 2. ^{1}H NMR spectrum of N,N-dibutylaminomethoxycyclohexane (IX)

RESULTS AND DISCUSSION

The bactericidal-inhibiting properties were studied according to OCT 39-234-89 at three concentrations (25; 50; 100 mg/l), *1143 strains of Desulfovibrio desulfuricans* were used as SBR, the nutrient medium was Postgate B, pH 7.0–7.5, the duration of incubation was thermostat at 30–32°C - 15 days.

The synthesized compounds (VII–X) were studied as inhibitor-bactericides against SRB according to the procedure [11]. For this purpose, 1% solutions of compounds (VII–X) in isopropanol were prepared. The bactericidal effect of the reagents is studied mainly by observing for 15 days and calculating the amount of H_2S formed at the end of the experiment. The formation of H_2S is determined by iodometric titration. For comparison, 2 samples without reagent were taken: control 1 and control 2. Control 1 – only Postgate B nutrient medium, control 2 – nutrient medium and SRB cultures. The results of the study are presented in table 2.

Table 2

Inhibitor-bactericidal properties of 1% solutions of compounds (VII-X) in isopropanol

Reagent	Concentration, c, mg/l	Number of bacteria (number of cell/ml)	Amount of H_2S, mg/l	Bactericidal effect, Z-%
VII	25	10^7	213	16.4
	50	10^4	89	60
	100	10^1	9.6	96.2
VIII	25	10^6	162	36.4
	50	10^3	57	76
	100	10^1	8.2	98
IX	25	10^4	105	52.7
	50	10^1	25	91
	100	–	–	100
X	25	10^2	45	82
	50	10^1	7.8	97.6
	100	–	–	100
Control 1		–	14.0	–
Control 2		10^8	222.0	–

Table 2 shows that all three samples showed high bactericidal properties. Moreover, 1% solutions of compounds (IX) and (X) at a concentration of 100 mg/l showed 100% bactericidal effect. A 1% solution of compounds (VII) and (VIII) at a concentration of 100 mg/l showed 96.2% and 98% bactericidal effect. Compounds (VII-X) at a concentration of 50 mg/l showed 60%, 76%, 91%, 97.6% bactericidal effect, respectively. And at a concentration of 25 mg/l, the bactericidal effect of compounds (VII–X) was 16.4%, 36.4%, 52.7, and 82%, respectively.

CONCLUSION

1. Three-component Mannich reaction of cyclohexanol, formaldehyde and secondary aliphatic amines was used to obtain aminomethoxy derivatives of cyclohexanol. The yield of compounds was 63–80%. Their physicochemical properties

ISNN: print 2663-7006; online 2709-2666

were determined, the composition and structure of the obtained compounds were confirmed using elemental analysis data, IR, ^{1}H, ^{13}C NMR spectroscopy.

2. The influence of the synthesized compounds on SRBs of the "*Desulfovibrio desulfuricans*" type was tested at three concentrations (25; 50; 100 mg/l). Based on the amount of hydrogen sulfide formed, the bactericidal effect of the presented samples was calculated. It was found that at a concentration of 100 mg/l, compound (VII-X) had 96.2%, 98%, and 100% bactericidal effect, respectively. It has been established that 1% solutions of aminomethoxy derivatives of cyclohexanol exhibit high bactericidal activity, and they act on bacteria at very low concentrations.

REFERENCES

1. Tsygankova L.Ye., Lebedev P.V., Kovynev S.G., Dubinskaya Ye.V. Bakteritsidnoye deystviye ingibitora korrozii INKORGAZ-11TD po otnosheniyu k sulphatredut-siruyushchim bakteriyam // Vestnik TGU. 2012, T. 17, № 4, pp.1138-1142
2. Lia X., Lana Sh., Zhuc Zh., Zhanga Ch., Zenga G., Liua Y., Caoa W., Songa B., Yanga H., Wanga Sh., Wua Sh. The bioenergetics mechanisms and applications of sulfate-reducing bacteria in remediation of pollutants in drainage: A review // Ecotoxicology and Environmental Safety. 2018, Vol.158, pp. 162-170
3. Andreev N.N., Kuznetsov Yu.I., Fedotova T.V. On corrosion protection of steel with solutions of volatile inhibitors // Protection of Metals. 2001, Vol.37, № 1 pp.1-8 doi.org/10.1023/A:1004875630903
4. Guan F., Zhai X., Duan J., Zhang M., Hou B. Influence of sulfate-reducing bacteria on the corrosion behavior of high strength steel EQ70 under cathodic polarization // PLOS ONE. 2016, Vol.11(9), pp 1-22
5. Ismailova S.V., Mammadbeyli E.H., Gurbanov A.I., Muradova S.A. Synthesis and properties of chiral dialkylaminomethoxy derivatives of *l*-(–)-menthol // PPOR. 2019, Vol. 20(2), pp. 168–176
6. Sarvesh S.H., Raymond J.B., Vivekanand V.G., Sanket K.G., Luann R.D. Synthesis, characterization and antimicrobial properties of mononuclear copper (II) compounds of N,N′-di(quinolin-8-yl)cyclohexane-1,2-diamine // Inorganica Chimica Acta Reviews. 2019, Vol.498, pp.119–129 doi.org/10.1016/J.ICA.2019.119020
7. Allochio Filho, J.F., Lemos, B.C., de Souza A.S., Pinheiro S. Multicomponent Mannich reactions: General aspects, methodologies and applications // Tetrahedron.2017,Vol.73(50),pp.6977-7004.doi.org/10.1016/J.TET.2017.10.063
8. Shuai Sh., Wenting Q., Pannan M., Ruining Li., Xianfeng L., Zhankui S. Three-component radical homo Mannich reaction // Nature Communications. 2021, Vol. 12(1), pp.1006-1012. doi.org/10.1038/s41467-021-21303-3
9. Hajieva G.E. Aminomethoxy derivatives of norbornenylmethanol as biocorrosion inhibitors // Theory and Practice of Corrosion Protection. 2020, Vol. 25(1),pp. 31-38.
10. Mamedbeyli E.G., Gadzhieva G.E., Ibragimli S.I., Agamalieva D.B. Norbornen-soderjashie osnovaniya Mannikha kak ingibitori biokorroziya // Neftepererabotka i neftekhimiya. 2020, № 2, pp. 20-23
11. Postgate J.R. The Sulfate-Reducing Bacteria (2nd Edition). University Press: Cambridge, 1984, 224 p

АМИНОМЕТОКСИПРОИЗВОДНЫЕ ЦИКЛОГЕКСАНОЛА КАК ИНГИБИТОРЫ БИОКОРРОЗИИ

С.В. Исмайылова[0000-0001-7399-5510]
Институт Нефтехимических Процессов НАН Азербайджана
ismayilova_s_ch@mail.ru

На основе циклогексанола, алифатических аминов (диэтиламин, дипропиламин, дибутиламин, дигексиламин) и формальдегида синтезированы новые основания Манниха. Реакцию проводили при температуре 78–80ºС в течение 4–5 ч в растворе бензола при эквимолярном соотношении исходных компонентов. Выход соединений составил 63–80%. Определены физико-химические свойства синтезированных соединений. Состав и строение целевых продуктов подтверждены методами элементного анализа, ИК, ^{1}H и ^{13}C ЯМР спектроскопии. Исследовано влияние их на жизнедеятельность сульфатвосстанавливающих бактерий типа "Desulfovibrio desulfuricans" в трех концентрациях (25; 50; 100 мг/л). Полученные соединения проявили высокие бактерицидные свойства. 1%-ые растворы этих соединений в изопропиловом спирте при концентрации 100 мг/л проявили 100%-ный бактерицидный эффект. Учитывая то, что указанные аминометоксипроизводные циклогексанола влияют на бактерии при очень низких концентрациях, их можно предложить в качестве эффективных ингибиторов против сульфатвосстанавливающих бактерий.
Ключевые слова: *циклогексанол, алифатические амины, основания Манниха, сульфатредуцирующие бактерии, ингибитор-бактерициды, биокоррозия.*

TSİKLOHEKSANOLUN AMİNOMETOKSİ TÖRƏMƏLƏRİNİN BİOKORROZİYA İNHİBİTORU KİMİ

S.V. İsmayılova[0000-0001-7399-5510]
Azərbaycan Milli Elmlər Akademiyasının Neft-Kimya Prosesləri İnstitutu
ismayilova_s_ch@mail.ru

Tsikloheksanol, alifatik aminlər (dietilamin, dipropilamin, dibutilamin, diheksilamin) və formaldehid əsasında yeni Mannix əsasları sintez olunmuşdur. Reaksiya 78–80℃ temperaturda, 4–5 saat ərzində, benzol məhlulunda ilkin maddələrin bərabər mol nisbətində aparılmışdır. Birləşmələrin çıxımı 63–80% təşkil edir. Sintez olunmuş birləşmələrin fiziki-kimyəvi göstəriciləri müəyyən edilmişdir. Maddənin quruluş və tərkibi element analizi, İQ, 1H, 13C spektroskopiya üsulları ilə təsdiq edilmişdir. Onların üç qatılıqda (25; 50; 100 mq/l) "Desulfovibrio desulfuricans" tipli sulfatreduksiyaedici bakteriyaların həyat fəaliyyətinə təsiri öyrənilmişdir. Alınmış birləşmələr yüksək bakterisid xassə göstərmişdir. Bu birləşmələrin izopropil spirtində 1%-li məhlulları 100mq/l qatılıqda 100% bakterisid təsir göstərmişdir. Tsikloheksanolun aminometoksi törəmələrinin çox aşağı qatılıqlarda bakteriyalara təsir göstərdiklərini nəzərə alaraq, onları sulfatreduksiyaedici bakteriyalara qarşı effektli inhibitorlar kimi təklif edilə bilər.
Açar sözlər: *tsikloheksanol, alifatik aminlər, Mannix əsasları, sulfatreduksiyaedici bakteriyalar, inhibitor-bakterisidlər, biokorroziya.*

ISNN: print 2663-7006; online 2709-2666

AJCN, Vol 4, No.1, 2022, pp. 60-64

https://doi.org/10.32010/AJCN5012022-60

UDC:546(656.87.21.22)

X-RAY DIFFRACTION STUDY OF BINARY ZINC-OXIDE CATALYSTS

T.Ch.Taghiyeva[0000-0002-0692-9043]
Azerbaijan State Oil and Industrial University
tahmina.taghiyeva@ufaz.az

The phase composition of binary zinc-containing catalysts was studied by X-ray diffraction. It was found that the formation of two phases of the initial oxides is observed in all the studied catalytic systems. So, samples of the Zr-Zn-O catalytic system consist of phases of zirconium and zinc oxides, samples of the Ce-Zn-O catalytic system consist of phases of cerium and zinc oxides, while samples of the Mg-Zn-O catalytic system consist of phases of magnesium and zinc oxides. It has been established that the crystallinity of binary zinc-containing catalysts varies in the range from 70% to 89%.

Keywords: *X-ray phase analysis, binary catalysts, zinc oxide, cerium oxide, zirconium oxide, magnesium oxide.*

INTRODUCTION

One of the most important monomers widely used in the petrochemical industry is acetone. It is used as a solvent and as a raw material in different chemical industries. Acetone is widely used in the chemical, paint, varnish, food, perfume, and textile industries [1,2]. There are different methods for production of acetone. Nowadays, the most widely used method is the cumene method of acetone production. This method is widely used in many countries, such as the USA, Italy, France, Germany, and others. However, this method has disadvantages. Benzene which is raw material of this process is carcinogenic. Cumene obtained as an intermediate product in this process is not environmentally friendly either. Moreover, in this reaction acetone is obtained together with phenol, what decreases the yield of acetone. Thus, the production of acetone is dependent on the market demands for phenol. The cumene route, the three-step process, not only uses fossil feedstock and shows low yields, but also is highly energy-consuming [1]. For this reason, new methods for acetone production are searched [2]. One of the most interesting methods for acetone production is the vapor phase reaction of ethanol. The vapor phase reaction of ethanol is an interesting method for producing acetone for many researchers. It is known from periodic literature that ethanol is converted to acetone in high yield on zinc containing catalysts [2–4]. It has been previously shown that ethanol is converted to acetone in high yield on binary zinc containing catalysts [5,6]. It is shown that the yield of acetone and the selectivity of the process with respect to acetone depend both on the reaction temperature and on the composition of the zinc oxide catalyst, which may be due to a change in the phase composition of binary zinc-containing catalysts, as well as the degree of their crystallinity. In this regard, in this work, an X-ray study of binary zinc-containing catalysts was carried out and the degrees of crystallinity of the synthesized samples were calculated. The phase compositions of binary zinc-containing catalysts were studied.

EXPERIMENTAL PART

Binary zinc oxide catalysts were prepared by mixing aqueous solutions of nitrate salts of cerium, zirconium, magnesium, and zinc. The resulting mixture was evaporated and dried at the temperature of 100°C, after which it was transferred into a porcelain cup and calcined at the temperature of 200–300°C until the complete release of nitrogen oxides. After that, the catalyst was calcined at the temperature of 700°C for 10 hours.

Thus, in each catalytic system Zr-Zn-O, Ce-Zn-O and Mg-Zn-O, 9 samples were prepared in various ratios of components, satisfying the following conditions:

$$mA/nB, \text{ where A- Zr, Ce and Mg; B-Zn; } m,n = 1 \div 9; \; m+n = 10.$$

X-ray studies were carried out on a "D2 Phaser" automatic powder diffractometer of the "Bruker" firm (CuKα-radiation, Ni-filter, $5 \leq 2\theta \geq 75°$). The degrees of crystallinity of all the formed phases were calculated using the DIFFRAC.EVA program on the D2 Phaser device.

RESULTS AND DISCUSSION

The results of the conducted X-ray studies showed that two phases of the initial oxides are formed in the Zr-Zn-O system: ZrO_2 and ZnO. Figure 1 shows the diffraction patterns of all nine ratios of the Zr-Zn-O catalyst system put together. ZrO_2 and ZnO oxides are also present at the beginning and end of these diffraction patterns. The analyzes of the obtained X-ray diffraction patterns show that all the samples consist of two phases and the percentage ratio of the components is preserved in all of them, which is evidenced by the regular change in the intensities of reflections in the diffraction patterns.

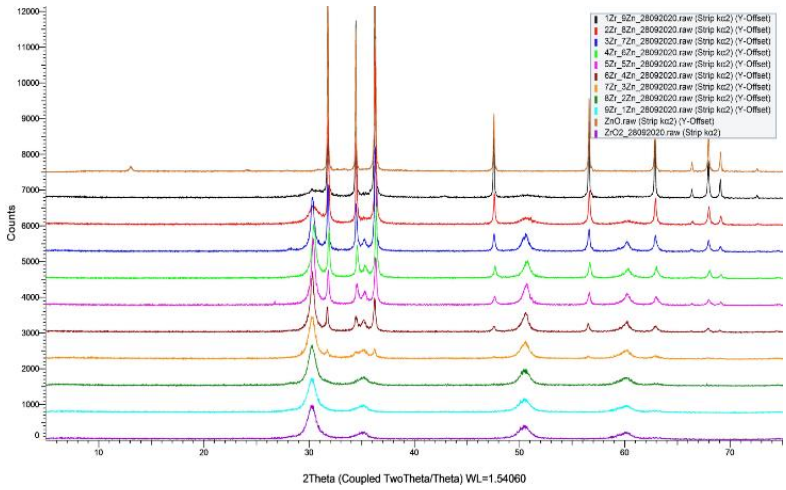

Fig. 1. X-ray diffraction patterns of zirconium and zinc oxides, as well as all nine samples of the Zr-Zn-O catalytic system.

Analysis and interpretation of diffraction patterns in the Ce-Zn-O system showed that at all ratios of cerium to zinc, the samples consist of two phases, namely, CeO_2 and ZnO. Figure 2 shows X-ray diffraction patterns of all nine ratios (mCr/nCu) put together. For comparative analysis, X-ray patterns of CeO_2 and ZnO are also presented at the beginning and end of these diffraction patterns. Analysis of X-ray

ISNN: print 2663-7006; online 2709-2666

patterns shows that all the studied samples of this catalytic system consist of two phases of cerium and zinc oxides. In all samples, the percentage ratio of the components is also preserved, as evidenced by the regular change in the intensities of reflections in the diffraction patterns.

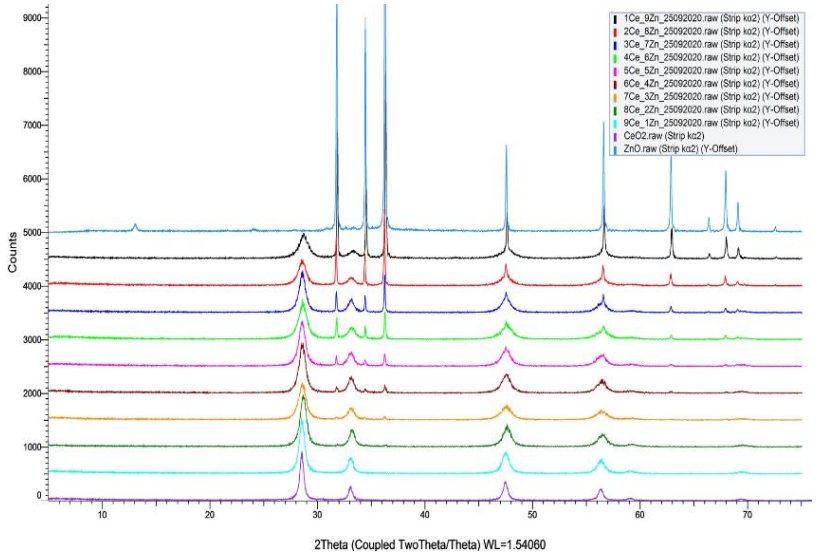

Fig. 2. X-ray diffraction patterns of cerium and zinc oxides, as well as all nine samples of the Ce-Zn-O catalytic system.

Figure 3 shows the diffraction patterns of all nine ratios of the Mg-Zn-O catalyst system put together. At the beginning and at the end of these diffraction patterns, X-ray diffraction patterns of the initial oxides of MgO and ZnO are also presented. An analysis of the obtained diffraction patterns showed that, as in the previous samples, the MgO and ZnO phases are formed at all ratios.

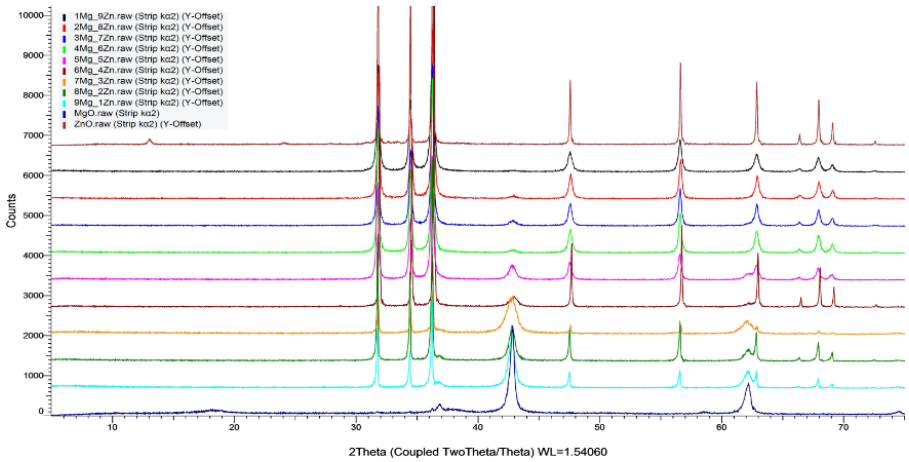

Fig.3. X-ray diffraction patterns of magnesium and zinc oxides, as well as all nine samples of the Mg-Zn-O catalytic system.

The results of calculating of degrees of crystallinity of all the formed phases presented in table 1. As can be seen from table 1, the crystallinity of the catalytic

systems Ce-Zn-O and Mg-Zn-O systems practically does not change with a change in the atomic ratio of cerium and magnesium to zinc in the composition of a binary catalyst, while with an increase in the content of zirconium in the composition of a binary catalyst, its crystallinity decreases from 80.7% on a Zr-Zn=1-9 sample to 70% on a Zr-Zn sample =9-1.

Table 1.

Crystallinity of samples of catalytic systems Zr-Zn-O, Ce-Zn-O and Mg-Zn-O

Ratio of the atoms	1-9	2-8	3-7	4-6	5-5	6-4	7-3	8-2	9-1
Zr-Zn-O	80,7	75,9	79,8	79,0	78,0	79,9	73,5	72,4	70,1
Ce-Zn-O	76,3	75,5	78,7	75,4	77,5	78,4	75,7	79,0	79,5
Mg-Zn-O	85.1	84.4	84	84.8	84	87.3	71.3	85.6	83.7

CONCLUSION

1. Binary zinc oxide catalysts with additions of zirconium, cerium, and magnesium consist of two phases of the initial oxides; from oxides of zirconium and zinc, oxides of cerium and zinc, as well as from phases of magnesium and zinc oxides.
2. The degree of crystallinity of binary zinc containing catalysts varies from 70% to 89%.

REFERENCES

1. R.Silva Calpa., Priscila C.Zonetti., Daniela C.de Oliveira., Roberto R.de Avillez., Lu cia G.Appel.Acetone from ethanol using ZnxZr1-xO2-y, Catalysis today. 2017, doi 10.1016/j.cattod.2016.09.011,pp.1-2
2. Nakajima T., Nameta H., Mishima S., Matsuzaki I., Tanabe K. A highly active and highly selective oxide catalyst for the conversion of ethanol to acetone in the presence of water vapour // Journal of Material Chemistry. 1994, 4(6). pp. 853–858. https://doi.org/10.1039/JM9940400853
3. Murthy R.S., Patnaik P., Sidheswaran P., Jayamani M. Conversion of ethanol to acetone over promoted iron oxide catalysis. J Catal. 1988,109. pp.298–302. doi:10.1016/0021-9517(88)90212-6
4. Bussi J., Parodi S., Irigaray B., Kieffer R. Catalytic transformation of ethanol into acetone using copper–pyrochlore catalysts. Applied Catalysis A. 1998, 172, pp. 117–129. doi 10.1016/S0926-860X(98)00106-9
5. Taghiyeva T.C., Baghiyev V.L.Phase composition and activity of Zr-Zn-O catalysts in the reaction of conversion ethanol // 2nd International Conference on Reaction Kinetics, Mechanism and Catalysis, Book of Abstracts, Budapest, Hungary. 2021, pp.26
6. Taghiyeva T.C., Baghiyev V.L. About Ethanol Conversion over Mg-Zn-O Catalyst. 6th International School-Conference on Catalysis for Young Scientists, Catalyst Design: From Molecular to Industrial Level. Abstracts. Novosibirsk, Russia. 2021, pp.284

ISNN: print 2663-7006; online 2709-2666

РЕНТГЕНОГРАФИЧЕСКОЕ ИССЛЕДОВАНИЕ БИНАРНЫХ ЦИНК ОКСИДНЫХ КАТАЛИЗАТОРОВ

Т.Ч.Тагиева.[0000-0002-0692-9043]
Азербайджанский Государственный Университет Нефти и Промышленности
tahmina.taghiyeva@ufaz.az

Рентгенографическим методом изучен фазовый состав бинарных цинк содержащих катализаторов. Найдено, что во всех изученных каталитических системах наблюдаются образование двух фаз исходных оксидов. Так образцы каталитической системы Zr-Zn-O состоят из фаз оксидов циркония и цинка, образцы каталитической системы Ce-Zn-O состоят из фаз оксидов церия и цинка, а образцы каталитической системы Mg-Zn-O состоят из фаз оксидов магния и цинка. Установлено, что кристалличность бинарных цинк содержащих катализаторов меняется в интервале от 70% до 89%.
Ключевые слова: *рентгенофазовый анализ, бинарные катализаторы, оксид цинка, оксид церия, оксид циркония, оксид магния.*

BİNAR SİNK-OKSİD KATALİZATORLARININ RENTGENOQRAFİK TƏDQİQİ

T.Ç.Tağıyeva.[0000-0002-0692-9043]
Azərbaycan Dövlət Neft və Sənaye Universiteti
tahmina.taghiyeva@ufaz.az

Rentgenoqrafik üsulla binar sink tərkibli katalizatorların faza tərkibi öyrənilmişdir. Aşkar edilmişdir ki, öyrənilmiş sistemlərin hamısında ilkin oksidlərin iki fazasının əmələ gəlməsi müşahidə olunur. Beləliklə, Zr-Zn-O katalitik sisteminin nümunələri sirkonium və sink oksidlərinin, Ce-Zn-O katalitik sisteminin nümunələri serium və sink oksidlərinin, Mg-Zn-O katalitik sisteminin nümunələri isə maqnezium və sink oksidlərinin fazalarından ibarətdir. Müəyyən edilmmişdir ki, binar sink tərkibli katalizatorların kristallikliyi 70%-dən 89%-dək aralığında dəyişir.
Açar sözlər: *rentgen faza analizi, binar katalizatorlar, sink oksid, serium oksid, sirkonium oksid, maqnezium oksid.*

AJCN, Vol 5, No. 1, 2022, pp. 65-72

https://doi.org/10.32010/AJCN05012022-65

UDC: 541.128.34:549.67:541.64:547:313

SEAL PRODUCTS AND THEIR ROLE IN THE PROCESS OF CONVERSION OF ISOBUTENE ON A HIGH SILICA ZEOLITE CATALYST

I. J. Ahmedova [0000-0003-3004-4242]
Azerbaijan State Oil and Industry University
ahmadovairada63@gmail.com

Conversion of isobutene on a high silica zeolite catalyst in the temperature interval (473-773 K) has been studied. The formation of liquid reaction products is observed at the temperature 473 K, whereas gaseous products form after 523K. Maximum yield of liquid products is observed at the temperature 573 K and makes up 67 %. With increase of contact time the yield of liquid reaction products shifts towards high temperatures. Formation of aromatic hydrocarbons is observed at the reaction temperature higher than 573 K. At the temperature 673 K the main mass of liquid products consists of aromatic hydrocarbons. The activity of H-form of HSZ (HHSZ) in the process of conversion of isobutene in the formation of liquid reaction products occurs only when 6-8% of seal products accumulate on its surface. By the method of ammonia adsorption on the initial and coked catalyst their acidic properties have been studied. It was shown that at the beginning of the process decrease in acidic properties of the catalyst occurs due to accumulation of seal products on it.

Keywords: *catalyst, activity, isobutene, zeolite, seal products, temperature, heterogen, chromatography, spectroscopy.*

INTRODUCTION

In a number of industrial processes of oil refinery and petrochemistry low molecular weight hydrocarbons C_2-C_5 form at different stages as by-products that can serve as raw materials for obtaining oligomers, high molecular weight and aromatic compounds. A large number of works are devoted to the low molecular weight hydrocarbons conversion study, mainly on natural and synthetic zeolites [1-3]. In these works the ways of different hydrocarbons conversion routes, affect of technological parameters on conversion rate and yield of different products, effect of the composition of a catalyst (ratio Si/Al) on the conversion rate were studied in detail. However, as final products of conversion of hydrocarbons only gaseous or liquid compounds were considered. Nevertheless, we know that in many heterogeneous-catalytic processes of conversion of initial hydrocarbons is followed by accumulation of coked seal products (SP) on the surface of catalyst, which, on the one hand, are final products of the process, on the other hand, they can affect on physico-chemical properties of a catalyst, and, therefore, on the process flow. Participation of SP in the catalytic process was mentioned before [6]. However, in the works listed above [1-3] formation of LH and their influence on the character of conversion of initial hydrocarbons wasn't considered.

In this work, along with the study of the general laws of isobutene conversion on a zeolite catalyst, the dynamics of SP accumulation on the catalyst surface has been

ISNN: print 2663-7006; online 2709-2666

studied, and an attempt is made to identify the cause of their influence on the hydrocarbon conversion process.

EXPERIMENTAL PART

In our work, the H-form of a high-silica zeolite (HHSZ, SiO_2/Al_2O_3 = 54.2, Na_2O (0.1 %)) was used as a catalyst. The process of isobutene conversion was carried out in a flow-through laboratory unit with an integral reactor at atmospheric pressure. The catalyst volume comprised 2 cm^3. Isobutene was obtained by dehydration of trimethyl carbinol on an alumina oxide catalyst at a temperature of 623 K. Before the carrying out the experiment, the catalyst was treated in a stream of air at a temperature of 773 K during 3 h, after which the oxygen from the system was removed with a stream of nitrogen purified from oxygen with copper chips at 573 K. The duration of the experiments was ~ 10 hours. The reaction products were analyzed on an LHM-8M1 chromatograph and on a PC-2O spectrophotometer. The activity of the catalyst was evaluated by the yield of liquid products.

Differential-thermal analysis of carbonized samples at different temperatures of the catalyst samples was carried out on a derivatograph of E. Paulik, N. Eddei of the "MOM" company in the temperature range of 20-1000 °C.

The accumulation of seal products on the HHSZ during the conversion of isobutene and the adsorption of ammonia on the initial and coked catalyst at different temperatures were studied on a gravimetric installation with McBen weights with a quartz coil.

RESULTS AND DISCUSSION

The isobutene conversion process at the HHSZ was carried out at 423-723 K and various volumetric speeds (300, 500 and 1000 h^{-1}) of its supply. The results of these experiments are presented in fig.1.

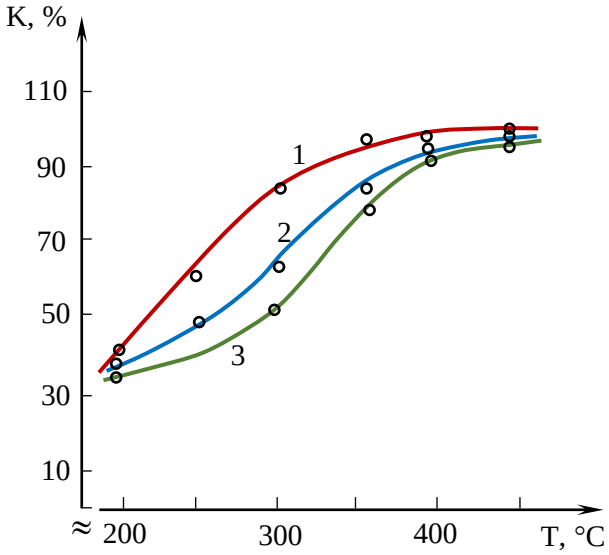

Fig.1. The dependence of isobutene conversion on temperature at various volumetric speeds: 1-300; 2-500 and 3-1000 h^{-1}.

At 473 K, the isobutene conversion degree made up 40.0; 38.4; 36.5 % at volumetric speeds of 300, 500, 1000 h^{-1}, respectively. With increase in temperature, the conversion degree increases and at 673-723 K almost complete (more than 98 %) conversion of isobutene is achieved at all the volumetric rates studied.

By means of chromatographic and infrared spectroscopic analysis, it was found that gaseous products consist of C_2-C_5 saturated and unsaturated aliphatic hydrocarbons, while liquid products, along with aliphatic ones, contain aromatic (benzene, toluene and xylenes) and 2.8 % unidentified hydrocarbons as well. On this basis, it may be assumed that, in addition to oligomerization, isobutene and the intermediate products of its conversion undergo dehydrogenation, isomerization, cracking, dehydrocyclization, etc.

The formation of gaseous products begins at a temperature of 523 K. In the process, C_2, C_3H_6 and C_3H_8 hydrocarbons are contained in the gas phase. The yield of gases at this temperature does not exceed 3 %. An increase in temperature to 573 K leads to the appearance of n-butane, butene-1, cis- and trans-butenes-2 in the products of the isomerization process. The yield of gases in this case reaches 18 % at large contact times. In the temperature range of 673-723 K, in addition to the listed gaseous products, C_5 hydrocarbons are also formed. The total yield of gaseous products is at the same time is 50-55 % and slightly depends on the contact time.

The formation of liquid hydrocarbons begins at 453 K. Up to a temperature of 523 K, as well as on other types of zeolites, the collected condensate consists only of isobutene dimers and trimers, the output of which at 473K is 33-40 % and weakly depends on the contact time. Increase in temperature to 573 K leads to a significant decrease in the yield of oligomers, however, the aromatic hydrocarbons benzene, toluene, and m-xylene appear in the reaction products. The dependence of the yield of liquid products on temperature is extreme. The dependence on the value of the volumetric rate, the maximum yield of liquid hydrocarbons falls at different temperatures. At low volumetric velocities (300-500 h^{-1}), the maximum yield of liquid products is reached at 573-623 K and amounts to 67 and 56 %, respectively. Increasing the volumetric rate leads to a shift of the maximum to higher temperatures. So, with a space velocity of 1000 h^{-1}, the largest yield of liquid hydrocarbons takes place at 673 K and makes up 65 %. Increase in temperature to 723 K leads to a decrease in the yield of liquid products, which is accompanied by an increase in the yield of gases.

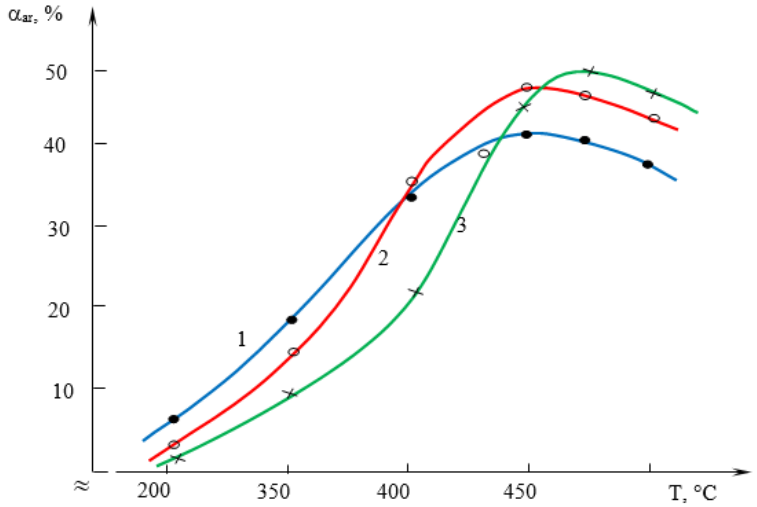

Fig.2. Dependence of the yield of aromatic compounds on temperature at different volumetric rates during the conversion of isobutene: 1-300; 2-500; and 1000 h^{-1}.

ISNN: print 2663-7006; online 2709-2666

The yield of aromatic hydrocarbons increases with temperature, and at 723K their total amount at volumetric rates of 300, 500, 1000 h^{-1}, makes up 41.9; 46.1; 46.4 %, respectively (fig.2). A further increase in temperature above 723 K leads to a decrease in the yield of aromatic hydrocarbons.

A characteristic feature of this process is the fact that in the initial period the catalyst exhibits non-stationary activity. Depending on the reaction conditions during the first 10-30 minutes after the start of the supply of isobutene, a high (more than 90 %) degree of isobutene takes place, however, there are no liquid hydrocarbons among the products of the process, and the gas phase contains only hydrogen and small amounts of methane. Then the degree of isobutene conversion decreases slightly, the hydrogen content in the gas decreases significantly, and methane almost disappears. At the same time, the formation of liquid products is detected, the yield of which first grows and then stabilizes. It was also found that during this period, coke-like compaction products are deposited on the catalyst.

Figure 3 depicts the accumulation of SP, the yield of liquid products as a function of time in the process of isobutene conversion, and the regeneration curve of the coked catalyst. As can be seen, under these conditions, 7.8 % of SP accumulates on the surface of the HHSZ catalyst during the transformation of isobutene (fig.3,cr.1) within 20–25 min from the beginning of the process. Only after this the catalyst acquires activity in the formation of liquid hydrocarbons, the output of which at 673 K amounts for 70 % (fig.3,cr.2). The regeneration curve of the coked catalyst (fig.3,cr.3) indicates the heterogeneity of the forming SP. The major part of them is removed by simply heating to 700 K in a stream of nitrogen. The remaining part can only be removed by oxidation with air at a higher temperature (723-773 K). The presence of heterogeneity of the composition of SP was previously detected by us in the processes of conversion of ethylene and butanes on a zeolite catalyst [4-6].

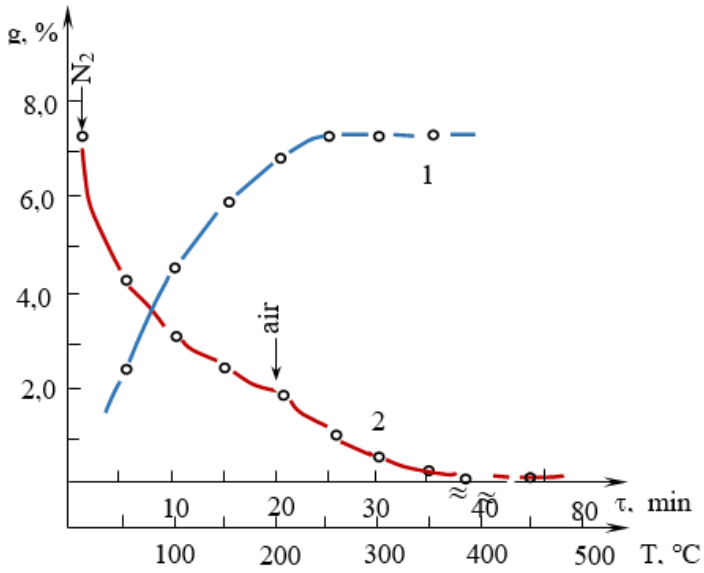

Fig.3. Dependence of the accumulation of PU (1), the yield of liquid products on time (2) and the regeneration of the catalyst on the temperature during the conversion of isobutene at 500 °C

In order to study the nature of accumulated compaction products, a differential thermal analysis was carried out on HHSZ samples coked in the process of isobutene conversion during 10 hours and without losing its activity (fig.4). On the DTA-curve of the initial samples, a small endothermic effect is observed, which can be attributed to the process of dehydration of the initial sample, and a smooth decrease in its mass takes place on the TG curve.

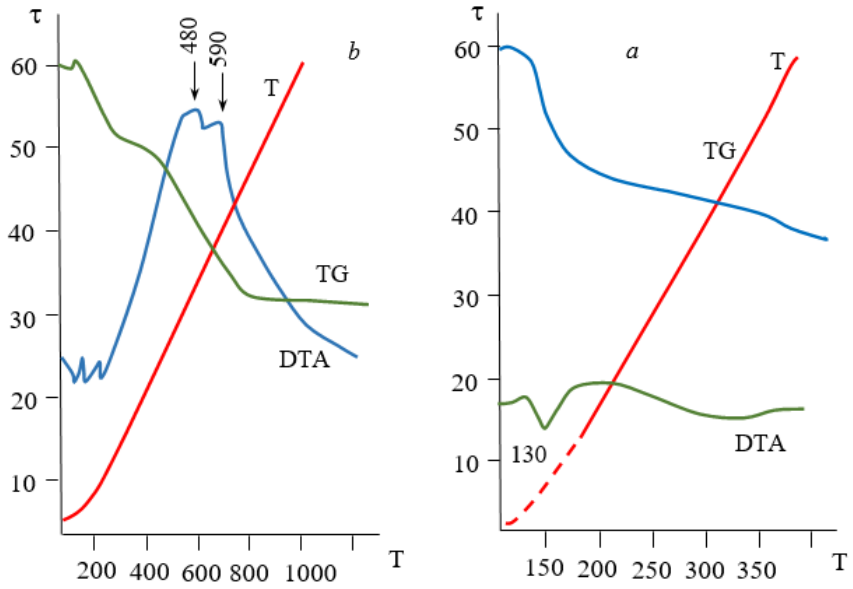

Fig.4. Differential thermal analysis of the initial (a) and carbonized HCB catalyst during the transformation of isobutene (b) at 673K.

On the thermogram of the sample coked at 673 K, the DTA curve has a vast exothermic effect with two maxima at temperatures of 753 K and 833 K (fig.4). The presence of two maxima on the DTA curve indicates the presence of two different components in the SP composition. The step form of the TG curve also proves the two-phase composition of PU accumulated at 673 K.

To explain this phenomenon, it may be assumed that there are a large number of strong acid sites on the surface of the initial catalyst, which provide strong adsorption of isobutene, which ultimately leads to its conversion into seal products. As the SP accumulate on the catalyst, some of these centers are blocked, what leads, on the one hand, to a decrease in the conversion of isobutene, and on the other, to its conversion to liquid products. After deposition on the surface of the maximum amount of SP for the given conditions, the process proceeds for a long time stationary and is characterized by stable in time values of the yields of gaseous and liquid products.

The acidic properties of the initial and coked catalysts were studied by measuring the amount of ammonia adsorption on a gravimetric unit with McBen weights at room temperature. The results are shown in fig.5.

As can be seen from the presented data, the initial catalyst is able to adsorb 8.6 % (mass., %) of NH_3, which is, as the calculation shows, about 3.10^{21} molecules of NH_3/g of the catalyst. Assuming that one molecule of NH_3 is sorbed at one acid center, it may be supposed that the concentration of acid centers on the surface of the initial catalyst makes up $3 \cdot 10^{21} g^{-1}$.

ISNN: print 2663-7006; online 2709-2666

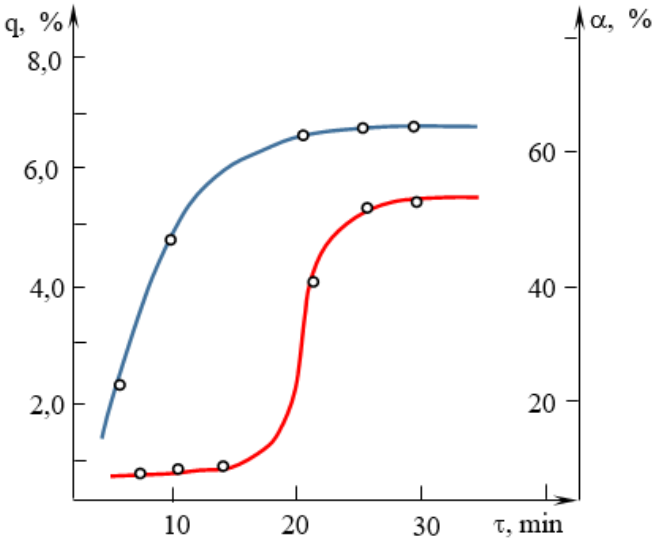

Fig.5. Dependence of the amount of adsorbed ammonia at room temperature on the initial (1) and on the coked at 673(2) catalysts during the conversion of isobutene on time.

It is obvious that the acidity of the catalyst is due to the presence of both Brensted and Lewis acid sites. Taking into account that oligomerization of olefins on zeolite catalysts takes place at both types of acid sites [4], it may be assumed that coke formation in this case takes place at both Brensted and Lewis acid sites. The termination of the formation of SP in 20 minutes after the start of the process suggests that during this period, seal products block all initial acid sites. However, new Brensted acid sites (H^+) are formed on the catalyst surface, at which olefin conversion can also occur. The presence of such acid sites is confirmed by the fact that NH_3 adsorption occurs on the coked catalyst (fig.5,cr. 2). The presence of such acid sites accounts for $1.8 \cdot 10^{21} g^{-1}$. Taking into account that coke formation does not occur at such acid sites, it can be assumed that they have less acidic strength .

CONCLUSION

1. The obtained experimental results indicate that in the initial period of the process, characterized by a high degree of conversion of the initial hydrocarbon and low yields of gaseous and, especially, liquid products, at the strong acid sites of the zeolite catalyst, mainly condensation reactions occur, accompanied by the formation of low molecular weight gaseous products (CH_4 and H_2).

2. At the same time, new Bronsted acid centers are formed on the surface of the resulting SP, at which the initial hydrocarbon is transformed into liquid aliphatic and aromatic products of the process. The stable activity of the catalyst is maintained for a long time. HHSZ - H-form of high-silic a zeolite (SiO_2/Al_2O_3 = 54.2, Na_2O<0.1 %) SP - seal products

REFERENCES

1. Andreia F., Silva, Auguste Fernandes, Margarida M. Antunes, Maria F. Ribeiro, Carlos M. Silva, Anabela A. Valente. Catalytic conversion of 1-butene over modified

versions of commercial ZSM-5 to produce clean fuels and chemicals. Chem. Cat. Chem. August 21, 2019, pp. 4196-4209. https://doi.org/10.1002/cctc.201801975
2. Blay V., Epelde E., Miravalles R., Perea LA. Converting olefins to propene: ethene to propene and olefin cracking. Catal Rev Sci Eng 2018; 60: 278e335. https:// doi.org/10.1080/01614940.2018.1432017
3. Dagle V.L, Smith C., Flake M., Albrecht K.O, Gray M.J., Ramasamy K.K, et al. Integrated process for the catalytic conversion of biomass-derived syngas into transportation fuels. Green Chem 2016; 18: 1880e91. https://doi.org/10.1039/ c5gc02298c.
4. Warnecke F., L. Lin, S. Haag., and Hannsjörg Freund. Identification of reaction pathways and kinetic modeling of olefin interconversion over an H-ZSM-5 catalyst. Ind. Eng. Chem. Res., Just Accepted Manuscript. . Publication Date (Web): 18 Jun 2020. doi.org /10.1021/acs.iecr.0c01747
5. Luqman Buchori., W. Widayat., Oki Muraza., Muhamad Iqbal Amali., Rahma Wulan Maulida, and Jedy Prameswari. Effect of Temperature and Concentration of Zeolite Catalysts from Geothermal Solid Waste in Biodiesel Production from Used Cooking Oil by Esterification–Transesterification // Process. Processes 2020, №8, pp.1629. https://doi.org/10.3390/pr8121629
6. Tobias C., Keller, Stéphane Isabettini., Danny Verboekend., Elodie G. Rodrigues and Javier Pérez-Ramírez. Hierarchical high-silica zeolites as superior base catalysts // Chem. Sci., 2014, №,5, pp.677-684. https://doi.org/10.1039/C3SC51937F

ПРОДУКТЫ УПЛОТНЕНИЯ И ИХ РОЛЬ В ПРОЦЕССЕ КОНВЕРСИИ ИЗОБУТЕНА НА ВЫСОКОКРЕМНЕЗЕМНОМ ЦЕОЛИТНОМ КАТАЛИЗАТОРЕ

И.Дж.Ахмедова, *0000-0003-3004-4242*
Азербайджанский Государственный Университет Нефти и Промышленности
ahmadovairada63@gmail.com

Изучена конверсия изобутена на высококремнеземистом цеолитном катализаторе в интервале температур (473-773 К). Образование жидких продуктов реакции наблюдается при температуре 473К, тогда как газообразные продукты образуются после 523 К. Максимальный выход жидких продуктов наблюдается при температуре 573 К и составляет 67%. С увеличением времени контакта выход жидких продуктов реакции смещается в сторону высоких температур. Образование ароматических углеводородов наблюдается при температуре реакции выше 573К. При температуре 673 К основная масса жидких продуктов состоит из ароматических углеводородов. Активность Н-формы НВКЦ в процессе превращения изобутена с образованием жидких продуктов реакции проявляется только тогда, когда на его поверхности накапливается 6-8% продуктов уплотнения. Методом адсорбции аммиака на исходном и закоксованном катализаторе изучены их кислотные свойства. Показано, что в начале процесса происходит снижение кислотных свойств катализатора за счет накопления на нем продуктов уплотнения.

Ключевые слова: *катализатор, активность, изобутен, цеолит, продукты уплотнения, температура, гетероген, хроматография, спектроскопия.*

ISNN: print 2663-7006; online 2709-2666

İZOBUTENİN YÜKSƏK SİLİSİUMLU SEOLİT KATALİZATORU ÜZƏRİNDƏ ÇEVRİLMƏSİ NƏTİCƏSİNDƏ ƏMƏLƏ GƏLƏN SIXLAŞMA MƏHSULLARI VƏ ONLARIN PROSESDƏ ROLU

İ. C. Əhmədova [0000-0003-3004-4242]
Azərbaycan Dövlət Neft və Sənaye Universiteti
ahmadovairada63@gmail.com

Yüksək silisiumlu seolit katalizatoru üzərində müxtəlif temperatur intervalında (473-773 K) izobutenin konversiyası tədqiq edilmişdir. Maye reaksiya məhsullarının əmələ gəlməsi 473 K temperaturunda müşahidə olunur, qazvari məhsullar 523 K temperaturdan sonra əmələ gəlir .Maye məhsulların maksimal çıxımı 573 K temperaturunda müşahidə olunur və 67% -təşkil edir. Kontaktın artması ilə, maye reaksiya məhsullarının çıxımı yüksək temperaturlara doğru dəyişir. Aromatik karbohidrogenlərin formalaşması 573K-dən yuxarı temperaturunda müşahidə olunur. 673K temperaturunda maye məhsulların əsas kütləsi aromatik karbohidrogenlərdən ibarətdir. Müəyyən olunmuşdur ki, izobutenin H-formalı yüksək silisiumlu seolit katalizatoru (HYSS) üzərində çevrilmə prosesində katalizatorun aktivliyi prosesin başlanğıc anından 25 dəqiqə müddətində 6-8% sıxlaşma məhsulları əmələ gəldikdən sonra müşahidə olunur. Ammonyak adsorbsiyası üsulu ilə onların turşu xüsusiyyətləri ilkin və oksigenlənmiş katalizatorda öyrənilmişdir. Göstərilmişdir ki, prosesin başlanğıcında katalizatorun turşu xassələrinin azalması onun üzərində sıxlaşma məhsullarının yığılması hesabına baş verir.

Açar sözlər: *katalizator, aktivlik, izobuten, seolit, sıxlaşma məhsulları, temperatur, heterogen, xromatoqrafiya, spektroskopiya.*

AJCN, Vol 4, No. 1, 2022, pp. 73-80

ttps://doi.org/10.32010/AJCN03032021-73

UDC:547.022.547.8

SYNTHESIS OF COMPLEXES OF DIAZACROWN ETHERS AND TRANSITION METALS AND INVESTEGATION OF THEIR BIOLOGICAL ACTIVITY

L.Z.Vazirova [0000-00030008-8973]
Azerbaijan State Oil and Industry University
vazirova.leyla@gmail.com

The synthesis of diazacrown ethers was carried out using efficient methods. New dibenzoazacrown ethers with functionally substituted hydroxyl and amino groups in the macrocyclic (MC) ring have been synthesized. The structure of the synthesized crown compounds - determined by IR mass NMR, -spectroscopy. Methods for the preparation of transition metal complexes with organic functional ligands based on diazacrown ethers having four, five, and six coordinating atoms in the rings. The synthesized new diazacrown ethers, due to hydroxyl and amino groups, increase the degree of intermolecular interactions and transfer from a two-dimensional structure to a three-dimensional one, which has an increased their biological activity.

Keywords: *Crown ethers, transition metals, biological activity,complex.*

INTRODUCTION

Methods for the synthesis of macrocyclic compounds are numerous and varied. On the other hand, complex macrocycles with multifunctional groups containing azacrown fragments have been studied to a much lesser extent [1,2]. One of the reasons for this is the instability of the obtained compounds in chemical reactions, which complicates the synthesis of aza crown ethers. In this regard, the search for new ways to obtain azacrown compounds under "soft" conditions is an urgent chemical problem. Basically, new methods of analysis and selective extraction of different inorganic ions, separation of isotopes of radioactive elements, obtaining special monomers, polymers and radiofrequency abrasions are formed on the basis of crown ethers [3]. Great works are on the application of production of crown-ethers for the creation of photo- and chemo sensors, selective for cations of metals, for photometric and fluorescent analysis of soil and water. At the same time, crow-ethers are all the more studied and used in excellent areas of science, for example, are actively conducting research on the biological and medical potential of these compounds and their metal complexes [4].

At the same time investigation of new antibacterial substances and associated with resistance to classical antibiotics and strains of pathogenic microorganisms is a main problem of modern medicine. The most interesting direction in the study of crown ethers and their metal complexes is the possibility of their use as amicrobial agents especially against gram negative and gram positive microorganisms [5-8].

EXPEREMENTAL PART

In order to further use new azacrown compounds were obtained. We studied the macrocyclization reactions of salicylic aldehyde with 1,4-dibromobutene-2 followed by

condensation with diamino compounds. We synthesized new dibenzoazacrown ethers by macrocyclization of salicylaldehyde with 1,4-dibromobutene-2 form 1,4-bis(2-formylphenoxy)-butene-2.Further condensation with diamino compounds, namely, ethylenediamine and triethyltetramine, and subsequent reduction of the corresponding bis-imine derivatives with sodium tetrahydroborate, led to the formation of new diazacrown ethers.

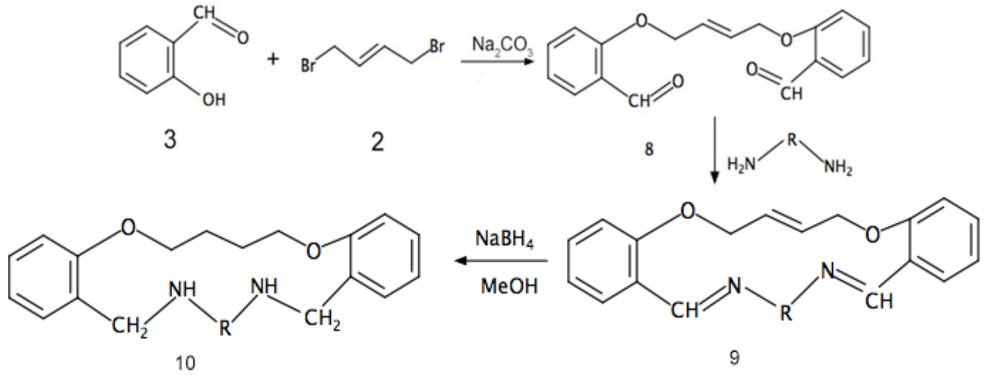

R = $(CH_2)_2$, $(CH_2)_3$, $(CH_2)_2NH(CH_2)_2$, $(CH_2)_2NH(CH_2)_2NH(CH_2)_2$, $(CH_2)_2O(CH2)_2O(CH_2)$

An alternative synthesis was also carried out by a two-stage method, including, at the first stage, the condensation of salicylaldehyde with the corresponding diamines, followed by the reduction of bis-imine derivatives with sodium tetrahydroborate. The second stage of the synthesis was a ring closure reaction of the corresponding derivative with 1,4-dibromobutene-2, leading to the formation of a diazacrown ether.

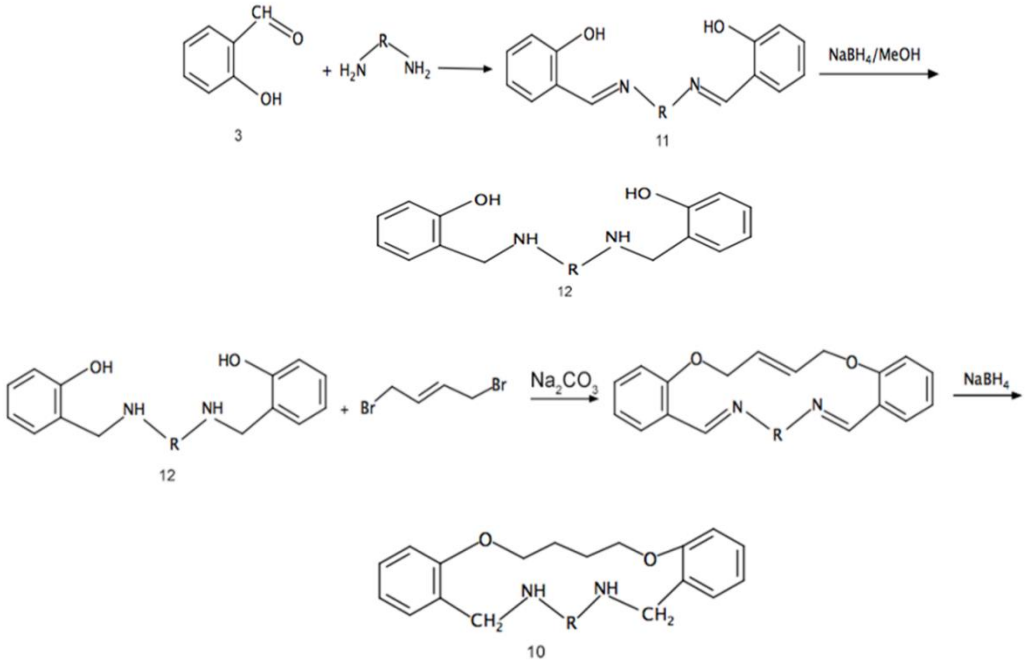

R=$(CH_2)_2$, $(CH_2)_3$, $(CH_2)_2NH(CH_2)_2$, $(CH_2)_2NH(CH_2)_2NH(CH_2)_2$, $(CH_2)_2O(CH_2)_2O(CH_2)$

It has been established that when the macrocyclization reaction is carried out in a three-component system, the yield is 30-35%. An alternative two-stage synthesis is completed with a lower yield of the target product (20-25%).

The purity and individuality of the synthesized compounds were determined by thin-layer chromatography on a Silufol plate (eluent - a mixture of ethanol with diethyl ether in a volume ratio of 1:1) and by melting temperature. The structure of the obtained crown compounds was established on the basis of elemental analysis data, by mass and NMR spectroscopy, and by studying the IR spectra of the samples.

In order to investigate physical chemical and biological properties of sintezed substances some complexes of transition metals (cobalt and nickel) with synthesized diazacrown ethers, which were used as polydentate ligands were obtained. (fig.1). The elements cobalt and nickel, as is known have 2 electrons at the external energy level. These electrons participate in chemical reactions with the electrons of the 3d orbitals of the second level from the outside. Due to this, a chemical bond is formed in the complexes.

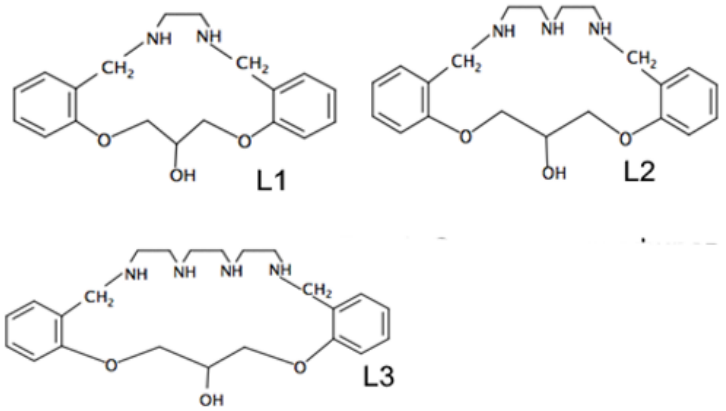

Fig.1. Crown ether schemes used as ligands for (L) complexes

Ligands L1, L2, and L3 have four, five, and six potential coordinating atoms in the rings, respectively. These crown ether complexes readily reacted with some transition metals by adding the appropriate ligand to the appropriate metal chloride in methanol. In this case, multi-colored crystals of the complexes are precipitated. Microanalytical data confirm the stoichiometry of the complexes 1:1 (ligand:metal) for all obtained complexes. The melting points of the complexes show that all complexes are thermally stable.

Composition, yield, melting points and elemental analysis data of crystalline solid complexes are given in table. 1.

Table.1

Transition metal complexes with synthesized diazacrown ethers date analysis

Complex	Color	Melting point (C)	Yield (%)	Elemental analysis		
				C	H	N
$CoL_1Cl_2 \cdot 3H_2O$	Dark-blue	188-192	78	44,7 (44,5)	5,6 (5,9)	5,4 (5,5)
$NiL_1Cl_2 \cdot H_2O$	Blue	>250	86	48,0(47,9)	5,4 (5,5)	5,7 (5,9)
$CoL_3Cl_2 \cdot 3H_2O$	Brown	190-194	74	45,5 (45,4)	6,1 (6,4)	7,5 (7,5)
$NiL_3Cl_2 \cdot 3H_2O$	Blue	216-220	81	45,3 (45,4)	6,3 (6,4)	7,3 (7,6)
$NiL_3(ClO_4)_2$	Light-blue	314-316	82	40,1 (40,1)	4,6 (4,7)	6,7 (6,7)
$CoL_4Cl_2 \cdot 3H_2O$	Dark-green	168-170	71	46,0 (46,2)	6,6 (6,7)	9,1 (9,4)
$NiL_4Cl_2 \cdot 2H_2O$	Blue	207–209	79	47,3 (47,6)	6,5 (6,6)	9,3 (9,7)

ISNN: print 2663-7006; online 2709-2666

RESULTS AND DISCUSSION

IR study of the resulting complexes shows that the absorption band v (C-N-C) at 1128-1140 cm-1 in free ligands shifts to 1110-1120 cm-1 during the formation of complexes (fig. 2). This shows that the nitrogen atoms of the macrocyclic ring are coordinated with metal ions. The absorption band v (Ar-OC) at 1245 cm-1 in free ligads shifts to the region 1232-1240 cm-1, which indicates that oxygen atoms also take part in coordination with metal ions.

In the complex of the synthesized diazacrown ether based on diethylenetriamine with nickel perchlorate, strong bands are observed in the spectrum in the region of 1100 cm–1, which belong to the vibrational absorption bands of ClO4–.

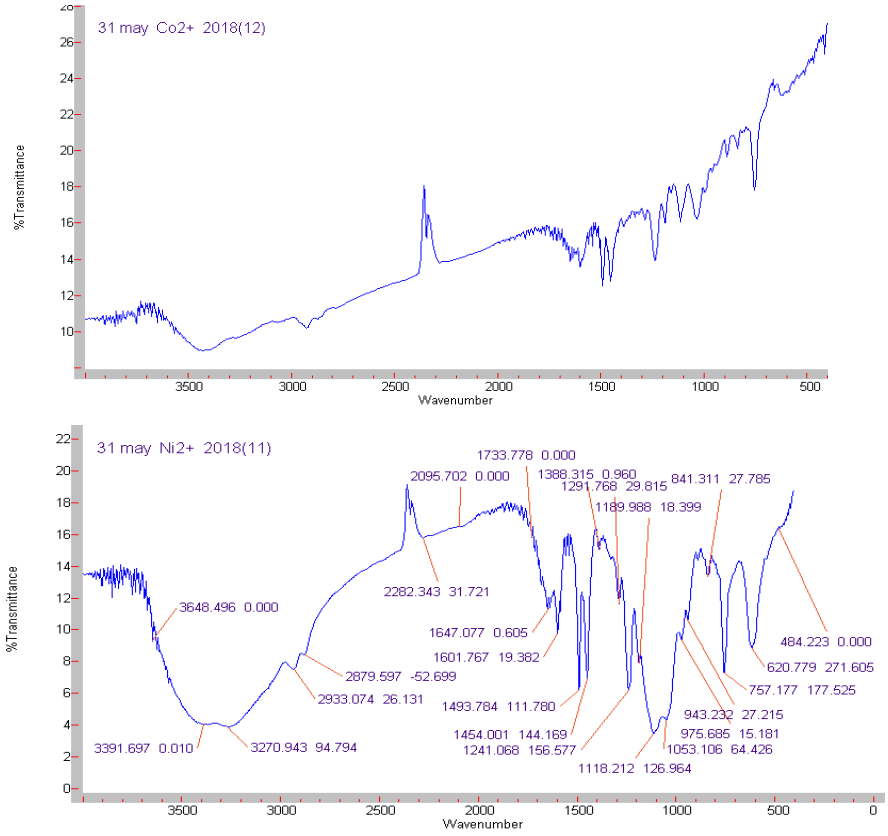

Fig 2. IR study of complexes.

The essence of the procedure for obtaining complexes is as follows: to a hot solution of the corresponding salt (0.3 mmol) in methanol (20 ml) was added solution of the ligand (0.3 mmol) in methanol (20 ml). The resulting mixture was heated to reflux for 0.5 h and then cooled to room temperature. The complex precipitated from the solution was filtered off, washed with methanol and diethyl ether, and dried in a vacuum.

The above method for the synthesis of complexes involving crown compounds is also more profitable from an economic point of view. Since this method of synthesis does not include the labour -intensive and resource-consuming process of obtaining intermediate compounds.

Table. 2

Data of ir spectroscopic analysis of the obtained transition metal complexes with the synthesized diazacrown ethers

Complex	IR date (sm^{-1})
L_1	3350, 3330, 1610, 1585, 1459, 1245, 1131, 758
$CoL_1Cl_2 \cdot 3H_2O$	3300, 1602, 1585, 1494, 1240, 115, 575
$NiL_1Cl_2 \cdot H_2O$	3300, 1598, 1489, 1235, 1118, 750
L_3	3350, 3330, 3200, 1600, 1585, 1496, 1245, 1135, 758
$CoL_3Cl_2 \cdot 3H_2O$	3350, 1600, 1584, 1492, 1237, 1110, 756
$NiL_3Cl_2 \cdot 3H_2O$	3350, 1600, 1582, 1490, 1238, 1112, 750
$NiL_3(ClO_4)_2$	3380, 3200, 1607, 1584, 1492, 1238, 1100, 752, 622
L_4	3350, 3330, 3320, 1600, 1583, 1494, 1245, 1137, 756
$CoL_4Cl_2 \cdot 3H_2O$	3350, 1598, 1487, 1238, 1115, 755
$NiL_4Cl_2 \cdot 2H_2O$	3350, 1598, 1489, 1237, 1114, 752

It was assumed that the resulting ligands would have biological activity against microorganisms, so they were tested against Gram-positive Staphylococcus aureus and Gram-negative strains of Escherichia coli. Tests of the antimicrobial activity of some synthesized new chemical compounds were carried out by the disk diffusion method and the method of serial dilutions.

The antibacterial activity of MC@Co and MC@Ni was tested by the micro-diffusion method, performed on Petri dishes, against Staphylococcus aureus and Escherichia coli.

Synthesized substances were taken in an amount equal to 30 μg. The colony of Escherichia coli was cultivated on Endo's medium, Staphylococcus aureus on Baird-Parker agar (the cultures were kindly provided by one of the clinical laboratories in Baku).

Table 3.

Antimicrobial activity of synthesized compounds

Culture	Concentration (mg)	(MC@Co) (SAMPLE № 1)		(MC@Ni) (SAMPLE №2)	
		zone of inhibition (mm)		zone of inhibition (mm)	
St. Aureus	5	24	25	28	28
	2.5	12	12	15	15
E. coli	5	-	-	-	-
	2.5	-	-	-	-

The microbial load in all tests was 1 billion microbial bodies per 1 ml, of which one drop was added to each tube. For a comparative study of the activity of the studied preparations, well-known preparations (ethyl alcohol, rivanol, furacillin, nitrofungin, ceftriaxon) were taken as controls. The results of the microdiffusion method showed that the diameter of the inhibition zone as a result of exposure to the studied MC@Co at a concentration of 5 on Staphylococcus aureus was 24 mm, and at a concentration of 2.5 it was 12 mm. (fig.3). The table shows that sample 1 and 2 has a strong anti-microbial effect against St. Aureus. The zones of inhibition for MC@Ni at concentrations of 2.5

ISNN: print 2663-7006; online 2709-2666

and 5 were 15 and 28 mm respectively. The data obtained show that the bactericidal effect of MC@Co and MC@Ni is associated with their inhibitory effect on the formation of the cell wall of microorganisms, protein denaturation, impaired permeability of the cytoplasmic membrane, and inhibition of enzymes important for the life of bacteria.

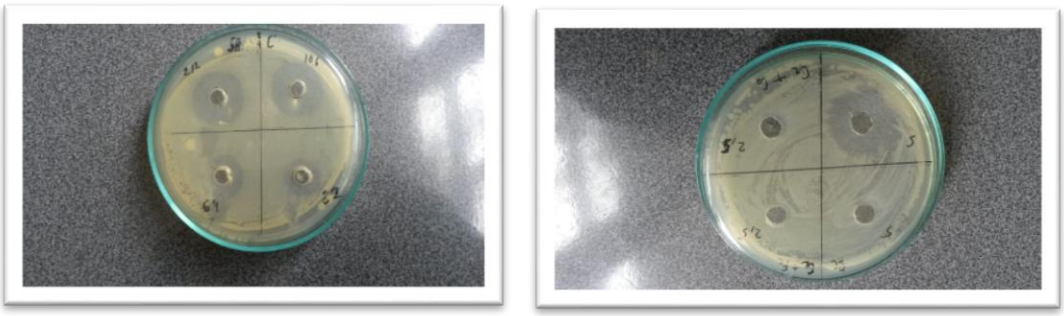

Fig 3. The results of the microdiffusion method

CONCLUSION

Summarizing the results of our studies, we assume that the synthesis of complexes based on azacrown ethers and transition metals have great potential for creating new effective antimicrobial drugs against gramm positive microorganisms.

REFERENCES

1. Lakovidis I., Delimaris, I., & Piperakis, S.M. (2011). Copper and its complexes in medicine: a biochemical approach. Mol. Bio. Int., 594529,pp28-35. https://doi.org/10.4061/2011/594529
2. Dmitrieva S.N., Churakova, M.V., Vedernikov, A.I., Kuzmina, L.G., & Gromov, S.P. (2011). New approach to the synthesis of dibenzodiazacrown ethers by ring transformation of dibenzocrown ether. Tetrahedron, 67(14), pp.2530 - 2535. https://doi.org/10.1016/j.tet.2011.02.038.
3. Adamu J. Y., Raufu A. I., Chimaroke F. C., Ameh J. A., Antimicrobial susceptibility testing of Staphylococcus aureus isolated from apparently healthy humans and animals in Maiduguri, Nigeria, International. Journal of Biomedical and Health Sciences, 2010,Vol. 6,№ 4, pp. 149-155. 0794-4748/2010, IJBHS 2010108/6404
4. Sadovskaya,N.Yu., Glushko V.N., Baryshnikova, M.A., Afanasyeva, D.A., Zhila, M.Yu., & Belus,S.K.). Synthesis and investigation of copper complexes of some derivatives of azomethinic monobenzone-esters.Russian Journal of General Chemistry.2019 89(3), pp. 440 - 445. https://doi.org/10.1134/S1070363219030125.
5. Anacona J., Maried Lopez, Mixed-Ligand Nickel(II) Complexes Containing Sulfathiazole and Cephalosporin Antibiotics: Synthesis, Characterization, and Antibacterial Activity, International Journal of Inorganic Chemistry. 2012, Vol.2, doi:10.1155/2012/106187
6. Brin L., Lantero M., de Diego I., Alvarez M., Zarazaga M., Torres C., Mechanisms of resistance to expanded-spectrum cephalosporins in Escherichia coli isolates,

recovered in a Spanish hospital, // Journal of Antimicrobial Chemotherapy.2005,56,pp.1107–1110. doi:10.1093/jac/dki370
7. Kline T., Fromhold M., McKennon T., Cai S., Treiberg J., Ihle N., Sherman D., Schwan W., Hickey M., Warrener P., Witte P., Brody L., Goltry L., Barker L., Anderson S., Tanaka S., Shawar R., Nguyen L., Langhorne M., Bigelow A., Embuscado L. and Naeemi E., Antimicrobial Effects of Novel Siderophores Linked to β-Lactam Antibiotics, // Bioorganic & Medicinal Chemistry. 2000, 8, pp.73-93. doi: 10.1016/S0968-0896(99)00261-8
8. Mayrhofer S., Domig K., Mair C., Zitz U., Huys G. and Kneifel W., Comparison of Broth Microdilution, Etest, and Agar Disk Diffusion Methods for Antimicrobial Susceptibility Testi21ng of Lactobacillus Acidophilus Group Members, // Applied and Environmental Microbiology. 2008, Vol.12, pp.3745-3748. doi: 10.1128/AEM.02849-07

СИНТЕЗ КОМПЛЕКСОВ ДИАЗАКРАУН ЭФИРОВ С ПЕРЕХОДНЫМИ МЕТАЛЛАМИ И ИССЛЕДОВАНИЕ ИХ БИОЛОГИЧЕСКОЙ АКТИВНОСТИ

Л.З.Вазирова[0000-00030008-8973]
Азербайджанский Государственный Университет Нефти и Промышленности
vazirova.leyla@gmail.com

Синтез диазакраун-эфиров проводили эффективными методами. Были синтезированы новые дибензоазакраун-эфиры с функционально замещенными гидроксильными и аминогруппами в макроциклическом (МК) кольце. Строение синтезированных краун-соединений - определено методами ИК, масс и ЯМР спектроскопии. Методы получения комплексов переходных металлов с органическими функциональными лигандами на основе диазакраун-эфиров, имеющих четыре, пять и шесть координирующих атомов в кольцах были изучены. Синтезированные новые диазакраун-эфиры за счет гидроксильных и аминогрупп увеличивают степень межмолекулярных взаимодействий и переходят от двумерной структуры к трехмерной, что повышает их биологическую активность.
Ключевые слова: *Краун-эфиры, переходные металлы, биологическая активность, комплексы.*

DIAZAKRAUN EFIRLƏRI VƏ KEÇID METALLARINDAN İBARƏT KOMPLEKSLƏRIN SINTEZI VƏ ONLARIN BIOLOJI AKTIVLIYININ TƏDQİQİ

L.Z.Vəzirova[0000-00030008-8973]
Azərbaycan Dövlət Neft və Sənaye Universiteti
vazirova.leyla@gmail.com

Diazakron efirlərinin sintezi səmərəli üsullarla aparılmışdır. Makrosiklik (MC) halqada funksional əvəzli hidroksil və amin qrupları olan yeni dibenzoazakraun efirləri sintez edilmişdir. Sintez olunmuş kraun efirlərin strukturu IQ, kütlə və NMR spektroskopiya üsulları

ISNN: print 2663-7006; online 2709-2666

ilə tədqiq edilmişdir. Makrotsiklik həlqədə dörd, beş və altı koordinasiya edici atoma malik olan diazakraun efirləri əsasında üzvi funksional liqandlarla keçid metal kompleksləri sintez olunmuşdur. Hidroksil və amin qrupları hesabına sintez edilmiş yeni diazakraun efirləri molekullararası qarşılıqlı təsirlərin artması nəticəsində ikiölçülü strukturdan bioloji aktivliyə malik olan üçölçülü quruluşa keçir.
***Açar sözlər**: Keçid metalları, kraun-efirləri, bioloji aktivlik, komplekslər.*

AJCN, Vol 4, No. 1, 2022, pp. 81-86

https://doi.org/10.32010/AJCN05012022-81

UDC 541.128

HYDROGENATION OF CARBON DIOXIDE ON SIRAL ALUMINOSILICATES MODIFIED WITH COBALT AND PALLADIUM

Sh.F.Tagiyeva[0000-0003-4913-3907]

Y.H.Mamedaliyev Institute of petrochemical Processes, Azerbaijan National Academy of Sciences

tshaxla@mail.ru

The reaction of hydrogenation of CO_2 in flow mode at atmospheric pressure on Siral aluminosilicates with 1, 10, and 40 wt.% SiO_2 and containing Co and Co-Pd has been studied. The synthesized catalysts were characterized by XRD and EPR spectroscopy. It has been established that on catalysts containing only cobalt, at a reaction temperature of ≤ 300°C, practically only methane is formed, and at a reaction temperature of T ≥ 300°C, methane and no more than 1% CO are formed. It is shown that with an increase in the SiO_2/Al_2O_3 ratio, a decrease in the methane yield is observed. The introduction of palladium into the composition of the Co/Siral catalyst stimulates the formation of methanol, the yield of which increases with an increase in the reaction temperature and reaches its maximum value at a reaction temperature of 500°C for the Co,Pd/Siral-10 catalyst. The mechanism of the reaction of CO_2 hydrogenation to methanol and the role of palladium in this reaction are discussed.

Keywords: *carbon dioxide, hydrogenation, methane, methanol, Siral, Pd, Co.*

INTRODUCTION

In recent years, the search for non-traditional raw materials for hydrocarbon production has been intensively conducted. At present, the problem of converting CO_2 into valuable chemical products is gaining importance, since this process can also be used for the utilization of CO_2 emitted in large quantities into the atmosphere [1]. One of the uses of CO_2 is its hydrogenation into methane, a synthetic substitute for natural gas, and methanol [2, 3]. The involvement of a stable carbon dioxide molecule in chemical processes is hampered by the lack of effective catalysts that allow the conversion of CO_2 into hydrocarbons, alcohols, and other valuable products with high yields and selectivity [4].

Despite the fact that a large number of theoretical studies and experimental observations have been carried out using a variety of catalysts and metal-based modifiers, the mechanisms for the hydrogenation of CO_2 to methanol are still controversial. There is still no consensus on how the CO_2 molecule is activated on the catalyst surface. In the literature, there are two ways describing the route of obtaining methanol. One of them is the formate pathway, where the rate of formation of the intermediate HCOO is usually considered to be the determining one [5]. The other way goes through the formation of CO by the water-gas shift reaction (WGSR) reaction and the usual conversion of synthesis gas to methanol ($CO + 2H_2 \rightarrow CH_3OH$). The formate mechanism suggests that CO can be formed by the decomposition of methanol, while the second mechanism can explain the direct formation of CO from WGSR as the main product [6]. This paper presents the results of studying the reaction of CO_2 hydrogenation on Co- and Co,Pd- containing samples of Siral aluminosilicate,

phase composition and magnetic properties, previously reduced at 450 °C in a hydrogen flow.

EXPERIMENTAL PART

SİRAL aluminosilicates (SASOL, Germany) with SiO_2 content of 1, 10 and 40 wt % were used as carriers for the preparation of catalysts [4]. Catalysts were prepared by impregnating supports with an aqueous solution of $Co(NO_3)_2$ $6H_2O$ and $PdCl_2$. After drying, the catalyst was molded into balls with a diameter of 2-3 mm and calcined at 500°C for 4 hours. The reduction of the catalysts was carried out in a stream of hydrogen at a temperature of 450°C for 1 hour.

The phase composition, structure, and magnetic properties of the synthesized catalysts were characterized using an XRD 3500 TD X-ray diffractometer, China, and EMRmicro electron magnetic resonance spectrometer, Bruker, Germany.

Catalytic testing of samples in CO_2 hydrogenation was carried out in a flow reactor with on-line chromatographic analysis of gas-phase reaction products using a Perkin Elmer Instruments Auto System XL chromatograph.

RESULTS AND DISCUSSION

Tables 1 and 2 show the compositions of CO_2 hydrogenation products over 10% Co/S-1,10,40 and 10% Co,0.5%Pd/S-1,10,40 catalysts (reaction conditions: atmospheric pressure, CO_2 : H_2 ratio is 1:3, space velocity - 120 h^{-1}).

Table 1

Composition of CO_2 hydrogenation products into hydrocarbons on Co/Siral-1,10,40 oxide catalysts: P = 0.1 MPa, CO_2 : H_2 = 1:3, vol. W = 120 h^{-1}*

*Chromatographic analysis was performed every 30 min. from the start of the reaction.

Catalyst	T, °C	Conversion of CO_2, %	Selectivity, Yield, %					
			CH_4		C_2H_6		CO	
			sel.	yield	sel.	yield	sel.	yield.
Co/SİRAL-1	200	55	99.5	55.7	0.5	0.28	-	–
	300	58	99.6	57.8	0.4	0.23	–	–
	400	52	98.7	51.3	–	–	1.3	0.68
	500	41	97.8	40	–	–	2.2	0.9
Co/SİRAL-10	200	38	100	38	–	–	–	–
	300	41	100	41	–	–	–	–
	400	37	97.3	36	–	–	2.7	0.99
	500	28	96.8	27.1	–	–	3.2	0.89
Co/SİRAL-40	200	29	100	29	–	–	–	–
	300	33	100	33	–	–	–	–
	400	29	96.6	28	–	–	3.4	0.98
	500	25	98.8	24.7	–	–	1.2	0.3

Table 2

Composition of CO_2 hydrogenation products to hydrocarbons on Co,Pd/Siral-1,10,40 oxide catalysts, P = 0.1 MPa, $CO_2 : H_2 = 1:3$, vol.W-120 h^{-1}*

*Chromatographic analysis was performed every 30 min. from the start of the reaction.

Catalyst	T, °C	Conversion of CO_2, %	Selectivity, Yield, %					
			CH_4		C_2H_6		CO	
			sel.	yield	sel.	yield	sel.	yield.
Co, Pd/SİRAL-1	200	49	98.8	48.4	1.2	0.6	-	-
	300	54	93.9	50.7	4.1	3.1	2.0	0.2
	400	57	84.7	48.3	4.7	3.5	10.6	5.2
	500	65	67.2	43.7	9.1	5.9	23.7	15.4
Co, Pd/SİRAL-10	200	54	98.5	53.2	0.93	0.5	0.57	0.3
	300	56	89.8	50.3	1.96	1.1	8.24	4.6
	400	62	76.5	47.4	5.0	3.1	18.5	11.5
	500	69	57.4	39.6	13.5	9.3	29.1	20.1
Co, Pd/SİRAL-40	200	41	99.2	40.6	0.49	0.2	0.48	0.2
	300	43	96.3	41.4	1.4	0.6	2.3	1
	400	44	92.3	40.6	2.27	1.0	5.43	2.4
	500	45	79.1	35.6	5.6	2.5	15.3	6.9

The results of catalytic tests show that the main products of the reaction of a $CO_2/H_2 = 1:3$ mixture with the studied catalysts are methane, ethane, carbon monoxide, methanol and water ($5CO_2 + 15H_2 = CH_4 + C_2H_6 + CO + CH_3OH + 8H_2O$). On catalysts containing cobalt, at a reaction temperature of ≤ 300°C, practically only methane is formed, at a reaction temperature of T ≥ 300 °C, methane and no more than 1% CO, and with an increase in the SiO_2/Al_2O_3 ratio, a decrease in the methane yield is observed. The introduction of palladium into the composition of the catalyst stimulates the formation of methanol, the yield of which increases with an increase in the reaction temperature and reaches its maximum value at a reaction temperature of 500 °C. The maximum yields of methane (57% and 41%) at a reaction temperature of 300°C are observed on the Co/S-1 and Co/S-10 catalysts, respectively. The maximum yield of methanol (21%) is observed on the Co,Pd/S-10 catalyst at a temperature of 500°C and atmospheric pressure. The activity of the Co,Pd/Siral catalyst with a SiO_2 content of 1 and 10% compared to catalysts with S-40 is noticeably higher, which indicates that the reaction of CO_2 hydrogenation to methane and methanol depends on the SiO_2/Al_2O_3 ratio.

Figure 1, a, b shows X-ray diffraction patterns of samples reduced in a stream of hydrogen at 450°C for one hour: a) Co/S-10 and b) Co,Pd/S-10. As can be seen from the given X-ray diffraction patterns for Co/S-10 and Co,Pd/S-10 samples reduced in a hydrogen flow at 450°C, Co_3O_4 and Co_3O_4, metallic Pd phases, respectively, are detected, that is processing first in a stream of air at 500 °C for 4 hours and then in a stream of hydrogen at 450 °C for one hour of samples of aluminosilicate matrix S-10 with salts of cobalt(II) nitrate

ISNN: print 2663-7006; online 2709-2666

and palladium(II) chloride deposited at room temperature from aqueous solutions leads to formation of cobalt oxide Co_3O_4 and metallic Pd.

The EPR spectra shown in fig.2, a, b belong to ferromagnetic CoOx particles, most likely Co_3O_4. The introduction of palladium into Co/S-10 noticeably affects the EMR spectra of the Co/S-10 samples, which is associated with a change in the magnetic state of the Co_3O_4 particles, most likely caused by a change in their dispersed state.

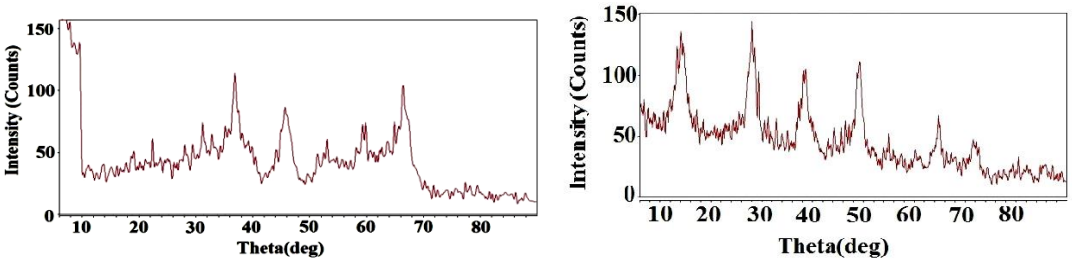

a b

Fig.1, a, b. X-ray diffraction patterns recorded at room temperature of samples reduced in a hydrogen flow at 450°C for one hour: a) Co/S-10 and b) Co,Pd/S-10.

Figures 2,a and 2,b show the EMR spectra of Co,Pd/S-10 and Co/S-10 samples recorded at room temperature

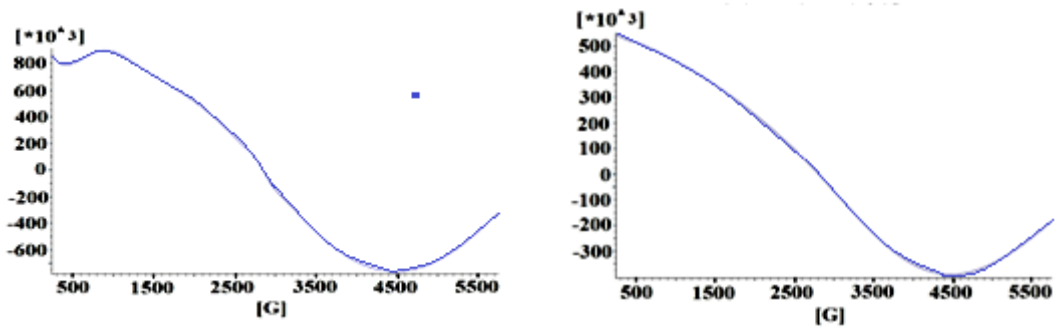

a **b**

Fig.2. EMR spectra of recorded at room temperature samples:
a) Co,Pd/ S-10 and b) Co/ S-10.

This, in turn, affects the catalytic properties and changes in the composition of the reaction products. We assume that the hydrogenation of CO_2 to methanol is catalyzed by nanodispersed palladium particles. With the participation of palladium, it is very likely that the following stepwise mechanism of the conversion of CO_2 into methanol takes place. At the initial stage, molecular hydrogen reacts with palladium particles to form Pd-H particles ($Pd_n + H_2 = 2Pd\text{-}H + Pd_{n-2}$), then CO_2 is hydrogenated upon interaction with Pd-H particles to form first mono

and then bidentate formate, which then converted to methanol through a series of intermediates. The second possible route of CO_2 conversion in the presence of dissociated hydrogen is the formation of carboxyl, which is converted into methanol through a number of intermediates, including formyl [6, 7].

REFERENCES

1. E.C. Ra, K.Y. Kim, E.H. Kim, L. Hojeong, A. Kwangjin, and L. Jae Sung. Recycling Carbon Dioxide through Catalytic Hydrogenation: Recent Key Developments and Perspectives. *ACS Catal.* 2020,Vol.10, №19,pp.11318-11345
2 Huš M., . Kopač D and Likozar B. Catalytic Hydrogenation of Carbon Dioxide to Methanol: Synergistic Effect of Bifunctional Cu/Perovskite Catalysts. *ACS Catal*. 2019, Vol.9, №1, pp.105-116
3. R. Guil-López, N. Mota, J. Llorente, E. Millán, B. Pawelec, J.L.G. Fierro, and R.M. Navarro. Methanol Synthesis from CO_2: A Review of the Latest Developments in Heterogeneous Catalysis. *Materials.* 2019, Vol.12, P.3902
4.Saeidi S., Najari S.,Hessel V.,Wilson K., Frerich J.K. P. Concepción, S.L. Suib, and A.E. Rodrigues. Recent advances in CO_2 hydrogenation to value-added products – Current challenges and future directions. *Progress in Energy and Combustion Science*. 2021, P.85. 100905
5 .https://www.sasol.com/siral-and-siralox.
6.Y. Hu, W. G. Gao, H. Wang [et al.] Structure–activity relationships of Cu–ZrO_2 catalysts for CO_2 hydrogenation to methanol: interaction effects and reaction mechanism // **RSC Adv.,** - 2017,- v. **7**, - pp. 8709-8717
7.Grabow L.C and Mavrikakis M. Mechanism of Methanol Synthesis on Cu through CO_2 and CO Hydrogenation // ACS Catal. 2011,Vol.1, № 4, pp. 365–384
8.Volnina E.A.,Kipnis M.A. Sovremenniye vzglyadi naa mexanizm sinteza metanola na Cu –soderzhashix kaatalizatorax.//Kinetika I Kataliz (Russian). 2020, Vol.61, № 1, pp. 107–118

ГИДРИРОВАНИЕ ДИОКСИДА УГЛЕРОДА НА МОДИФИЦИРОВАННЫХ КОБАЛЬТОМ И ПАЛЛАДИЕМ АЛЮМОСИЛИКАТАХ SIRAL

Ш.Ф.Тагиева[0000-0003-4913-3907]
Институт Нефтехимических Процессов им. Ю.Г.Мамедалиева
tshaxla@mail.ru

Исследована реакция гидрирования CO_2 в проточном режиме при атмосферном давлении на алюмосиликатах Siral с содержанием SiO_2 1, 10 и 40 мас.% и содержащих Co и Co-Pd. Синтезированные катализаторы охарактеризованы методами РФА и ЭПР спектроскопии. Установлено, что на катализаторах, содержащих лишь кобальт, при температуре реакции ≤ 300°C образуется практически лишь метан, при температуре реакции T ≥ 300°C – метан и не более 1% CO. Показано, что с ростом соотношения SiO_2/Al_2O_3 наблюдается уменьшение выхода метана. Введение палладия в состав катализатора

ISNN: print 2663-7006; online 2709-2666

Co/Siral стимулирует образование метанола, выход которого увеличивается с ростом температуры реакции и достигает максимального значения при температуре реакции 500°C для катализатора состава Co,Pd/Siral-10. Обсуждается механизм реакции гидрирования CO_2 в метанол и роль палладия в этой реакции.
Ключевые слова: *диоксид углерода, гидрирование, метан, метанол, Siral, Pd, Co.*

Co VƏ Pd – LA MODIFIKASIYA EDILMIŞ SIRAL ALÜMINOSILIKATLARIN KARBON DIOKSIDLƏ HIDROGENLƏŞMƏSI

Ş.F.Tağiyeva[0000-0003-4913-3907]
Y.H. Məmmədəliyev adına Neft Kimya Prosesləri İnstitutu
tshaxla@mail.ru

Tərkibində 1,10 və 40% SiO_2 olan, Co- və Co,Pd-la modifikasiya olunmuş Siral alüminosilikatların üzərində atmosfer təzyiqdə axın rejimində karbon dioksidin hidrogenləşmə reaksiyası tədqiq edilmişdir. Sintez edilmiş katalizatorlar rentgen difraktometriyası və electron maqnit rezonansı metodları ilə xarakterizə edilmişdir. Müəyyən edilmişdir ki, tərkibində yalnız kobalt olan katalizatorlarda ≤ 300°C reaksiya temperaturunda praktiki olaraq yalnız metan, T ≥ 300°C temperaturda isə metan və miqdarı 1%-dən çox olmayan CO əmələ gəlir və SiO_2/Al_2O_3 nisbətinin artması ilə metanın çıxımında azalma müşahidə edilir. Katalizatorun tərkibinə palladiumun daxil edilməsi metanolun əmələ gəlməsini stimullaşdırır, onun çıxımı reaksiya temperaturunun artması ilə artır və 500°C temperaturda maksimum olur. Karbon dioksidin metanola hidrogenləşmə reaksiyasının mexanizmi və bu reaksiyada palladiumun rolu müzakirə olunur.
Açar sözlər*: karbon dioksid, hidrogenləşmə, metan, metanol, Siral, Pd, Co.*

ATTENTION FOR AUTHORS!

"Azerbaijan Journal of Chemical News" approved by the Higher Attestation Commission under the President of Azerbaijan Republic and it is included to the list of journals and periodicals that should be published by major scientific results of dissertations in Azerbaijan Republic.